Mechanisms in suppressing chromosomal translocations and maintaining genome stability

by

Cheryl Jacobs Smith

A dissertation submitted in partial fulfillment
of the requirements for the degree of
Doctor of Philosophy
(Human Genetics)
in The University of Michigan
2014

Doctoral Committee:

Associate Professor JoAnn M. Sekiguchi, Chair
Professor John V. Moran
Assistant Professor Raymond C. Chan
Associate Professor Thomas E. Wilson
Professor Wesley Dunnick

Dedication

This thesis is dedicated to my parents, Verlinda and Darwin Jacobs, without whose love, guidance, and sacrifice I would not be here today and to Elizabeth Oosterhouse, an excellent science buddy and friend who I will miss always.

Acknowledgements

I would like to give a heartfelt thanks to JoAnn Sekiguchi for her mentoring and guidance throughout my tenure in the Sekiguchi lab. After each of our discussions, I would leave feeling that you had taught me not only about science, but also more about myself. I really appreciate the heartfelt conversations we have had over the years. After the loss of my father, my life was in disarray. I now know that without the professional support and personal friendship of you, JoAnn, I would have left graduate school. It is thanks to you that I have stayed the course. Thank you. I would also like to reiterate what a previous graduate student, Jennie Mason, had acknowledged about JoAnn: “that her eternal optimism and her willingness to allow me to pursue my own line of investigations were instrumental to my development during my graduate career”.

I would also like to thank my thesis committee members for their intellectual contributions to my dissertation and their continued support as I pursue my professional goals. I have enjoyed our conversations and have benefited from the experimental advice. I am thankful from funding from Rackham as a Rackham Merit Fellow, the Human Genetics Training Grant (T32-GM-07544 (NIGMS)) and from the NCI (F31 CA163530-01A1).

I would also like to thank past and present members of the “Fergiguchi” labs. I have benefited from your friendship and intellectual discussions. You all have made lab truly an enjoyable and supportive environment. I would like to especially acknowledge a previous Sekiguchi-Fergiguchi, Billy Giblin. At first, I thought you hated me but then I realized that you were only critical to people when you truly cared about their scientific mentoring. Thank you for believing in me as a rotation student before I even believed in myself! I would like to thank Jennifer (Jennie) Mason for her leadership, guidance, and friendship. You truly helped me feel like I belonged in the Sekiguchi lab and your advance knowledge

about many of the protocols in the lab helped me get a great start on my project. Plus, I will always remember our dance moves when we made metaphase preps. You know how to truly make a long, boring protocol fun. I would like to thank Ishita Das, Kalyla Nelson, William Lu, Hilary Moale, Elizabeth Spehalski, Todd Festerling, and Andrea Hartlerode for their boisterous energy, friendly attitudes and overall cheer. A special acknowledgment goes to Andrea Hartlerode as my bowling buddy on our bowling team at Colonial Lanes, the Molecular Bowl-ologists. We are currently in second place and I hope we clinch 1st! I would also like to acknowledge my other teammates, Allison Johnson and Diane Flasch. You ladies are awesome bowlers and I look forward to Monday nights every week because you are a great group of ladies! I would also like to say it has been a pleasure getting to know our newest members, Jordann Smak and Mary Morgan. I know you two will be great Fergiguchis. I would also like to express my deepest thanks for the hard work and commitment of Jeffrey Xie. You are one of the most dedicated undergraduates I have worked with and I know your future will be bright as you continue your M.D./Ph.D. pursuit.

No one goes through graduate school without the help of administrators, so I would like to thank the Human Genetics administration for their adept problem solving skills and commitment to figure out any problem I presented. I would also like to thank the MMG administrator, Sherry Taylor, as she has contributed to making sure any administrative queries I have are answered.

A happy and well-adjusted graduate student has amazing friends and I am no exception. Thank you to Heather McLaughlin (Harville), Valerie Schaibley, Kaanan Shah, Kadee Luderman, Ilea Swineheart, and Stephanie Coomes. Without you PIBs girls I do not know to whom else I would have shared my joys and failures. I am overwhelmingly thankful for my high school and college friends, Nicole Phillips Austin, Lena Lotsana Brower, and Erin Lattin who were able to take time out of their busy schedules and support me on my special day. You ladies are wonderful and your friendship means so much to me!

I am thankful to all my family members (new and old) and for their continued support throughout graduate school. That you believed in me first,

helped me to believe in myself. Last but not least, I would like to think my best friend and husband, Kyle Alexander Smith. These past 10 years have been amazing and ‘oh, the places we will go!’ I honestly could not imagine anyone else to share this life with nor could I imagine that anyone else would show me unconditional love and support throughout this arduous process. Now we can finally be the Drs’ Smith!

Table of Contents

List of Figures

Chapter 1 Figures

Chapter 2 Figures

Chapter 3 Figures

Chapter 4 Figures

Chapter 5 Figure

List of Abbreviations

DSB	double strand break
MRN	MRE11/RAD50/NBS1
MRE11 complex	MRE11/RAD50/NBS1
ATM	ataxia telangiectasia mutated
DNA-PKcs	DNA-dependent protein kinase catalytic subunit
PIKK	phosphoinositide 3-kinase (PI3K)-related protein kinase
ATR	ATM and RAD3-RELATED PROTEIN
mTOR	mammalian target of rapamycin
HR	homologous recombination
NHEJ	nonhomologous end joining
cNHEJ	classical nonhomologous end joining
MMEJ	microhomology-mediated end joining
aNHEJ	alternative nonhomologous end joining
ssDNA	single stranded DNA
NBS	Nijmegen breakage syndrome
ATLD	Ataxia-telangiectasia-like disorder
CPSF	Cleavage and polyadenylation-specific factor
RS-SCID	Radio-sensitive severe combined immunodeficiency
TCR	T-cell receptor
BCR	B-cell receptor
IgH	Immunoglobulin heavy chain
DN	Double negative
DP	Double positive
RSS	Recombination signal sequence
RAG1/2	Recombination activating genes 1 and 2

PCC	Post-cleavage complex
PHD	Plant homeodomain
P70	ARTEMIS C-terminal deletion mutant
AT	Ataxia-telangiectasia
NBSLD	RAD50-associated NBS-like disorder
CSR	class switch recombination

Abstract

Double strand breaks (DSBs) represent one of the most dangerous forms of DNA damage. DSBs are generated during normal metabolic processes, such as DNA replication, or upon exposure of cells to exogenous agents, such as ionizing radiation. In addition, DSBs are formed as intermediates during programmed DNA rearrangements that occur during early B and T lymphocyte development, a process known as V(D)J recombination. Unrepaired or mis-repaired DNA ends can engender detrimental outcomes for cells and organisms such as aberrant genomic events like chromosomal translocations. The classical nonhomologous end joining (cNHEJ) pathway is one of the major DNA DSB repair pathways operative in mammalian cells and is required for both general DSB repair and V(D)J recombination.

The studies of my dissertation investigate the functions of DNA nucleases in the repair of double strand breaks during V(D)J recombination. I have undertaken two independent, but related, lines of investigation to address this question. One project sought to elucidate the regulation of the ARTEMIS nuclease during V(D)J recombination. I examined the molecular mechanisms underlying tumorigenesis caused by an *Artemis* hypomorphic disease allele and identified that the ARTEMIS C-terminus suppresses tumorigenesis associated with misrepair of DNA DSBs generated during V(D)J recombination. My findings raise the possibility that particular defects in ARTEMIS that result in partial loss of function, can predispose to lymphoma, but not complete immunodeficiency.

The second project focused on determining the interplay between the ARTEMIS and MRE11 nuclease in facilitating normal and aberrant V(D)J rearrangements. My results indicate that mutation of the MRE11 complex prevents tumorigenesis associated with aberrant end joining of V(D)J loci, an in

turn, implicates the MRE11 complex in promoting tumorigenesis associated with DNA damage. Both projects have led to a greater understanding of the mechanisms underlying human lymphoma caused by impaired ARTEMIS nuclease activity, and additionally, identified the MRE11 complex as a possible chemotherapeutic target for improved treatment for lymphoid malignancies.

I. CHAPTER 1 Introduction

A. DNA double strand break repair in genome stability and development

DNA double strand breaks (DSBs) are amongst the most cytotoxic lesions to a cell. These dangerous DNA lesions are generated as a result of exposure to exogenous DNA damaging agents and endogenous products resulting from cellular metabolism. In addition, programmed DSBs arise by highly regulated processes, such as V(D)J recombination, which is necessary for the development of mature T- and B-cells. If unrepaired or misrepaired, DSBs can lead to an accumulation of mutations and/or chromosomal aberrations such as chromosomal translocations, which can then play an initiating role in carcinogenesis. Therefore, understanding the mechanisms that result in efficient repair of DNA damage is critical to our understanding of genome stability and cancer.

A1.1 DNA double strand break repair response

The DNA double stand break (DSB) response can be modeled as a three-tiered signaling cascade. The signal transduction mechanism that disseminates the DNA damage alarm begins with sensor proteins that senses the damage or chromatin alterations emanating from it and mediate the activation of transducers, that in turn, convey the alarm to numerous downstream effectors involved in specific mechanisms that induce cell cycle checkpoints, repair the damage, or if the damage is too great, induce senescence or apoptosis, depending on the type of damage and cell type (Figure 1.1) (1). One of the main sensors of DSBs consists of the MRE11/RAD50/NBS1 complex best known as the MRN complex or the MRE11 complex (Figures 1.1 and 1.3). The MRE11 complex is a critical component of DSB repair and plays multiple roles during the repair of broken DNA ends such as DNA damaging sensing, checkpoint activation, and repair (2). In response to DSBs, the MRE11 complex initiates the

DNA damage response via activation of the ataxia telangiectasia mutated (ATM) protein kinase also recognized as the primary transducer of the DSB alarm (Figures 1.1 and 1.3) (3, 4).

ATM is a member of the phosphoinositide 3-kinase (PI3K)-related protein kinase (PIKK) family, which also includes ATM and RAD3-RELATED protein (ATR), and the catalytic subunit of DNA-DEPENDENT PROTEIN KINASE (DNA-PKcs), among others (5). Activated ATM phosphorylates numerous 'effector' substrates that are key factors in the DNA damage response pathway like chromatin-associated repair factors (e.g., H2AX, SMC1, and Kap1) and members of the cNHEJ pathway (e.g., KU, XRCC4, LIG4, and ARTEMIS (4, 6). Additionally, ATM phosphorylates DNA-PKcs suggesting that this phosphorylation event may serve to regulate DNA-PKcs function (7).

ATM has been documented primarily as a critical component to the response to DSBs; however, crosstalk between ATM and DNA-PKcs can occur during the DNA DSB response (8). The exact interplay between ATM and DNA-PKcs is still unclear; however, recent studies highlighted the functional overlap of these kinases in the repair of DSB intermediates and in the DNA damage response (8-12). Thus, mice deficient in either DNA-PKcs or ATM are live born, but DNA-PKcs and ATM double deficiency lead to early embryonic lethality (12, 13). Ablation of both kinase activities in cells undergoing immunoglobulin class switch recombination, lymphocyte-specific DNA rearrangement, lead to compound defects in switching and a synergistic increase in chromosomal aberrations. The phenotypes were attributed, in part, to the requirement of both kinases to phosphorylate p53 and induce p53-dependent apoptosis of cells harboring aberrant events (11). Additionally, the overlapping activities of ATM and DNA-PKcs have been implicated in joining endonuclease-induced DSBs during lymphocyte development (9).

In response to DNA damage, distinct DNA damage sensors regulate ATR, ATM, and DNA-PKcs. ATM is recruited to the DNA break and activated by the DNA end-binding complex composed of MRE11, RAD50, and NBS1, whereas DNA-PKcs is recruited to the DNA break and activated by the DNA end-binding

complex composed of the KU70-KU80 heterodimer (Figure 1.3) (14, 15). ATR, through ATRIP, recognizes ssDNA at sites of DNA damage or stressed replication forks (16). In this way, particular kinases are activated as a result of particular types of DNA damage.

The ATM kinase phosphorylates numerous downstream substrates to disseminate the DNA DSB repair response; however, the phosphorylation of the histone variant H2AX by ATM is critical for eliciting DNA repair (3, 17). Original observations by the Bonner lab identified by chromatin immunoprecipitation (ChiP) assays in the yeast strain *S. cerevisiae*, that phosphorylation of H2AX (γH2AX) was induced when an HO endonuclease-inducible break was unable to be repaired (18). Work in mammalian cells identified that γH2AX is spread over several hundred kilobases from the break whether it be induced by the lymphocyte-specific endonuclease, RAG1/2, or triggered by the accumulation of unprocessed DNA ends (18, 19). ATM is the major kinase responsible for histone H2AX phosphorylation as a result of DSBs; however, other PIKK kinases, such as DNA-PKcs also participate (8). The resultant phosphorylation of histone H2AX is thought to recruit 'docking' proteins such as MDC1 to damaged ends, which in turn recruit effector proteins such as 53BP1 to regulate DNA repair pathway choice (Figure 1.3) (18).

The efficient repair of DSBs relies on a complex signaling network which involves a tiered signaling cascade involving sensor' proteins that sense DNA damage and/or chromatin alteration, transducer's which convey the signal, and numerous downstream 'effectors' involved in the DNA DSB response including cell cycle checkpoint activation, senescence or apoptosis, and repair.

A1.2 DNA Damage Repair Pathways

Specific types of DNA lesions are repaired by dedicated pathways (Figure 1.2). A subset of pathways removes damaged and/or mis-matched DNA bases. For example, chemical alterations of bases that occur due to by-products of normal cellular metabolism, helix distorting lesions such as cyclobutane pyrimidine dimers that are induced by ultraviolet light, and interstrand crosslinks that are produced by agents such as cisplatin are repaired by base excision

repair, nucleotide excision repair and interstrand crosslink repair, respectively (20, 21). Mismatch repair primarily repairs DNA bases that have been improperly added during DNA replication as well as small DNA loops (20). Generally, when a base(s) is removed it is followed by polymerase addition to fill in the resulting gap and ligation.

DSBs represent one of the most dangerous forms of DNA damage. Indeed, defective DSB repair is associated with various developmental, immunological, and neurological disorders, and can be a major driver in cancer (22, 23). DSBs can also arise pathologically such as following exposure to exogenous agents, like ionizing radiation and when DNA replication forks encounter unrepaired DNA lesions, triggering fork collapse (24). In some instances, the cell programs DSBs. During the first meiotic prophase, the evolutionary conserved SPO11 protein induces hundreds of DNA DSBs along chromosomes in order to promote homologous recombination between homologs during meiosis (25). These DSBs are essential for correct chromosome segregation at the first meiotic division and generates gametes with allele combinations distinct from the parental germline (26). DSB-induced rearrangements at immunoglobulin genes are also critical for the multiplicity of antigen receptor diversity (27). Typically, molecular events at damage sites ensure that developmental programmed DSBs are steered toward the appropriate repair outcome, yet upon misrepair of the developmental DSBs, aberrant repair events may result (28).

The two major DSB repair pathways that have been studied extensively are homologous recombination (HR) and nonhomologous end joining (NHEJ) (Figure 1.3). As their names imply, NHEJ involves direct ligation of the broken ends; in contrast HR requires an undamaged homologous sequence to serve as a template for repair of broken strands. There is very efficient error-free NHEJ and error-prone NHEJ associated with small insertions, deletions, or substitutions at the break point junction (29). Studies in human cells using linearized plasmids with complementary, blunt ends and non-complementary ends of various configurations demonstrated that although the efficiency of the plasmid

substrates were similar, the plasmids containing complementary or blunt ends were repaired at earlier time points as compared to the plasmids with non-complementary ends suggesting that non-complementary ends require additional processing time prior to ligation. Additionally, human cells with linearized non-complementary plasmids treated with wortmannin, a PIKK inhibitor, blocked the repair of non-complementary plasmids. DNA-PKcs is a PIKK protein kinase and the authors hypothesized that the wortmannin treatment inhibited DNA-PKcs activities resulting in inhibition of recruitment of downstream DNA end processing factors such as nucleases, polymerases, and ligases to the break (30). Indeed, activated DNA-PKcs interacts with nucleases such as ARTEMIS and the NHEJ ligation complex (31-35).

Another modality of end joining, microhomology-mediated end joining (MMEJ), has come to be appreciated (Figure 1.3). MMEJ utilizes annealing of short homologous sequences (2-20 bp in length), revealed by DNA end-resection, to align ends prior to ligation (36). Since the activities of MMEJ have been observed when NHEJ is deficient, MMEJ is referred to as an alternative end joining mechanism. Recent observations of chromosomal translocation junctions have identified microhomology at the junction suggesting MMEJ contributes to chromosomal translocations. Thus MMEJ is error-prone and contributes to genome instabilities but its use and regulation is poorly understood.

A1.3 Homologous Recombination

Research studies have shown that the choice among these DNA repair pathways depends on the DSB end structure mediated by resection (37-39). Once a DSB is resected to generate 3′ single stranded DNA, it must be repaired by homologous recombination (HR) or by single-strand annealing, which relies on sequence homology between the broken DNA ends (Figure 1.3) (40).

Factors within the Rad52 epistasis group including Mre11, Rad50 and Xrs2 were identified due to their inability to repair ionizing irradiation-induced damage in *S. cerevisiae* (41). Subsequent biochemical and yeast two-hybrid studies identified that Mre11, Rad50, and Xrs2 exist in a complex known as the

MRX or Mre11 complex that promotes homologous recombination in DNA repair and cellular replication (41, 42). The Rad52 epistasis group is highly conserved among eukaryotes (41); however, Xrs2 is less well conserved and is divergent from its mammalian counterpart, NBS1. Nonetheless, NBS1 associates with mammalian MRE11 and mammalian RAD50 to form the MRN or MRE11 complex that is functionally analogous to yeast MRX in its role in HR (41, 43).

Although the purified MRE11 protein exhibits 3'- 5' exonuclease and endonuclease activities in vitro, MRE11 is implicated in the 5'-3' resection at DNA ends necessary for HR (40, 42). This was a conundrum in the field for years because HR requires resection of 5'-termini to generate 3'-single-strand DNA and the nuclease activities of MRE11 were incongruent with its role in HR-mediated resection (44, 45). However, studies from the Neale lab proposed a working model that suggested use of bidirectional end resection instead of unidirectional resection at a DSB. The data from the group suggests that MRE11 can nick the strand to be resected up to 300 nucleotides from the 5′-terminus of the DSB subsequently enabling resection in a bidirectional manner, using another nuclease, EXO1. The Neale lab then suggests EXO1 nuclease activities chew DNA ends in the 5′–3′ direction away from the DSB, and MRE11 in the 3′–5′ direction towards the DSB end resulting in 5'-3' resection at the DSB and a 3' single stranded DNA end (46).

Subsequent to the 5'-3' resection, RPA coats single stranded DNA ends to protect them from degradation whereby later RPA is replaced by RAD51 filaments. RAD51-single stranded DNA filaments perform one of the central functions of HR: strand invasion, homology search, and DNA strand exchange (47). Oftentimes, a sister chromatid rather than a homolog serves as a template for these processes, thus restoring the original sequence before damage (40, 47). It is likely cohesion of the sister chromatids facilitates this preference (47). These observations suggests HR is most active in the phases of the cell cycle where a sister chromatid is present, in S- and G2 phases of the cell cycle (47). Overall, HR occurs in several distinct steps that prepare a broken DNA substrate

for strand invasion into a homologous template and eventual resolution of strand invasion intermediates.

A1.4 Classical nonhomologous end joining

DNA end-to-end joining mechanisms, by which DNA DSBs are repaired, has been studied in mammalian cells for over 30 years. Early studies using the simian virus 40 (SV40) genome demonstrated that by creating chimeras of the genome with plasmids, subsequent cellular survival depended upon deletion of the plasmid sequence without altering the viral sequence. Sequence analysis identified that the deletional/joining events relied upon end-to-end joining at a relatively high frequency (48). Subsequent studies identified similar results in mammals (49).

The efficient repair of DNA DSBs by the ubiquitously expressed classical nonhomologous end joining (cNHEJ) factors requires the intricate coordination of multiple events at DNA ends. After DSB generation, mammalian KU70/KU80 heterodimer binds selectively to the DNA ends (Figure 1.3) (50, 51). KU70/KU80 is highly abundant within the mammalian cell and was originally identified as an antigen found in sera from various autoimmune patients (52). Therefore, initially it was thought that KU70/KU80 played a role in mediating autoimmune disease. However, subsequent studies identified the KU70/KU80 heterodimer as a DNA end-binding protein owing to the fact that KU70/KU80 binds specifically to DSBs as well as other discontinuities in the DNA double helix (53). The KU70/KU80 heterodimer binds DNA ends with a high affinity and translocates along the DNA break and acts as the targeting subunit for the DNA PROTEIN KINASE CATALYTIC SUBUNIT (DNA-PKcs) to make the holoenzyme DNA-PK (51, 53-55).

DNA-PKcs is a nuclear protein a part of the PIKK family of serine/threonine protein kinases. It is active when it is bound to DNA through the KU70/KU80 heterodimer (53, 56). In this bound state, DNA-PK facilitates DNA end synapsis and autophosphorylation of DNA-PK proceeds (57-59). Autophosphorylation of DNA-PK causes a conformational change within the protein complex to allow accessibility of the DNA ends to additional factors for

processing. In addition to its DNA end binding capabilities, DNA-PK (DNA-PKcs) recruits and phosphorylates the nuclease, ARTEMIS (Figure 1.3). The ARTEMIS:DNA-PKcs complex induces ARTEMIS endonucleolytic activity critical for DNA hairpin opening and 3' and 5' overhang processing on a subset of DNA ends to prepare ends for ligation (60, 61).

Direct end-to-end ligation proceeds when the ligation complex consisting of LIG4:XRCC4:XLF ligates the DNA ends together (62, 63). During this process, DNA end-to-end synapsis is facilitated by the DNA-PK complex and DNA-PK not only autophosphorylates its subunits but also the ligation complex (35). LIG4:XRCC4:XLF is capable of ligating incompatible DNA ends as well as over gaps (64). Therefore, the ligation junction of non-compatible DNA ends can be altered by nucleotide deletion or nucleotide addition by polymerases such as polymerase mu and X which have been shown to interact with LIG4:XRCC4 and KU70/KU80 (65, 66). Although, cNHEJ repair does not necessarily result in modification at the break point junction as ligation of compatible DNAs can be directly re-ligated and thus, the break point junction conserved.

A1.5 Alternative nonhomologous end joining

Inhibition of cNHEJ by use of KU- or LIG4-deficient cells revealed end joining activity later referred to as alternative NHEJ (aNHEJ) (67, 68). This activity likely reflects an alternative mode of repair that probably comprises several mechanisms, where one of which includes MMEJ (Figure 1.3). Of these, only MMEJ requires DNA end resection (69, 70). Initially, aNHEJ was first thought to be a backup repair pathway operating only in the absence of cNHEJ; however, recent studies indicate that aNHEJ works even when cNHEJ is functional (37, 38, 71).

Unlike cNHEJ, MMEJ (within aNHEJ) requires limited resection and always results in deletions flanking the original breaks (69). The genes required for MMEJ in mammals and budding yeast include MRE11, RAD50, NBS1 (Xrs2), CTIP (Sae2), and ATM (Tel1), indicating that resection initiation is an essential step. Consistent with the yeast studies, the MRE11 complex/CTIP pathway promotes MMEJ in mammalian cells (37, 39, 72, 73).

The development of chromosomal reporters to measure the repair of DSBs has been advantageous for the identification of DNA repair genes involved in resection-mediated repair. One such assay using the Direct repeat–green fluorescent protein (DR-GFP), measures HR by the ability of the GFP reporter to be repaired subsequent to endonuclease damage. Specifically, DR-GFP is composed of two differentially mutated green fluorescent protein (GFP) genes oriented as direct repeats. The upstream repeat contains the recognition site for the rare-cutting I-SceI endonuclease and the downstream repeat is a 5′ and 3′ truncated GFP fragment. Transient expression of I-SceI leads to a DSB in the upstream GFP gene. HR-mediated repair of the I-SceI-induced DSB results in GFP^+ cells, which are quantified by flow cytometry (74). Thus, this system allows for the monitoring of repair pathways requiring end resection in rodent and human cells such as homology-dependent repair, single-strand annealing, and MMEJ (39, 72, 75-77). However, this system only measures imperfect repair (repair requiring resection) and thus, limits its use. Although, reporter constructs developed in the Jeremy Stark lab have improved detection of NHEJ events by creating a construct whereby the GFP promoter region is separated by a *puro* gene flanked by I-SceI cut sites (39). When I-SceI is expressed, the *puro* gene is excised leaving 3' overhangs, and if repaired by NHEJ, result in restoration of the regulatory region of GFP and thus, expression of GFP (i.e. green cells) (39). Alternatively, NHEJ could fail to restore the I-SceI site, leading to an I-SceI-resistant site. These constructs are advantageous as flow cytometric analysis can sort both GFP^+ and GFP^- populations and the junctional sequences analyzed to infer what type of NHEJ-mediated repair event occurred.

Downregulation of MRE11 via siRNA depletion or molecule inhibition with mirin, resulted in a decrease in MMEJ capacity in *Xrcc4*$^{-/-}$ cells defective in cNHEJ as measured using a plasmid substrate (72). These results indicate that MRE11 is important for MMEJ activity within aNHEJ (or just aNHEJ in general), when cNHEJ is deficient (72). Likewise, using a different reporter specific for MMEJ, inactivation of NBS1 or CTIP decreased MMEJ repair (39, 75). Together,

these data suggest that resection by the CTIP/MRE11 pathway is critical during MMEJ and this likely facilitates MMEJ of DNA DSBs within the aNHEJ pathway.

Several lines of evidence suggest that the cNHEJ nuclease, ARTEMIS, and the aNHEJ nuclease, MRE11, may act in concert during the repair of DNA DSBs. Upon exposure of cells to DSB inducing agents, ARTEMIS undergoes hyperphosphorylation that is dependent on the NBS1 component of the MRE11 complex and the ATM protein kinase (78-80). This hyperphosphorylated form of ARTEMIS physically interacts with the MRE11 complex (79). ARTEMIS is required to repair a subset of modified DNA ends in the context of the cNHEJ pathway during the G1 phase of the cell cycle, and likewise, the MRE11 complex also functions in G1 DSB repair events and has been implicated in cNHEJ repair (72, 77, 81, 82). In addition, recent evidence suggests that ARTEMIS also has significant roles in HR during the G2 phase of the cell cycle (83). However, the functional interactions between ARTEMIS and the MRE11 complex remain unclear. Additionally, the interplay between aNHEJ and cNHEJ is still poorly understood. Therefore, the major goals of my dissertation have been to better understand the molecular and functional interactions that control DNA end processing focusing on ARTEMIS and the MRE11 complex.

A1.6 The MRE11/RAD50/NBS1 complex

The MRE11 complex is a sensor of DSBs that binds DNA ends in a DNA damage-dependent manner and controls the DNA damage response by governing the activation of the central transducing kinase, ATM (15, 84-87). Additionally, the MRE11 complex has multiple roles in the metabolism of DSBs that involve both its enzymatic and structural functions. The 3′–5′ exonuclease and ssDNA endonuclease activities of MRE11 do not depend on RAD50 and NBS1 but are enhanced when complexed with RAD50 and NBS1 (42). Thus, MRE11 possesses intrinsic nuclease activity that is enhanced when MRE11 is a part of the MRE11 complex.

A non-enzymatic, but structural role for MRE11 via its interaction with RAD50 supports a role for the MRE11 complex in bringing together long stretches of DNA, namely during HR. Electron microscopic and atomic force

imaging indicated that DNA-bound heterotetrameric, $MRE11_2RAD50_2$, bridges DNA ends via two arrangements: DNA binding within one $MRE11_2RAD50_2$ DNA-binding head for “short-range” bridging of DNA ends (also MRE11:MRE11 dimers coordinate “short-range” bridging) and via the RAD50 hook domain assembly erects two $(MRE11_2RAD50_2)_2$ scaffolds to tether DNA ends over “long-distances” (88, 89).

During both meiotic and mitotic repair, the MRE11 complex influences DSB repair structurally, by forming various protein complexes (i.e. MRE11:MRE11 dimers—end bridging, the $MRE11_2RAD50_2$ heterotetramer—“short range” DNA end binding, and the $(MRE11_2RAD50_2)_2$ conformation—“long range” DNA end binding/tethering) appropriate for bringing DNA ends together and then to subsequently enzymatically process the ends to promote end resection and resection-mediated repair, such as HR and MMEJ (2, 15, 42, 89).

Another component of the MRE11 complex, NBS1, is important for the regulation of the MRE11 complex, influencing DNA binding, nuclease activity, and the propagation of the DNA damage response via the NBS1 subunit (42). Patient cell cultures with Nijmegen breakage syndrome (NBS, NBS1 hypomorphism) and ataxia-telangiectasia-like disorder (ATLD, MRE11 hypomorphism) exhibit checkpoint defects in S-phase and at the G2/M transition, while the G1/S transition is largely unaffected indicating the MRE11 complex mediates S- and G2/M checkpoint activation. These checkpoint defects are associated with reduced MRE11 complex chromatin association in both human and mouse cells of NBS and ATLD (87, 90-92). Molecular and genetic observations provide support for the role of the MRE11 complex particularly in the S- and G2 phases of the cell cycle (42). The MRE11 complex can also regulate DSB repair, through HR and both c/aNHEJ (42, 72, 77, 82).

Studies have identified a role of the MRE11 complex in both cNHEJ and aNHEJ (72, 77, 82). These studies support a model in which the nuclease activity of MRE11, which is required for the generation of ssDNA during HR, can also favor aNHEJ associated with MMEJ by initiating ssDNA resection. It is thought that the MRE11 complex (with additional nucleases such as EXO1 and CTIP can

initiate resection, which then can be followed by HR or aNHEJ associated with MMEJ, depending on the presence of homologous sequences, cell cycle phase and the size of the resection (72, 77).

The role of the MRE11 complex in cNHEJ is less clear. Most studies that have investigated the contribution of the MRE11 complex to cNHEJ have used plasmid substrates and observed an increase in cNHEJ-mediated events (72, 77). Or, they have observed a decrease in cNHEJ-mediated events when the MRE11 complex is deficient (82). However, few, if any studies, have investigated how the MRE11 complex promotes cNHEJ with other cNHEJ factors. Thus, it is poorly understood how the MRE11 complex promotes cNHEJ alongside critical cNHEJ factors such as KU70/KU80, DNA-PKcs, ARTEMIS, and the ligation complex. One of the studies of my dissertation focuses on better understanding the contribution of the MRE11 complex to cNHEJ-mediated events and provides novel observations that will be the groundwork for future investigations.

A1.7 ARTEMIS is a part of the metallo-β-lactamase/βCASP superfamily of enzymes

ARTEMIS (*DCLRE1C*, DNA crosslink repair 1C, OMIM#605988, but conventionally ARTEMIS is used) was initially identified as the gene mutated in a human T^-B^- severe combined immunodeficiency associated with cellular radiosensitivity (RS-SCID) (93-95). It was later identified that ARTEMIS activity is important for V(D)J recombination, a lymphocyte-specific DNA rearrangement that occurs in both B- and T-cells and is necessary to create antigen receptor multiplicity (93).

The V(D)J recombination/DNA repair factor, ARTEMIS, belongs to the metallo-β-lactamase superfamily of enzymes (Figure 1.4). Three regions comprise the ARTEMIS protein: 1) the β-Lact homology domain, which is adjacent to 2) the β-CASP region (78). The β-CASP region is specific to members of the β-Lact superfamily of enzymes that acts on nucleic acids. The third domain is the COOH-terminal domain (Figure 1.4B) (96, 97). Metallo-β-lactamases are enzymes that were first described in bacteria due to their cleavage of the β-lactam ring of certain antibiotics. Particular sequence motifs

within ARTEMIS designate its catalytic core with sequence motifs mostly comprising histidine and aspartic acids (Figure1.4B). The metallo-β-lactamase and β-CASP motifs are conserved in ARTEMIS and in other nucleases such as SNM1A, SNM1B, PSO2 (Snm1a), (involved in DNA repair) and the RNA cleavage and polyadenylation-specific factor, CPSF (Figure 1.4B) (96, 98). Based on these homologies, the de Villartay group named this new domain the β-CASP domain (98). This domain, which is conserved in all living organisms, is associated with the metallo-β-lactamase domain (97, 98).

When *ARTEMIS* was initially discovered to be the gene mutated in RS-SCID, much of its biological activity was initially inferred from the patient phenotypes (93). Specifically, its role in general DSB and in lymphocyte development, namely during V(D)J recombination. RS-SCID patients possess defects in V(D)J recombination leading to an early arrest of B- and T-cell maturation and defects in general DSB repair resulting in cellular sensitivity to DNA damaging agents (93). Given the potential enzymatic function of its metallo-β-lactamase/β-CASP domain, it was hypothesized that ARTEMIS could be involved in nucleolytic processing of DSB intermediates during V(D)J recombination and in the repair of general cellular DNA damage. The Lieber group demonstrated that ARTEMIS indeed possesses endonucleolytic and exonucleolyic activity. However, the exonucleolytic activity of ARTEMIS is unclear as the Turchi group was able to purify ARTEMIS without exonucleolytic activity and demonstrated that enzymatic activity was likely a contaminant (99). Although the intrinsic nucleolytic activity of ARTEMIS still remains to be further defined, when in complex with DNA-PKcs, ARTEMIS is capable of opening and processing hairpin structures generated by the lymphocyte-specific endonuclease, RAG1/2, as well as endonucleolytically cleaving overhangs (60, 100).

B. Antigen receptor gene diversification

B1.1 V(D)J Recombination

In 1976, Hozumi and Tonegawa reported the first direct evidence for somatic rearrangement of immunoglobulin genes, a process now referred to as V(D)J recombination (101). Seven loci (α, β, γ, and δ for T cell receptors (TCR) and heavy and light chain—κ and λ for immunoglobulins) undergo V(D)J recombination during lymphocyte development. These loci have similar gene rearrangements consisting of variable (V), diversity (D, present only in β, δ, and μ), and joining (J) gene segments that combinatorially recombine to form the diverse exons that encode for the variable regions of antigen receptors expressed on the cellular surface of both T- and B-cells.

During early B-cell development, rearrangement of the heavy chain locus initiates in the bone marrow (Figure 1.5A). Only one gene locus is rearranged at time, in a fixed sequence of events: for B-cells this is the immunoglobulin heavy chain (IgH) locus (102). Productive rearrangements allow the cells to progress to the next stage. Rearrangement of a D gene segment to a J_H gene segment occurs in early pro-B cells, generating late pro-B cells in which V_H to DJ_H rearrangement occurs. A successful V_H-DJ_H rearrangement leads to the expression of a complete immunoglobulin heavy chain as part of the pre-B-cell receptor that stimulates the cell to become a pre-B-cell. Here, the light chain rearranges and upon successful light chain gene assembly, a cell becomes an immature B-cell that expresses a complete IgM molecule composed of the rearranged light and heavy chains (Figure 1.5A) (102). This somatic recombination event generates a variable region that determines antigen recognition and specificity. The constant region is encoded by separate exons located downstream of the variable region many kilobases away.

T-cell lymphoid progenitors are located in the thymus and are designated as double negative (DN) for CD4 and CD8 surface expression (Figure 1.5B). There are various stages to DN thymocyte development that correspond to the rearrangement status of the TCRβ chain (in this instance, rather than the TCRα, TCRγ or TCRδ). DN2 cells begin to rearrange D-Jβ gene segments and progress

to the DN3 stage. DN3 cells are arrested until they productively rearrange Vβ-DJβ gene segments. Then, the in in-frame β chain pairs with a surrogate chain called the pre-T-cell receptor and is expressed on the cell surface triggering entry into the cell cycle. Expression of the surrogate chain signals the cessation of β-chain gene rearrangement and initiates cell proliferation. The cells are then known as DN4 cells where eventually these cells cease to proliferate and CD4 and CD8 are co-expressed on the cell surface. The small $CD4^+CD8^+$ double-positive (DP) cells begin rearrangement at the α-chain locus. The cells then express α:β TCR, CD4 or CD8, and are ready for selection and migration to peripheral lymphoid organs (Figure 1.5B) (102). Similar to B-cell gene rearrangement, productive rearrangements at each stage allow the cells to proceed to the next developmental stage.

Conserved sequence motifs known as recombination signal sequences (RSSs) flank one or both sides of V, D, or J gene segments (Figure 1.5C). The genomic architecture of the RSS is characterized by palindromic heptamer sequences directly adjacent to the coding element and an A/T rich nonamer separated from the heptamer by spacer nucleotides containing nonconserved sequences (103). The heptamer of the recombination signal is critical for precise and efficient targeting of cleavage. In contrast, the nonamer plays an important role in initial sequence specific DNA binding (104). The length of the spacer defines two types of RSSs, either by 12(±1) or 23(±1) nucleotides, with efficient joining requiring one RSS of each type that is reflected in the gene structure of joining partners (Figure 1.5C) (104).

V(D)J recombination is initiated in progenitor lymphocytes by the recombination activating genes 1 and 2 comprising the endonucleolytic RAG1/2 core complex (Figure 1.5C) (103-105). The RAG1/2 complex is quite unique. In most vertebrate animals, RAG1 and RAG2 are located tandemly along the chromosome and are comprised of one large exon each (104). Although similar in their enzymatic properties, the RAG1 and RAG2 proteins do not share sequence identity suggesting that the two proteins have co-evolved to function during V(D)J recombination. It has been proposed that the antigen receptor

genes, and the RAG1 and RAG2 proteins that mediate their rearrangement, may have evolved from an ancestral transposon (106, 107). The presence of RSSs facing in opposite directions is similar to the inverted repeat architecture of many transposon ends, thus, the RAG1/2 proteins could have originated from genes encoded by a transposon. If so, perhaps, after the initial invasion, such a transposon must have lost its ability to reintegrate after excision.

Initial DNA recognition occurs by RAG1 via the nonamer sequence and the RAG1 complex is stabilized to an RSS via RAG2 binding to the heptamer sequence using the 12/23 rule whereby coupled cleavage combines a RSS with a 12(±) nucleotide spacer and a 23(±) nucleotide spacer (104). The RAG1/2 complex initiates V(D)J recombination by nicking DNA ends located at the RSSs adjacent to numerous V, D and J coding exons (Figure 1.5C) (108, 109). At each RSS, a nick is first introduced on one strand using water as the nucleophile to generate a 3′-hydroxyl group and a 5′-phosphate. The 3′-hydroxyl then attacks a phosphodiester bond on the other strand in a trans-esterification reaction. This process of hydrolysis (nicking) followed by strand transfer yields two dissimilar ends: a blunt end that terminates in the heptamer of the RSS (referred to as the signal end) and a covalently sealed “hairpin” end that terminates in the last residues of the V, D, or J coding segment (and hence is referred to as a coding end) (109). The two step trans-esterification reaction for the RAG1/2-mediated DNA cleavage, the ability of alcohols to serve as the nucleophile in the nicking reaction, and the ability of the RAG1/2 complex to reverse the hairpin formation step by using the 3′-hydroxyl of the signal end to attack a hairpin coding end, all strongly resembled aspects of DNA cleavage and joining by transposases and retroviral integrases (107). This mechanistic convergence of V(D)J recombination and transposition was supported with the discovery that the RAG1/2 complex is capable of performing transposition of pairs of signal ends in vitro (107).

The RAG1/2 complex generates four broken DNA ends in a post cleavage complex (PCC) that facilitates DNA repair pathway-choice control (110-113). The resultant DNA DSBs within the PCC contain two distinct end structures, blunt, 5' phosphorylated recombination signal (RS) ends and covalently closed, hairpin

coding ends (Figure 1.5C) (114). One model posits that the PCC forms a scaffold, retaining broken DNA ends to facilitate proper repair by cNHEJ and discourage repair by HR and aNHEJ (113, 115, 116).

The broken ends are then processed and joined by the ubiquitously expressed cNHEJ DNA repair factors, including KU70, KU80, DNA-PKcs, ARTEMIS, DNA LIG4, XRCC4 and XLF (117). The blunt RS ends are precisely ligated without further processing; however, nucleotide additions and deletions can occur at a subset of ends (118-120). The hairpin coding ends are nicked by the ARTEMIS:DNA-PKcs complex and cleavage at positions located away from the apex can result in addition of palindromic, "P", nucleotides within the junctions (60). In addition, non-templated, "N", nucleotides can be added by the pol X family, lymphoid-specific DNA polymerase, terminal deoxynucleotidyl transferase (TdT), and nucleotides can also be deleted (121, 122). DNA polymerase mu (pol μ), a close homolog of TdT that displays template-dependent polymerase activity, participates in the end processing of the immunoglobulin light chain, but not of heavy chain junctions (123). Rather, DNA polymerase lamda (pol λ), another close homolog to TdT that belongs to the pol X family and possesses template-dependent polymerase activity, participates in the end processing of the immunoglobulin heavy chain, likely before TdT (124).

V(D)J recombination is regulated in part, by cell cycle regulation of RAG2. The RAG2 C-terminus is phosphorylated by CDK to shuttle it for degradation during the G1 to S cell transition (125). RAG enzymatic activity is significantly diminished with only the enzymatic activity of RAG1 remaining (126). In vitro studies have shown that RAG1 and RAG2 co-expression increases V(D)J recombination 1000-fold indicating that the in vivo RAG1 and RAG2 complex act together as the core RAG1/2 complex to initiate V(D)J recombination (104, 126).

B1.2 Hairpin coding end processing by the ARTEMIS endonuclease

Biochemical studies indicate that ARTEMIS possesses intrinsic robust 5' to 3' single strand exonucleolytic activity and is activated as an endonuclease upon interaction with DNA-PKcs (60). However, a recent paper by the Turchi group found that a purified product of ARTEMIS lacked the exonucleolytic

activity, yet, maintained its endonucleolytic activities when bound with DNA-PKcs putting into question the exonucleolytic activities of ARTEMIS (99). In contrast, the Lieber group recently identified that the exonucleolytic activity of ARTEMIS was intrinsic and that it is not dependent upon interaction with DNA-PKcs (127). The intrinsic exonuclease activities of ARTEMIS remain to be fully elucidated. Nonetheless, it is clear that ARTEMIS possesses robust endonucleolytic activity on 5' and 3' overhangs, hairpins, loops, and flaps (100, 128). The ARTEMIS:DNA-PKcs complex is likely the active form of the nuclease that functions during V(D)J recombination and general DNA DSB repair (60). The ARTEMIS C-terminal domain interacts with and is phosphorylated by DNA-PKcs; however, the functional importance of ARTEMIS phosphorylation in vivo is not clear (78, 128, 129). In this regard, although first proposed to be required for regulation of intrinsic nuclease activities, biochemical and cellular studies of mutant ARTEMIS proteins have provided evidence that phosphorylation by DNA-PKcs is not necessary for activation of endonucleolytic activities (32, 130, 131). In addition, in vitro cellular assays examining the V(D)J recombination and DNA repair activities of exogenously expressed C-terminally truncated ARTEMIS proteins that lack DNA-PKcs phosphorylation sites, or mutant forms that cannot bind DNA-PKcs, have suggested that DNA-PKcs-dependent phosphorylation of the ARTEMIS C-terminus is dispensable for complete activation (78). Thus, although the DNA-PKcs interaction is clearly required for activation of ARTEMIS endonucleolytic activity, the mechanism by which this occurs is not well understood and thus, was a focus of my dissertation in chapter 2.

B1.3 Defective V(D)J recombination and human disease

There are approximately 150 inherited primary immunodeficiency diseases, and the genetic defects underlying these diseases have been identified in more than 100 disorders (132). Mutations in nearly all of the known genes that play central roles in V(D)J recombination have been identified in human combined immunodeficiency patients, including *RAG1, RAG2, PRKDC (DNA-PKcs), LIG4, XLF,* and *DCLRE1C (ARTEMIS)* (Figure1.6A) and result in T^-B^- SCID (81, 93, 98, 130, 133-135) associated with radiosensitivity.

In addition, defective V(D)J recombination can lead to chromosomal translocations that juxtapose loci that undergo V(D)J rearrangements and cellular oncogenes are associated with human lymphoid malignancies (136, 137). One mechanism that results in oncogenic chromosomal rearrangements is misrepair of RAG1/2 generated DSBs (109, 138). In normal cells, the cNHEJ pathway ensures that DSBs are properly repaired; however, checkpoint failure and defects in processing and joining broken ends can render them available for repair by alternative pathways (Figure 1.6B) (115, 138). Mutations in cNHEJ genes can alter the fate of the DSBs and lead to chromosomal instability, including oncogenic translocations. Indeed, hypomorphic mutations in *LIG4* and *ARTEMIS* have been found in human patients with lymphoid malignancies (Figure 1.6A) (81) (98). In addition, mouse models harboring inactivating mutations in *Ku70, Ku80, DNA-PKcs* (*Prkdc*, convention is to annotate as *DNA-Pkcs*), *Xrcc4, Lig4* and *Artemis* in the context of p53 mutation are predisposed to early onset pro-B lymphoma associated with oncogenic chromosomal translocations involving the IgH locus (Figure 1.6) (139-147). Thus, the cNHEJ factors play critical roles in suppressing tumorigenesis.

The mechanisms of oncogenic translocation formation resulting from aberrant V(D)J recombination are not well understood. Chromosomal translocations associated with spontaneous human lymphoid malignancies are mediated by short regions of sequence homology (microhomology) at the breakpoint junction. Moreover, translocation breakpoints in the lymphomas arising in *cNHEJ/p53* double null mice contain microhomologies. The hallmark features of this error prone pathway, MMEJ, are deletions of flanking sequence and short homologies of 1 to 25 bases at the junctions that serve to align the DNA ends prior to joining. In addition to its apparent importance in the etiology of human cancers, MMEJ also appears to play a significant role in therapy-induced oncogenic chromosomal translocations.

B1.4 Recombination activating genes 1 and 2 (Rag1/2) and immunodeficiency

Null mutations of *RAG1/RAG2* are associated with SCID as no productive rearrangements at either the T- or B-cell receptor rearranging loci can be detected in patients. In contrast *RAG1/RAG2* mutations that result in hypomorphic alleles are associated with less severe immunodeficiency disorders such as Omenn Syndrome and leaky SCID that produces an oligoclonal population of circulating lymphocytes (Figure 1.7) (148).

Heterozygous and homozygous mutations in *RAG1/RAG2* associated with immunodeficiency disorders impact various domains of the proteins. Although not essential for catalytic activity, the N-terminus of RAG1 consists of a basic region, a nuclear localization signal, a recombination signal sequence recognition domain and a dimerization domain defined by a C2H2 Zinc finger and a C3HC4 zinc binding motif described as a RING motif associated with E3 ligases. RAG1 missense mutations in the nuclear localization domain impair recombination signal sequence recognition and cleavage (149, 150). Omenn Syndrome patients have been found to bear missense mutations in the *RAG1* nuclear localization domain, thus strengthening the importance of this region, spanning only 4% of the molecule (151). Omenn Syndrome was first described in 1965 and is characterized by early-onset generalized erythroderma, failure to thrive, protracted diarrhea, hepatosplenomegaly, and lymphadenopathy and is inherited in an autosomal recessive manner associated with autoimmunity (152).

The C-terminus of RAG1 contains the enzymatic activity for both nicking and hairpin formation in addition to sites for RAG2 protein interaction. Homozygous or compound heterozygous mutations in the region of RAG1 mediating interaction with RAG2 can result in decreased RAG1/RAG2 interaction and hence in reduced recombinational activity on extrachromosomal substrates while mutations in the catalytic domain, give rise to proteins highly inefficient in DNA nicking (149, 150).

RAG2 largely consists of an N-terminal β-propeller structure, which comprises the catalytic core. The C-terminus of RAG2 includes a plant

homeodomain (PHD). The stretch of amino acids falling between the core and the PHD-like region has been defined as the ‘‘hinge’’ or linker, holding the two structural domains together. The biological importance of the β-propeller structure and PHD fingers is demonstrated by the fact that heterozygous or homozygous mutations in these domains are reported to be responsible for diseases such as Omenn Syndrome and SCID in humans. Those mutations that are associated with functional null *RAG1/RAG2* mutations cluster within the RAG2 or RAG1 binding domain as well as the heptamer binding domain (RAG1) suggesting this region is essential to enzymatic activity at RSSs. Mutations that are associated with less severe immunodeficiency disorders such as Omenn syndrome, cluster mostly within the nonamer binding and the C-terminus (RAG1) and within the acidic hinge (RAG2) suggesting these regions are not essential for full enzymatic activity of the RAG1/2 complex.

B1.5 Mouse models of RAG1/RAG2

David Schatz and Margi Oettinger were the first to demonstrate the dependence of the RAG1/2 endonuclease to lymphoid development (105). The crucial role played by RAG1 and RAG2 in lymphoid cell development was demonstrated in vivo by results of gene targeting in mouse (153, 154). In fact *Rag1*$^{-/-}$ and *Rag2*$^{-/-}$ mice share an identical phenotype, with a severe and early block in differentiation of both T- (at the triple negative [$CD3^{-}CD4^{-}CD8^{-}$]$CD25^{+}$ stage) and B-cells (at the $B220^{lo}CD43^{+}$ IgM^{-}, pro-B stage), at the stage of development when V(D)J rearrangements are initiated (153, 154). In 1996, The Bartram lab showed that a portion of patients with a clinical picture of SCID with natural killer cells but no B and T lymphocytes (6 out of 14 cases analyzed) bear mutations in either RAG1 or RAG2 genes (155). All the mutations identified (missense, nonsense, deletion) proved to be devoid of recombinational activity (0.1–1.0% of wild-type), when assayed in transient transfection experiments with artificial extrachromosomal rearrangement substrates. The few signal and coding-joints that were detected appeared qualitatively normal, indicating that the RAG1/2-generated DSBs are repaired via the mechanisms of DSB repair and are unaffected in RAG1/2-deficient subjects (155).

Hypomorphic *Rag1* or *Rag2* murine mutations recapitulate Omenn syndrome and in one case in particular, predisposed to tumorigenesis (156) (157). The RAG1-S723C mouse is the only animal model currently available to investigate the contribution of hypomorphic *Rag* mutations to Omenn Syndrome and established that hypomorphic *rag* mutations in mice and humans are associated with autoantibody production (158). The RAG1-S723C knock-in mouse model exhibited impaired lymphocyte development and decreased V(D)J rearrangements; however, distinct from RAG nullizygosity, the RAG1-S723C hypomorph resulted in aberrant DNA breaks within rearranging loci that ultimately predisposed the mice to thymic lymphoma in a p53 deficient background (156, 159). RAG1/2 mutations had previously been identified in human tumors and this study provided in vivo evidence for the role of the RAG1/2 complex not only in lymphocyte development but also in suppressing tumorigenesis.

B1.6 DNA-PK deficiency in man and mice

The KU heterodimer, consisting of KU70 and KU80, can associate with DNA-PKcs to form the DNA-PK holoenzyme in turn activating the kinase activities of DNA-PKcs (57, 58). The ubiquitously expressed cNHEJ factor, KU70/KU80, serves as a sensor of DSBs during cNHEJ in the context of DNA DSB repair, including that incorporated into the V(D)J recombination reaction in developing lymphocytes.

Based on its intrinsic activities, KU may have a specific role in DNA end processing (160). On the other hand, KU may function primarily by recruiting and activating DNA-PKcs to form a synaptic complex (involving KU, DNA-PKcs, and DNA ends) that then recruits other factors involved in the reaction (161, 162). However, the differential effects of KU80 deficiency and the DNA-PKcs mutation on recombination signal joining during V(D)J recombination suggest the possibility of unique functions for the two molecules. In this regard, KU80-deficient mice have a phenotype that is distinctly different from that of *DNA-PKcs*$^{-/-}$ mice. Both deficiencies lead to severe combined immune deficiency (SCID). However, mice harboring a missense mutation in the C-terminus of DNA-PKcs

that results truncation of the C-terminus known as SCID (*DNA-PKcs*$^{Scid/Scid}$) mice are “leaky,” with some mature lymphocytes accumulating in older mice, whereas KU80-deficient mice (*Ku80*$^{-/-}$ mice) have thus far been found to be non-leaky, with B- and T- cell development arrested at an early progenitor stage (161, 163-165). Furthermore, *Ku80*$^{-/-}$ mice, unlike SCID mice, are smaller than their wild type or heterozygous littermates, and their cells show early senescence, suggesting a link between KU80 and growth control (164). The reason for the phenotypic differences between *DNA-PKcs*$^{Scid/Scid}$ and KU80-deficient mice is unknown. It may be that KU80 has functions distinct from its role as a DNA-binding subunit for DNA-PKcs or that the *DNA-PKcs*$^{Scid/Scid}$ murine mutation and the *DNA-PKcs*$^{Scid/Scid}$ chinese hamster cell line mutation, V-3, does not totally inactivate all DNA-PKcs functions (161) (166). Although *DNA-PKcs*$^{-/-}$ mice are severely impaired at the progenitor B- and T- cell stages of lymphocyte development, *DNA-PKcs*$^{-/-}$ mice largely recapitulate the SCID mouse phenotype except for the lymphocyte “leakiness” suggesting residual DNA-PKcs activity of the SCID mutation (147, 167-169). However, *Ku70*$^{-/-}$ mice are similarly small like their *Ku80*$^{-/-}$ counterparts and are characterized with defects in the joining phase of V(D)J recombination (170). Interestingly, although the *DNA-PKcs*$^{Scid/Scid}$ and the *Ku80*$^{-/-}$ mouse have some non-overlapping phenotypes, *Ku70*$^{-/-}$ mice have similar “leaky” lymphocyte development as *DNA-PKcs*$^{Scid/Scid}$ mice (164, 165, 170). Regardless of the overlapping and/or non-overlapping roles of these factors in cNHEJ during V(D)J recombination, it is clear from the animal studies the importance of these factors to process broken DNA end intermediates during V(D)J recombination.

There has yet to be patients identified with *KU70/KU80* mutations, but there have been patients with DNA-PKcs mutations reported (Figure 1.6A). The first human mutation in the gene encoding DNA-PKcs (*PRKDC*) was identified by the van Gent group in 2009 (171). The patient presented with radiosensitivity and few circulating T- and B-cells. As DNA-PKcs is not only important for the repair of RAG1/2-generated DSBs during lymphocyte development but also general DSBs that occur during normal cellular process, the patient also presented with

radiosensitivity to DNA damaging agents. Although SCID consists of a heterogeneous group of diseases, it is immunologically characterized by the absence or dysfunctioning of lymphocytes. Patients who are diagnosed with RS-SCID are additionally sensitive to DNA damaging agents (93), therefore, the patient was diagnosed with RS-SCID (171). The hypomorphic missense mutation (L3062R) did not result in decreased protein expression or reduced (auto)phosphorylation. Rather the mutation was shown to have defects in recruiting downstream effector proteins necessary for appropriate DNA repair (171). Recently a compound heterozygous patient was identified by the Jeggo group with *PRKDC* mutations (allele 1, splice site mutation resulting in skipping of exon 16, and allele 2, A3574V) where one allele resulted in an inactivating allele (A3574V, mutation in a well-conserved FAT domain), and the other severely reduced DNA-PKcs activity (Δ exon 16). Strikingly, this patient was marked with severe neurological abnormalities such as microcephaly-associated cortical and hippocampal dysplasia and seizures (172). Although loss of DNA-PKcs in mice, dogs, and horses was previously shown not to impair neuronal development, the findings from the Jeggo lab implicate a stringent requirement for DNA-PKcs during human neuronal development and suggest that high DNA-PK protein expression is required to sustain efficient pre- and postnatal neurogenesis (147, 172-174). This is quite interesting as it suggests roles for cNHEJ during neuronal development, which is not unfounded as other cNHEJ genes have been implicated during this process such as KU70/KU80, LIG4 and XRCC4 (175, 176).

B1.7 ARTEMIS mutations and immunodeficiency syndromes

DCLRE1C (*ARTEMIS*) mutation is associated with human immunodeficiency disorders and was initially discovered as the gene mutated in human RS-SCID (93, 94, 177). The majority of ARTEMIS mutations that cause RS-SCID are located within a highly conserved, metallo-β-lactamase/β-CASP catalytic domain (residues 1-385 of 692 aa) that distinguishes this family of proteins (Figure 1.8) (94). These mutations include genomic exon deletions, nucleotide deletions, nonsense and missence mutations and are presumed to

inactivate protein function. Inherited hypomorphic *ARTEMIS* alleles have also been identified in patients and cause combined immunodeficiency syndromes of varying severity, including Omenn syndrome (Figure 1.8) (133, 178, 179). One particularly interesting subset of inherited hypomorphic *ARTEMIS* alleles results in premature translation termination and is associated with partial immunodeficiency and lymphoma (Figure 1.8) (178). The patients harboring these mutations are predisposed to mature B lymphomas characterized by chromosomal aberrations, including translocations (178). The ARTEMIS C-terminal domain interacts with and is phosphorylated by DNA-PKcs; however, the functional importance of the ARTEMIS C-terminus during V(D)J recombination is not clear (78, 100, 129). Investigating the association between lymphoma and the hypomorphic *ARTEMIS* alleles that delete the C-terminus was a major focus of my thesis (Chapter 2) and my studies provided the first evidence that the ARTEMIS C-terminus suppresses tumorigenesis.

The Alt lab used gene targeting to disrupt the murine *Artemis* locus in a fashion analogous to a mutation found in human RS-SCID patients to elucidate the potential functions of ARTEMIS in V(D)J recombination and general DSB repair (93). *Artemis*$^{-/-}$ mice recapitulated the ARTEMIS inactivating patient phenotype and *DNA-PKcs*$^{-/-}$ mice, including normal size and cellular proliferation, severe combined immunodeficiency, a specific defect in V(D)J coding, and increased cellular sensitivity to ionizing radiation. Moreover, impaired T-cell development is associated with the accumulation of unresolved hairpin intermediates in *Artemis*$^{-/-}$ thymocytes, strongly supporting the ARTEMIS functions in processing hairpin coding ends. Interestingly, similar to *DNA-PKcs*$^{Scid/Scid}$ and *Ku70*$^{-/-}$ mice, a significant subset of young *Artemis*$^{-/-}$ mice showed “leaky” lymphocyte development (163, 170, 180). Like *DNA-PKcs*$^{Scid/Scid}$ or KU70-deficient mice, it is likely that the leakiness of *Artemis*$^{-/-}$ lymphocytes results from a low but significant level of productive V(D)J rearrangements suggesting the involvement of a nuclease other than ARTEMIS than can open hairpin coding ends.

Another mouse model of ARTEMIS deficiency sought to address the role of the ARTEMIS C-terminus in lymphocyte development and tumor suppression. *ARTEMIS* hypomorphic mutations that result in the deletion of the ARTEMIS C-terminus present with partial immunodeficiency and predisposition to lymphoma. This phenotype is quite distinct from the ARTEMIS inactivating patient mutations that completely block lymphocyte development, yet are not tumor prone. Prior to my dissertation work, the mechanistic basis for the distinct disease outcomes resulting from specific *ARTEMIS* mutations was not well understood. Furthermore, the regulation of ARTEMIS in vivo functions had not yet been fully elucidated. Together, my dissertation work in chapter 2 provided insight into the mechanisms that maintain genome stability and prevent the formation of lymphoma-associated chromosomal translocations associated with ARTEMIS mutations that diminish, but do not severely abrogate lymphocyte development.

B1.8 The ligation complex and immunodeficiency

The cNHEJ ligation complex consists of LIG4, XRCC4, and XLF. The ligation complex is an essential part of cNHEJ during V(D)J recombination as deficiency in any component of the complex results in immunodeficiency syndromes of varying severity in patients and animal models (81, 134, 140, 181-185). The ligation complex, specifically LIG4 and XRCC4 interact with DNA-PK and ARTEMIS in a complex containing XLF to facilitate ligation and repair of broken DNA ends (186). This close physical connection between the cNHEJ factors during V(D)J recombination results in dynamic and rapid repair of RAG1/2-induced DSBs.

XRCC4 deficiency in cells results in proliferation defects, DSB repair defects, and inability to support either the coding or RSS end-joining processes required to complete the V(D)J recombination reaction (176). These defects are quite similar to those observed with KU- and LIG4–deficient cells and likely result from impairment of an end-joining reaction that employs all of these proteins. However, XRCC4, in contrast to KU, is required for normal embryonic development, with XRCC4-deficient and LIG4-deficient embryos dying over a relatively broad period in late gestation (176). Analyses of the mutant embryos

revealed defects only in lymphocyte and neuronal development; massive apoptotic cell death of newly generated, post mitotic neurons was the only potential cause of death identified. Strikingly, LIG4 deficiency results in similar neuronal developmental defects. Therefore, this neuronal death phenotype almost certainly results from the absence of a shared XRCC4 and LIG4 function.

Among the patients with cNHEJ deficiencies, 16 cases with mutations in *LIG4* have been described to date with phenotypes varying from malignancy in developmentally normal individuals, to severe combined immunodeficiency early mortality, and developmental delay (Figure 1.6a, Figure 1.9) (184). Most patients developed thrombocytopenia and leucopenia later in childhood and were found to have previously unrecognized immunodeficiency following molecular diagnosis (184). Genotype-phenotype correlations can be ascribed to the position of truncating mutations corresponding to disease severity. For example, mutations associated with severe abrogation of LIG4 activity (located within the catalytic region of the protein—N-terminus) can result in SCID whereas other mutations (that disrupt the XRCC4/LIG4 interacting domain—C-terminus) can predispose to lymphoma (81, 187, 188). As of yet, there have not been XRCC4 patients identified (Figure 1.6a), but given the close interaction between LIG4 and XRCC4, any XRCC4-deficient patients could share many of the LIG4-deficient phenotypes.

The involvement of a third protein in the DNA LIG4 complex was first suggested by discovery of the yeast cNHEJ protein Nej1p (XLF) and the observation that it interacts with yeast Lif1p (XRCC4) (189-193). The inability of standard computational approaches to reveal apparent Nej1p (XLF homologues outside of budding yeasts, led to the idea that Nej1p was not a universally conserved cNHEJ protein. However, it was recently discovered that people with a form of V(D)J recombination/cNHEJ deficiency lack the protein XLF (also called Cernunnos) (Figure 1.6) (63, 134). XLF/CERNUNNOS was identified when a radiosensitive SCID condition (patient 2BN) without mutation in any of the known cNHEJ genes was identified (134). Various DNA repair assays detected in-check cell cycle checkpoints and DNA damage response post clastogen exposure.

Plasmid substrates transfected into patient fibroblasts revealed reduced V(D)J recombination indicating a defect in cNHEJ. Notably, the V(D)J deficiency observed in XLF-deficient patients was less severe than what was observed in RS-SCID patients with ARTEMIS mutations. Strikingly, the clinical phenotype of XLF-deficient patients shares several characteristics with Nijmegen breakage syndrome (NBS) and LIG4 deficiency such as combined immunodeficiency, microcephaly, growth retardation, and sensitivity to ionizing radiation (134, 188, 194). However, XLF deficiency does not lead to impaired cell-cycle checkpoints, as observed in NBS, a genome instability condition, but leads rather to a cNHEJ defect as observed in LIG4 deficiency, albeit less severe (87, 188).

Like Nej1p, XLF interacts directly with XRCC4 and is required for cNHEJ. Indeed, detailed computational analyses aided by this information and new genome sequences verified that Nej1p and XLF are ancestrally related, despite their low primary sequence conservation (195-197). Even more strikingly, these computational approaches indicated that XLF, and by inference Nej1p, are distantly related to XRCC4 (in yeast, Lif1p), and that these genes likely arose by an ancestral duplication (63, 196). The collected results from the literature support a model in both budding yeast and humans in which LIG4 (in yeast, Dnl4p) is predominantly bound to XRCC4 (in yeast, Lif1p), with XLF (in yeast, Nej1p) providing a further supporting role via direct contacts to both LIG4 and XRCC4. However, observable differences in these interactions between species, the relatedness of XRCC4 and XLF, and the weak and non-uniform conservation of these proteins all suggest a substantial flexibility in their use during cNHEJ (198).

B1.9 Ataxia-telangiectasia (AT) and human disease

Ataxia-telangiectasia (AT) is caused by mutations in the *ATM* gene and is inherited in a homozygously recessive manner (194). It is characterized by cerebellar ataxia and other developmental defects such as immunodeficiency that typically results in low immunoglobulin IgA, low IgG2, and lymphopenia, especially of the naive CD4 cells, and radiosensitivity. Approximately one-third of AT patients develop malignancies, with lymphomas and leukemias of T-cell origin

being predominant (Figure 1.9) (194). B-cell neoplasias are less common. The T-cell receptor loci, at chromosomes 7p14, 7q34, and 14q11, are often abnormally rearranged in a high proportion of T-cells from AT individuals, even before the onset of malignancy (194). The high incidence of T cell cancers and frequent involvement of the TCR loci in chromosomal rearrangements suggests that the tumorigenic trigger in AT is provided by impaired V(D)J recombination. Murine models of AT largely recapitulate the patient phenotype and present with defects in lymphocyte development such as a reduction in the number of mature naïve CD4 and CD8 T-cells, cell cycle checkpoint defects, and cancer predisposition (199). It is puzzling that the cerebellar defects are not recapitulated in mouse models of AT (199).

C. Mouse models of the MRE11 complex and human disease

Null mutations of *Mre11*, *Rad50*, and *Nbs1* are not viable in mouse models and presently no patient has been identified harboring null alleles. Therefore, this has necessitated the use of conditional murine alleles and hypomorphic alleles.

C1.1 Nijmegen breakage syndrome (NBS)

The Nijmegen breakage syndrome (NBS) was first described in two brothers with microcephaly, mental retardation, facial erythema, café-au-lait spots, IgA deficiency, and chromosomal instability (200). Molecular analysis of the mutation identified hypomorphic mutations in the *NBN* (*Nbs1*) gene inherited in a homozygously recessive manner (200). NBS patients are characterized by lymphopenia of B- and T-cells, short stature, ‘bird-like’ features, and have an increased risk for development of non-Hodgkins lymphomas with the majority being of B-cell origin (Figure 1.9) (201). Although each disease also has unique features (AT results in cerebellar ataxia and telangiectasia which is absent in NBS), NBS patients’ phenotypes overlap with those of patients with mutations in *ATM* such as increased sensitivity to DNA damaging agents, predisposition to malignancy harboring clonal translocations with rearranging loci (ch. 7 and ch. 14), and mental impairment (194). The overlapping phenotypes suggest a

functional relationship between the ATM protein and the NBS1 protein (42, 194, 201). Indeed, ATM phosphorylates NBS1 in response to damage, and this has been proposed to be a prerequisite for checkpoint activation by the MRE11 complex (42).

Hypomorphic mouse models of NBS interestingly are unique and do not completely recapitulate the ATM signaling defects observed in cells (Figure 1.10) (42). However, conditional and hypomorphic mutations (that truncate either the N- or C-terminus of NBS1) of NBS demonstrate defects in the cell cycle (S/G2), sensitivity to DNA damaging agents, chromosomal sensitivity, and defects in class switch recombination (CSR), a lymphocyte-specific DNA rearrangement (Figure 1.10) (42).

C1.2 RAD50 and human disease (NBS-like disorder)

Until recently, no human patient had been identified that harbored mutant alleles of *RAD50* so much of the biological understanding of the RAD50 protein came from model organisms. However, in 2009, an individual previously diagnosed with NBS due to short stature, 'bird-like' features, and microcephaly was identified to be compound heterozygous for *RAD50* (maternal allele: R1093X, suggested to be functionally null; paternal allele: A3939T, larger, unstable protein probably a hypomorph) (202). The lack of cancer predisposition in this individual spurred additional molecular characterization and resulted in identification of the RAD50-associated NBS-like disorder (NBSLD).

Conditional knock-out mice of *Rad50* largely present with an increase in genomic instability resulting in precipitous death of cultured cells, decrease in proliferation, and increase in DNA damage (Figure 1.10) (42). Other RAD50 murine mutations contain phenotypes ranging from embryonic lethality ($Rad50^{S}$, $Rad50^{\Delta}$), bone marrow failure, and cancer predisposition to chromosomal instability (*Rad50* conditional allele) (Figure1.10) (42).

C1.3 MRE11 and human genome instability disorders

As deficiency in ATM results in cerebellar ataxia, increased DNA damage, chromosomal radiosensitivity in lymphocytes and cancer predisposition (among

other phenotypes), another disorder similar to AT, is caused by hypomorphic mutations in MRE11 and is aptly named ataxia-telangiectasia like disorder (ATLD) (90). The clinical features of patients with ATLD are very similar to those of AT. The clearest similarity being with the progressive cerebellar ataxia that the ATLD patients show. In contrast to AT, ATLD patients show no telangiectasia nor immunodeficiency or cancer (203, 204). Compared with AT, ATLD is characterized by a later onset of the neurological features, and slower progression of the disorder to give the overall appearance of a milder condition than AT in the early years (205). ATLD patients also show normal levels of total immunoglobulins such as IgG, IgA and IgM although there may be reduced levels of specific functional antibodies (205). Since MRE11 is a component of a protein complex with NBS1 and RAD50, it is perhaps surprising that a deficiency in MRE11 gives rise to an AT-like disorder rather than a more NBS-like disorder (206, 207). Nonetheless, the patient phenotypes highlight the importance of MRE11 in DSB repair, as the patient clinical findings are associated with developmental defects that rely on rapid cellular proliferation and the repair of DNA breaks. Mouse models of different ATLD mutations recapitulate patient molecular findings including checkpoint defects, chromosomal defects, DNA damage sensitivity, and lack of malignancy (Figure 1.10) (42, 91).

The MRE11 component of the MRE11 complex possesses intrinsic nuclease activity whereby MRE11 is an endonuclease and also a 3'-5' exonuclease (208). Additionally, the nuclease domain of MRE11 is highly conserved suggesting the nuclease activities of MRE11 are essential (89). Early studies in yeast identified that the nuclease activities of MRE11 are essential to DNA repair (209). The Ferguson lab corroborated the yeast findings and observed that the mammalian MRE11 nuclease activities are essential to DNA repair as well as in checkpoint activation (15). In its homozygous state, both the *Mre11* null allele and the nuclease dead allele of *Mre11*, $Mre11^{H129N}$, resulted in embryonic lethality indicating essential roles for the MRE11 complex and the nuclease activities of MRE11 during development (15). Interestingly, even though the $Mre11^{H129N}$ allele is molecularly distinct from the *Mre11* null allele, the

Mre11^{H129N} allele shares similar DNA repair phenotypes such as rapid cellular senescence, cellular sensitivity to DNA damaging agents, increase in chromosomal aberrations, and HR deficiency (Figure 1.10) (15). However, uniquely, the *Mre11*^{H129N} allele is able to activate ATM while the *Mre11* null allele destabilizes the MRE11 complex resulting in loss of both RAD50 and NBS1 cellularly resulting in loss of ATM activation (15).

C1.4 The MRE11 complex and lymphocyte development

Conditional NBS1 or MRE11 deletion in B lymphocytes results in defects in class switch recombination (CSR), a lymphocyte-specific rearrangement that occurs in B-cells, raising the possibility that MRE11 or the MRE11 complex has a role in CSR (Figure 1.10) (82, 210). The nuclease-deficient *Mre11*^{H129N} allele also resulted in deficient CSR, and it has been suggested that defects in resection may underlie this phenotype (82). It has been observed that mice expressing the *Nbs1*$^{\Delta B}$ and *Mre11*^{ATLD1} alleles, hypomorphic C-terminal truncations with substantial defects in MRE11 complex formation and function, showed an increase in aberrant joining such as trans-rearrangements caused by abnormal V(D)J recombination (91, 92) Additionally, increased levels of unrepaired DNA were detected in these and similar animal models, suggesting a subtler defect in the fidelity of end joining (Figure 1.10) (91, 211). Taken together, the data suggest a role for the MRE11 complex in the repair of lymphocyte-specific DSBs that occur during developmental programs like V(D)J recombination and CSR.

The MRE11 complex also functions in an end-joining pathway denoted as aNHEJ (71, 72, 77, 82). *DNA-PKcs*$^{scid/scid}$*Nbs1*$^{\Delta B/\Delta B}$ mice are nearly inviable, but a limited number of double-mutant mice and cells have allowed the role of the MRE11 complex in cells lacking a primary component of cNHEJ to be investigated. Using a hyperactive RAG1/2 protein to initiate DNA breaks, it was demonstrated that an aNHEJ pathway could be activated in cells lacking DNA-PKcs (113). This system revealed that the MRE11 complex could facilitate aNHEJ-mediated joining of V(D)J substrates (71, 113). This study provided evidence for the role of the MRE11 complex in facilitating RAG1/2 DNA DSBs during V(D)J using aNHEJ. This finding is somewhat confusing as studies have

also cited a role for the MRE11 complex in facilitating cNHEJ to repair DNA DSB intermediates that occur during lymphocyte development during CSR (82), therefore, it is unclear how the MRE11 complex directly promotes end joining in both the cNHEJ and aNHEJ pathways during V(D)J recombination and thus, is a major focus of my dissertation, specifically in Chapter 4.

The MRE11 complex clearly plays a key role in DNA DSB repair processes that also involve the activities of the cNHEJ factors, including ARTEMIS; however, the interplay between these critical repair activities is not well understood and represents a focus of this thesis.

C1.5 Using the mouse model as a model organism to study V(D)J recombination and disease

The mouse is a highly relevant model system to better understand lymphocyte development and furthermore serves as an excellent model of various maladies associated with V(D)J recombination. The high relative sequence conservation of nonhomologous end joining genes between humans and mouse makes this organism appealing in a genetic context. The existence of inbred mouse strains with isogenic backgrounds is a strong advantage of using the mouse as a model system. In addition, the ability to rear mice in defined conditions permits control of potential environmental components that may impact V(D)J recombination.

The lack of large cohorts of individuals with V(D)J defects hampers large-scale studies to evaluate the causality of V(D)J mutations associated with primary immunodeficiencies. Therefore, molecular immunologists have relied heavily on the use of engineered mouse models with customizable alleles (i.e. deletions, knock-in of orthologous human mutations, and temporally or spatially conditional mutations), which I take full advantage of in the studies of my dissertation. These engineered mouse models that I used for my studies were integral to the novel studies within my dissertation.

D. Summary

Factors critical in the repair of DNA DSBs are important in preventing accumulation of unwanted mutations and also immune system development evidenced by patient mutations that predispose to tumorigenesis and immunodeficiency disorders of varying severity.

As we are able to gain more information on residues important for protein-protein interaction and protein-DNA interaction, it is becoming increasingly clear the intricate coordination of repair factors at DNA ends is specific and fine tuned to harmoniously repair damage. However, questions still remain how the intricacies behind the DNA damage response interplays with DNA repair pathway choice to ensure normal cellular function. In addition, questions remain about functions of factors within the DNA damage response and the consequences of disease associated alleles.

My dissertation seeks to further define these questions by focusing on the in vivo roles of the ARTEMIS DNA nuclease in maintaining genome stability, preventing oncogenic chromosomal translocations and ensuring proper immune system development. The precise mechanisms by which ARTEMIS activities are regulated in vivo are not well understood. To this end, I investigate the in vivo functions of the ARTEMIS C-terminus in preventing aberrant events associated with chromosomal translocations. Additionally, I investigate how other nucleases, such as MRE11, regulate ARTEMIS activity and the importance of nucleases such as ARTEMIS and MRE11 on the suppression or generation of oncogenic events associated with cancer. As a result, my dissertation has resulted in novel findings that have contributed to the DNA repair field. My studies lay critical foundation to future investigations into the interplay between ARTEMIS and MRE11, cNHEJ and aNHEJ, and HR and NHEJ. My thesis work has moved the DNA repair field closer to better understanding the coordination of DNA end processing events important to cellular development and in cancer prevention.

References

1. Ciccia A, Elledge SJ. The DNA damage response: making it safe to play with knives. Mol Cell. 2010;40(2):179-204. PMCID: 2988877.
2. Williams RS, Williams JS, Tainer JA. Mre11-Rad50-Nbs1 is a keystone complex connecting DNA repair machinery, double-strand break signaling, and the chromatin template. Biochem Cell Biol. 2007;85(4):509-20.
3. Shiloh Y. ATM and related protein kinases: safeguarding genome integrity. Nat Rev Cancer. 2003;3(3):155-68.
4. Lavin MF, Kozlov S. ATM activation and DNA damage response. Cell Cycle. 2007;6(8):931-42.
5. Lempiainen H, Halazonetis TD. Emerging common themes in regulation of PIKKs and PI3Ks. EMBO J. 2009;28(20):3067-73. PMCID: 2752028.
6. Derheimer FA, Kastan MB. Multiple roles of ATM in monitoring and maintaining DNA integrity. FEBS Lett. 2010;584(17):3675-81. PMCID: 2950315.
7. Weterings E, Chen DJ. DNA-dependent protein kinase in nonhomologous end joining: a lock with multiple keys? J Cell Biol. 2007;179(2):183-6. PMCID: 2064754.
8. Stiff T, O'Driscoll M, Rief N, Iwabuchi K, Lobrich M, Jeggo PA. ATM and DNA-PK function redundantly to phosphorylate H2AX after exposure to ionizing radiation. Cancer Res. 2004;64(7):2390-6.
9. Zha S, Jiang W, Fujiwara Y, Patel H, Goff PH, Brush JW, et al. Ataxia telangiectasia-mutated protein and DNA-dependent protein kinase have complementary V(D)J recombination functions. Proc Natl Acad Sci U S A. 2011;108(5):2028-33. PMCID: 3033273.
10. Martin M, Terradas M, Tusell L, Genesca A. ATM and DNA-PKcs make a complementary couple in DNA double strand break repair. Mutat Res. 2012.
11. Callen E, Jankovic M, Wong N, Zha S, Chen HT, Difilippantonio S, et al. Essential role for DNA-PKcs in DNA double-strand break repair and apoptosis in ATM-deficient lymphocytes. Mol Cell. 2009;34(3):285-97. PMCID: 2709792.
12. Sekiguchi J, Ferguson DO, Chen HT, Yang EM, Earle J, Frank K, et al. Genetic interactions between ATM and the nonhomologous end-joining factors in genomic stability and development. Proc Natl Acad Sci U S A. 2001;98(6):3243-8. PMCID: 30638.
13. Gurley KE, Kemp CJ. Synthetic lethality between mutation in Atm and DNA-PK(cs) during murine embryogenesis. Curr Biol. 2001;11(3):191-4.
14. Meek K, Dang V, Lees-Miller SP. DNA-PK: the means to justify the ends? Adv Immunol. 2008;99:33-58.
15. Buis J, Wu Y, Deng Y, Leddon J, Westfield G, Eckersdorff M, et al. Mre11 nuclease activity has essential roles in DNA repair and genomic stability distinct from ATM activation. Cell. 2008;135(1):85-96. PMCID: 2645868.

16. Liu S, Shiotani B, Lahiri M, Marechal A, Tse A, Leung CC, et al. ATR autophosphorylation as a molecular switch for checkpoint activation. Mol Cell. 2011;43(2):192-202. PMCID: 3155885.
17. Burma S, Chen BP, Murphy M, Kurimasa A, Chen DJ. ATM phosphorylates histone H2AX in response to DNA double-strand breaks. J Biol Chem. 2001;276(45):42462-7.
18. Scully R, Xie A. Double strand break repair functions of histone H2AX. Mutat Res. 2013.
19. Savic V, Yin B, Maas NL, Bredemeyer AL, Carpenter AC, Helmink BA, et al. Formation of dynamic gamma-H2AX domains along broken DNA strands is distinctly regulated by ATM and MDC1 and dependent upon H2AX densities in chromatin. Mol Cell. 2009;34(3):298-310. PMCID: 2744111.
20. Hoeijmakers JH. Genome maintenance mechanisms are critical for preventing cancer as well as other aging-associated diseases. Mech Ageing Dev. 2007;128(7-8):460-2.
21. Thompson LH, Hinz JM. Cellular and molecular consequences of defective Fanconi anemia proteins in replication-coupled DNA repair: mechanistic insights. Mutat Res. 2009;668(1-2):54-72. PMCID: 2714807.
22. Jackson SP, Bartek J. The DNA-damage response in human biology and disease. Nature. 2009;461(7267):1071-8. PMCID: 2906700.
23. McKinnon PJ. DNA repair deficiency and neurological disease. Nat Rev Neurosci. 2009;10(2):100-12. PMCID: 3064843.
24. Pfeiffer P, Goedecke W, Obe G. Mechanisms of DNA double-strand break repair and their potential to induce chromosomal aberrations. Mutagenesis. 2000;15(4):289-302.
25. Borde V, de Massy B. Programmed induction of DNA double strand breaks during meiosis: setting up communication between DNA and the chromosome structure. Curr Opin Genet Dev. 2013;23(2):147-55.
26. Keeney S, Neale MJ. Initiation of meiotic recombination by formation of DNA double-strand breaks: mechanism and regulation. Biochem Soc Trans. 2006;34(Pt 4):523-5.
27. Dudley DD, Chaudhuri J, Bassing CH, Alt FW. Mechanism and control of V(D)J recombination versus class switch recombination: similarities and differences. Adv Immunol. 2005;86:43-112.
28. Gostissa M, Alt FW, Chiarle R. Mechanisms that promote and suppress chromosomal translocations in lymphocytes. Annu Rev Immunol. 2011;29:319-50.
29. Lieber MR. The mechanism of double-strand DNA break repair by the nonhomologous DNA end-joining pathway. Annu Rev Biochem. 2010;79:181-211. PMCID: 3079308.
30. Smith J, Baldeyron C, De Oliveira I, Sala-Trepat M, Papadopoulo D. The influence of DNA double-strand break structure on end-joining in human cells. Nucleic Acids Res. 2001;29(23):4783-92. PMCID: 96706.
31. Niewolik D, Pannicke U, Lu H, Ma Y, Wang LC, Kulesza P, et al. DNA-PKcs dependence of Artemis endonucleolytic activity, differences between hairpins and 5' or 3' overhangs. J Biol Chem. 2006;281(45):33900-9.

32. Goodarzi AA, Yu Y, Riballo E, Douglas P, Walker SA, Ye R, et al. DNA-PK autophosphorylation facilitates Artemis endonuclease activity. EMBO J. 2006;25(16):3880-9. PMCID: 1553186.
33. Weterings E, Verkaik NS, Bruggenwirth HT, Hoeijmakers JH, van Gent DC. The role of DNA dependent protein kinase in synapsis of DNA ends. Nucleic Acids Res. 2003;31(24):7238-46. PMCID: 291856.
34. Block WD, Yu Y, Merkle D, Gifford JL, Ding Q, Meek K, et al. Autophosphorylation-dependent remodeling of the DNA-dependent protein kinase catalytic subunit regulates ligation of DNA ends. Nucleic Acids Res. 2004;32(14):4351-7. PMCID: 514382.
35. Wang YG, Nnakwe C, Lane WS, Modesti M, Frank KM. Phosphorylation and regulation of DNA ligase IV stability by DNA-dependent protein kinase. J Biol Chem. 2004;279(36):37282-90.
36. Villarreal DD, Lee K, Deem A, Shim EY, Malkova A, Lee SE. Microhomology directs diverse DNA break repair pathways and chromosomal translocations. PLoS Genet. 2012;8(11):e1003026. PMCID: 3493447.
37. Lee-Theilen M, Matthews AJ, Kelly D, Zheng S, Chaudhuri J. CtIP promotes microhomology-mediated alternative end joining during class-switch recombination. Nat Struct Mol Biol. 2011;18(1):75-9. PMCID: 3471154.
38. Zhang Y, Jasin M. An essential role for CtIP in chromosomal translocation formation through an alternative end-joining pathway. Nat Struct Mol Biol. 2011;18(1):80-4. PMCID: 3261752.
39. Bennardo N, Cheng A, Huang N, Stark JM. Alternative-NHEJ is a mechanistically distinct pathway of mammalian chromosome break repair. PLoS Genet. 2008;4(6):e1000110. PMCID: 2430616.
40. Symington LS, Gautier J. Double-strand break end resection and repair pathway choice. Annu Rev Genet. 2011;45:247-71.
41. Symington LS. Role of RAD52 epistasis group genes in homologous recombination and double-strand break repair. Microbiol Mol Biol Rev. 2002;66(4):630-70, table of contents. PMCID: 134659.
42. Stracker TH, Petrini JH. The MRE11 complex: starting from the ends. Nat Rev Mol Cell Biol. 2011;12(2):90-103.
43. Bressan DA, Baxter BK, Petrini JH. The Mre11-Rad50-Xrs2 protein complex facilitates homologous recombination-based double-strand break repair in Saccharomyces cerevisiae. Mol Cell Biol. 1999;19(11):7681-7. PMCID: 84807.
44. Zhu Z, Chung WH, Shim EY, Lee SE, Ira G. Sgs1 helicase and two nucleases Dna2 and Exo1 resect DNA double-strand break ends. Cell. 2008;134(6):981-94. PMCID: 2662516.
45. Nicolette ML, Lee K, Guo Z, Rani M, Chow JM, Lee SE, et al. Mre11-Rad50-Xrs2 and Sae2 promote 5' strand resection of DNA double-strand breaks. Nat Struct Mol Biol. 2010;17(12):1478-85. PMCID: 3059534.
46. Garcia V, Phelps SE, Gray S, Neale MJ. Bidirectional resection of DNA double-strand breaks by Mre11 and Exo1. Nature. 2011;479(7372):241-4. PMCID: 3214165.
47. Heyer WD, Ehmsen KT, Liu J. Regulation of homologous recombination in eukaryotes. Annu Rev Genet. 2010;44:113-39.

48. Wilson JH, Berget PB, Pipas JM. Somatic cells efficiently join unrelated DNA segments end-to-end. Mol Cell Biol. 1982;2(10):1258-69. PMCID: 369925.
49. Roth DB, Wilson JH. Relative rates of homologous and nonhomologous recombination in transfected DNA. Proc Natl Acad Sci U S A. 1985;82(10):3355-9. PMCID: 397774.
50. Getts RC, Stamato TD. Absence of a Ku-like DNA end binding activity in the xrs double-strand DNA repair-deficient mutant. J Biol Chem. 1994;269(23):15981-4.
51. Wang J, Dong X, Myung K, Hendrickson EA, Reeves WH. Identification of two domains of the p70 Ku protein mediating dimerization with p80 and DNA binding. J Biol Chem. 1998;273(2):842-8.
52. Francoeur AM, Peebles CL, Gompper PT, Tan EM. Identification of Ki (Ku, p70/p80) autoantigens and analysis of anti-Ki autoantibody reactivity. J Immunol. 1986;136(5):1648-53.
53. Gottlieb TM, Jackson SP. The DNA-dependent protein kinase: requirement for DNA ends and association with Ku antigen. Cell. 1993;72(1):131-42.
54. de Vries E, van Driel W, Bergsma WG, Arnberg AC, van der Vliet PC. HeLa nuclear protein recognizing DNA termini and translocating on DNA forming a regular DNA-multimeric protein complex. J Mol Biol. 1989;208(1):65-78.
55. Suwa A, Hirakata M, Takeda Y, Jesch SA, Mimori T, Hardin JA. DNA-dependent protein kinase (Ku protein-p350 complex) assembles on double-stranded DNA. Proc Natl Acad Sci U S A. 1994;91(15):6904-8. PMCID: 44306.
56. Morozov VE, Falzon M, Anderson CW, Kuff EL. DNA-dependent protein kinase is activated by nicks and larger single-stranded gaps. J Biol Chem. 1994;269(24):16684-8.
57. Chan DW, Lees-Miller SP. The DNA-dependent protein kinase is inactivated by autophosphorylation of the catalytic subunit. J Biol Chem. 1996;271(15):8936-41.
58. Chan DW, Ye R, Veillette CJ, Lees-Miller SP. DNA-dependent protein kinase phosphorylation sites in Ku 70/80 heterodimer. Biochemistry. 1999;38(6):1819-28.
59. Douglas P, Sapkota GP, Morrice N, Yu Y, Goodarzi AA, Merkle D, et al. Identification of in vitro and in vivo phosphorylation sites in the catalytic subunit of the DNA-dependent protein kinase. Biochem J. 2002;368(Pt 1):243-51. PMCID: 1222982.
60. Ma Y, Pannicke U, Schwarz K, Lieber MR. Hairpin opening and overhang processing by an Artemis/DNA-dependent protein kinase complex in nonhomologous end joining and V(D)J recombination. Cell. 2002;108(6):781-94.
61. Drouet J, Frit P, Delteil C, de Villartay JP, Salles B, Calsou P. Interplay between Ku, Artemis, and the DNA-dependent protein kinase catalytic subunit at DNA ends. J Biol Chem. 2006;281(38):27784-93.
62. Grawunder U, Zimmer D, Leiber MR. DNA ligase IV binds to XRCC4 via a motif located between rather than within its BRCT domains. Curr Biol. 1998;8(15):873-6.

63. Ahnesorg P, Smith P, Jackson SP. XLF interacts with the XRCC4-DNA ligase IV complex to promote DNA nonhomologous end-joining. Cell. 2006;124(2):301-13.
64. Gu J, Lu H, Tippin B, Shimazaki N, Goodman MF, Lieber MR. XRCC4:DNA ligase IV can ligate incompatible DNA ends and can ligate across gaps. EMBO J. 2007;26(4):1010-23. PMCID: 1852838.
65. Mahajan KN, Nick McElhinny SA, Mitchell BS, Ramsden DA. Association of DNA polymerase mu (pol mu) with Ku and ligase IV: role for pol mu in end-joining double-strand break repair. Mol Cell Biol. 2002;22(14):5194-202. PMCID: 139779.
66. Daley JM, Laan RL, Suresh A, Wilson TE. DNA joint dependence of pol X family polymerase action in nonhomologous end joining. J Biol Chem. 2005;280(32):29030-7.
67. Liang F, Romanienko PJ, Weaver DT, Jeggo PA, Jasin M. Chromosomal double-strand break repair in Ku80-deficient cells. Proc Natl Acad Sci U S A. 1996;93(17):8929-33. PMCID: 38571.
68. Wilson TE, Grawunder U, Lieber MR. Yeast DNA ligase IV mediates non-homologous DNA end joining. Nature. 1997;388(6641):495-8.
69. McVey M, Lee SE. MMEJ repair of double-strand breaks (director's cut): deleted sequences and alternative endings. Trends Genet. 2008;24(11):529-38.
70. Truong LN, Li Y, Shi LZ, Hwang PY, He J, Wang H, et al. Microhomology-mediated End Joining and Homologous Recombination share the initial end resection step to repair DNA double-strand breaks in mammalian cells. Proc Natl Acad Sci U S A. 2013;110(19):7720-5. PMCID: 3651503.
71. Deriano L, Stracker TH, Baker A, Petrini JH, Roth DB. Roles for NBS1 in alternative nonhomologous end-joining of V(D)J recombination intermediates. Mol Cell. 2009;34(1):13-25. PMCID: 2704125.
72. Rass E, Grabarz A, Plo I, Gautier J, Bertrand P, Lopez BS. Role of Mre11 in chromosomal nonhomologous end joining in mammalian cells. Nat Struct Mol Biol. 2009;16(8):819-24.
73. Yeo JE, Lee EH, Hendrickson E, Sobeck A. CtIP mediates replication fork recovery in a FANCD2-regulated manner. Hum Mol Genet. 2014.
74. Pierce AJ, Jasin M. Measuring recombination proficiency in mouse embryonic stem cells. Methods Mol Biol. 2014;1105:481-95.
75. Bennardo N, Gunn A, Cheng A, Hasty P, Stark JM. Limiting the persistence of a chromosome break diminishes its mutagenic potential. PLoS Genet. 2009;5(10):e1000683. PMCID: 2752804.
76. Fattah F, Lee EH, Weisensel N, Wang Y, Lichter N, Hendrickson EA. Ku regulates the non-homologous end joining pathway choice of DNA double-strand break repair in human somatic cells. PLoS Genet. 2010;6(2):e1000855. PMCID: 2829059.
77. Xie A, Kwok A, Scully R. Role of mammalian Mre11 in classical and alternative nonhomologous end joining. Nat Struct Mol Biol. 2009;16(8):814-8. PMCID: 2730592.

78. Poinsignon C, de Chasseval R, Soubeyrand S, Moshous D, Fischer A, Hache RJ, et al. Phosphorylation of Artemis following irradiation-induced DNA damage. Eur J Immunol. 2004;34(11):3146-55.
79. Chen L, Morio T, Minegishi Y, Nakada S, Nagasawa M, Komatsu K, et al. Ataxia-telangiectasia-mutated dependent phosphorylation of Artemis in response to DNA damage. Cancer Sci. 2005;96(2):134-41.
80. Riballo E, Kuhne M, Rief N, Doherty A, Smith GC, Recio MJ, et al. A pathway of double-strand break rejoining dependent upon ATM, Artemis, and proteins locating to gamma-H2AX foci. Mol Cell. 2004;16(5):715-24.
81. Riballo E, Critchlow SE, Teo SH, Doherty AJ, Priestley A, Broughton B, et al. Identification of a defect in DNA ligase IV in a radiosensitive leukaemia patient. Curr Biol. 1999;9(13):699-702.
82. Dinkelmann M, Spehalski E, Stoneham T, Buis J, Wu Y, Sekiguchi JM, et al. Multiple functions of MRN in end-joining pathways during isotype class switching. Nat Struct Mol Biol. 2009;16(8):808-13. PMCID: 2721910.
83. Beucher A, Birraux J, Tchouandong L, Barton O, Shibata A, Conrad S, et al. ATM and Artemis promote homologous recombination of radiation-induced DNA double-strand breaks in G2. EMBO J. 2009;28(21):3413-27. PMCID: 2752027.
84. Ajimura M, Leem SH, Ogawa H. Identification of new genes required for meiotic recombination in Saccharomyces cerevisiae. Genetics. 1993;133(1):51-66. PMCID: 1205298.
85. Alani E, Padmore R, Kleckner N. Analysis of wild-type and rad50 mutants of yeast suggests an intimate relationship between meiotic chromosome synapsis and recombination. Cell. 1990;61(3):419-36.
86. Ivanov EL, Korolev VG, Fabre F. XRS2, a DNA repair gene of Saccharomyces cerevisiae, is needed for meiotic recombination. Genetics. 1992;132(3):651-64. PMCID: 1205204.
87. Carney JP, Maser RS, Olivares H, Davis EM, Le Beau M, Yates JR, 3rd, et al. The hMre11/hRad50 protein complex and Nijmegen breakage syndrome: linkage of double-strand break repair to the cellular DNA damage response. Cell. 1998;93(3):477-86.
88. Hopfner KP, Craig L, Moncalian G, Zinkel RA, Usui T, Owen BA, et al. The Rad50 zinc-hook is a structure joining Mre11 complexes in DNA recombination and repair. Nature. 2002;418(6897):562-6.
89. Williams RS, Moncalian G, Williams JS, Yamada Y, Limbo O, Shin DS, et al. Mre11 dimers coordinate DNA end bridging and nuclease processing in double-strand-break repair. Cell. 2008;135(1):97-109. PMCID: 2681233.
90. Stewart GS, Maser RS, Stankovic T, Bressan DA, Kaplan MI, Jaspers NG, et al. The DNA double-strand break repair gene hMRE11 is mutated in individuals with an ataxia-telangiectasia-like disorder. Cell. 1999;99(6):577-87.
91. Theunissen JW, Kaplan MI, Hunt PA, Williams BR, Ferguson DO, Alt FW, et al. Checkpoint failure and chromosomal instability without lymphomagenesis in Mre11(ATLD1/ATLD1) mice. Mol Cell. 2003;12(6):1511-23.
92. Williams BR, Mirzoeva OK, Morgan WF, Lin J, Dunnick W, Petrini JH. A murine model of Nijmegen breakage syndrome. Curr Biol. 2002;12(8):648-53.

93. Moshous D, Callebaut I, de Chasseval R, Corneo B, Cavazzana-Calvo M, Le Deist F, et al. Artemis, a novel DNA double-strand break repair/V(D)J recombination protein, is mutated in human severe combined immune deficiency. Cell. 2001;105(2):177-86.
94. Le Deist F, Poinsignon C, Moshous D, Fischer A, de Villartay JP. Artemis sheds new light on V(D)J recombination. Immunol Rev. 2004;200:142-55.
95. de Villartay JP, Shimazaki N, Charbonnier JB, Fischer A, Mornon JP, Lieber MR, et al. A histidine in the beta-CASP domain of Artemis is critical for its full in vitro and in vivo functions. DNA Repair (Amst). 2009;8(2):202-8.
96. de Villartay JP, Fischer A, Durandy A. The mechanisms of immune diversification and their disorders. Nat Rev Immunol. 2003;3(12):962-72.
97. Poinsignon C, Moshous D, Callebaut I, de Chasseval R, Villey I, de Villartay JP. The metallo-beta-lactamase/beta-CASP domain of Artemis constitutes the catalytic core for V(D)J recombination. J Exp Med. 2004;199(3):315-21. PMCID: 2211804.
98. Moshous D, Callebaut I, de Chasseval R, Poinsignon C, Villey I, Fischer A, et al. The V(D)J recombination/DNA repair factor artemis belongs to the metallo-beta-lactamase family and constitutes a critical developmental checkpoint of the lymphoid system. Ann N Y Acad Sci. 2003;987:150-7.
99. Pawelczak KS, Turchi JJ. Purification and characterization of exonuclease-free Artemis: Implications for DNA-PK-dependent processing of DNA termini in NHEJ-catalyzed DSB repair. DNA Repair (Amst). 2010;9(6):670-7. PMCID: 2883643.
100. Ma Y, Pannicke U, Lu H, Niewolik D, Schwarz K, Lieber MR. The DNA-dependent protein kinase catalytic subunit phosphorylation sites in human Artemis. J Biol Chem. 2005;280(40):33839-46.
101. Hozumi N, Tonegawa S. Evidence for somatic rearrangement of immunoglobulin genes coding for variable and constant regions. Proc Natl Acad Sci U S A. 1976;73(10):3628-32. PMCID: 431171.
102. Kenneth Murphy PT, Mark Walport. Janeway's Immunobiology. Lawrence E, editor: Garland Science, Taylor & Francis Group; 2008.
103. Schatz DG, Oettinger MA, Schlissel MS. V(D)J recombination: molecular biology and regulation. Annu Rev Immunol. 1992;10:359-83.
104. Schatz DG. V(D)J recombination moves in vitro. Semin Immunol. 1997;9(3):149-59.
105. Oettinger MA, Schatz DG, Gorka C, Baltimore D. RAG-1 and RAG-2, adjacent genes that synergistically activate V(D)J recombination. Science. 1990;248(4962):1517-23.
106. van Gent DC, Mizuuchi K, Gellert M. Similarities between initiation of V(D)J recombination and retroviral integration. Science. 1996;271(5255):1592-4.
107. Schatz DG. Antigen receptor genes and the evolution of a recombinase. Semin Immunol. 2004;16(4):245-56.
108. Hiom K, Gellert M. Assembly of a 12/23 paired signal complex: a critical control point in V(D)J recombination. Mol Cell. 1998;1(7):1011-9.
109. Schatz DG, Ji Y. Recombination centres and the orchestration of V(D)J recombination. Nat Rev Immunol. 2011;11(4):251-63.

110. Agrawal A, Schatz DG. RAG1 and RAG2 form a stable postcleavage synaptic complex with DNA containing signal ends in V(D)J recombination. Cell. 1997;89(1):43-53.
111. Jones JM, Gellert M. Intermediates in V(D)J recombination: a stable RAG1/2 complex sequesters cleaved RSS ends. Proc Natl Acad Sci U S A. 2001;98(23):12926-31. PMCID: 60801.
112. Arnal SM, Holub AJ, Salus SS, Roth DB. Non-consensus heptamer sequences destabilize the RAG post-cleavage complex, making ends available to alternative DNA repair pathways. Nucleic Acids Res. 2010;38(9):2944-54. PMCID: 2875030.
113. Corneo B, Wendland RL, Deriano L, Cui X, Klein IA, Wong SY, et al. Rag mutations reveal robust alternative end joining. Nature. 2007;449(7161):483-6.
114. Roth DB, Menetski JP, Nakajima PB, Bosma MJ, Gellert M. V(D)J recombination: broken DNA molecules with covalently sealed (hairpin) coding ends in scid mouse thymocytes. Cell. 1992;70(6):983-91.
115. Lee GS, Neiditch MB, Salus SS, Roth DB. RAG proteins shepherd double-strand breaks to a specific pathway, suppressing error-prone repair, but RAG nicking initiates homologous recombination. Cell. 2004;117(2):171-84.
116. Tsai CL, Drejer AH, Schatz DG. Evidence of a critical architectural function for the RAG proteins in end processing, protection, and joining in V(D)J recombination. Genes Dev. 2002;16(15):1934-49. PMCID: 186421.
117. Sekiguchi J, Alt F.W., Oettinger M., Honjo T. Molecular Biology of B Cells. In: W. AF, editor. Elsevier Science2004. p. 57-78.
118. Iwasato T, Yamagishi H. Novel excision products of T cell receptor gamma gene rearrangements and developmental stage specificity implied by the frequency of nucleotide insertions at signal joints. Eur J Immunol. 1992;22(1):101-6.
119. Touvrey C, Couedel C, Soulas P, Couderc R, Jasin M, de Villartay JP, et al. Distinct effects of DNA-PKcs and Artemis inactivation on signal joint formation in vivo. Mol Immunol. 2008;45(12):3383-91.
120. Shimizu T, Yamagishi H. Biased reading frames of pre-existing DH--JH coding joints and preferential nucleotide insertions at VH--DJH signal joints of excision products of immunoglobulin heavy chain gene rearrangements. EMBO J. 1992;11(13):4869-75. PMCID: 556964.
121. Mickelsen S, Snyder C, Trujillo K, Bogue M, Roth DB, Meek K. Modulation of terminal deoxynucleotidyltransferase activity by the DNA-dependent protein kinase. J Immunol. 1999;163(2):834-43.
122. Mahajan KN, Gangi-Peterson L, Sorscher DH, Wang J, Gathy KN, Mahajan NP, et al. Association of terminal deoxynucleotidyl transferase with Ku. Proc Natl Acad Sci U S A. 1999;96(24):13926-31. PMCID: 24167.
123. Bertocci B, De Smet A, Berek C, Weill JC, Reynaud CA. Immunoglobulin kappa light chain gene rearrangement is impaired in mice deficient for DNA polymerase mu. Immunity. 2003;19(2):203-11.
124. Bertocci B, De Smet A, Weill JC, Reynaud CA. Nonoverlapping functions of DNA polymerases mu, lambda, and terminal deoxynucleotidyltransferase during immunoglobulin V(D)J recombination in vivo. Immunity. 2006;25(1):31-41.

125. Li Z, Dordai DI, Lee J, Desiderio S. A conserved degradation signal regulates RAG-2 accumulation during cell division and links V(D)J recombination to the cell cycle. Immunity. 1996;5(6):575-89.
126. Gellert M. V(D)J recombination: RAG proteins, repair factors, and regulation. Annu Rev Biochem. 2002;71:101-32.
127. Li S, Chang HH, Niewolik D, Hedrick MP, Pinkerton AB, Hassig C, et al. Evidence that the DNA Endonuclease ARTEMIS also has Intrinsic 5' Exonuclease Activity. J Biol Chem. 2014.
128. Ma Y, Schwarz K, Lieber MR. The Artemis:DNA-PKcs endonuclease cleaves DNA loops, flaps, and gaps. DNA Repair (Amst). 2005;4(7):845-51.
129. Ding Q, Reddy YV, Wang W, Woods T, Douglas P, Ramsden DA, et al. Autophosphorylation of the catalytic subunit of the DNA-dependent protein kinase is required for efficient end processing during DNA double-strand break repair. Mol Cell Biol. 2003;23(16):5836-48. PMCID: 166339.
130. van der Burg M, Ijspeert H, Verkaik NS, Turul T, Wiegant WW, Morotomi-Yano K, et al. A DNA-PKcs mutation in a radiosensitive T-B- SCID patient inhibits Artemis activation and nonhomologous end-joining. J Clin Invest. 2009;119(1):91-8. PMCID: 2613452.
131. Huang Y, Giblin W, Kubec M, Westfield G, St Charles J, Chadde L, et al. Impact of a hypomorphic Artemis disease allele on lymphocyte development, DNA end processing, and genome stability. J Exp Med. 2009;206(4):893-908. PMCID: 2715118.
132. Geha RS, Notarangelo LD, Casanova JL, Chapel H, Conley ME, Fischer A, et al. Primary immunodeficiency diseases: an update from the International Union of Immunological Societies Primary Immunodeficiency Diseases Classification Committee. J Allergy Clin Immunol. 2007;120(4):776-94. PMCID: 2601718.
133. Ege M, Ma Y, Manfras B, Kalwak K, Lu H, Lieber MR, et al. Omenn syndrome due to ARTEMIS mutations. Blood. 2005;105(11):4179-86.
134. Buck D, Malivert L, de Chasseval R, Barraud A, Fondaneche MC, Sanal O, et al. Cernunnos, a novel nonhomologous end-joining factor, is mutated in human immunodeficiency with microcephaly. Cell. 2006;124(2):287-99.
135. Villa A, Sobacchi C, Notarangelo LD, Bozzi F, Abinun M, Abrahamsen TG, et al. V(D)J recombination defects in lymphocytes due to RAG mutations: severe immunodeficiency with a spectrum of clinical presentations. Blood. 2001;97(1):81-8.
136. Lieber MR, Yu K, Raghavan SC. Roles of nonhomologous DNA end joining, V(D)J recombination, and class switch recombination in chromosomal translocations. DNA Repair (Amst). 2006;5(9-10):1234-45.
137. Alt FW, Zhang Y, Meng FL, Guo C, Schwer B. Mechanisms of programmed DNA lesions and genomic instability in the immune system. Cell. 2013;152(3):417-29.
138. Brandt VL, Roth DB. Recent insights into the formation of RAG-induced chromosomal translocations. Adv Exp Med Biol. 2009;650:32-45.

139. Difilippantonio MJ, Zhu J, Chen HT, Meffre E, Nussenzweig MC, Max EE, et al. DNA repair protein Ku80 suppresses chromosomal aberrations and malignant transformation. Nature. 2000;404(6777):510-4.
140. Frank KM, Sharpless NE, Gao Y, Sekiguchi JM, Ferguson DO, Zhu C, et al. DNA ligase IV deficiency in mice leads to defective neurogenesis and embryonic lethality via the p53 pathway. Mol Cell. 2000;5(6):993-1002.
141. Li GC, Ouyang H, Li X, Nagasawa H, Little JB, Chen DJ, et al. Ku70: a candidate tumor suppressor gene for murine T cell lymphoma. Mol Cell. 1998;2(1):1-8.
142. Nacht M, Strasser A, Chan YR, Harris AW, Schlissel M, Bronson RT, et al. Mutations in the p53 and SCID genes cooperate in tumorigenesis. Genes Dev. 1996;10(16):2055-66.
143. Rooney S, Sekiguchi J, Whitlow S, Eckersdorff M, Manis JP, Lee C, et al. Artemis and p53 cooperate to suppress oncogenic N-myc amplification in progenitor B cells. Proc Natl Acad Sci U S A. 2004;101(8):2410-5. PMCID: 356964.
144. Lim DS, Vogel H, Willerford DM, Sands AT, Platt KA, Hasty P. Analysis of ku80-mutant mice and cells with deficient levels of p53. Mol Cell Biol. 2000;20(11):3772-80. PMCID: 85695.
145. Vanasse GJ, Halbrook J, Thomas S, Burgess A, Hoekstra MF, Disteche CM, et al. Genetic pathway to recurrent chromosome translocations in murine lymphoma involves V(D)J recombinase. J Clin Invest. 1999;103(12):1669-75. PMCID: 408389.
146. Gao Y, Ferguson DO, Xie W, Manis JP, Sekiguchi J, Frank KM, et al. Interplay of p53 and DNA-repair protein XRCC4 in tumorigenesis, genomic stability and development. Nature. 2000;404(6780):897-900.
147. Gao Y, Chaudhuri J, Zhu C, Davidson L, Weaver DT, Alt FW. A targeted DNA-PKcs-null mutation reveals DNA-PK-independent functions for KU in V(D)J recombination. Immunity. 1998;9(3):367-76.
148. Schatz DG, Swanson PC. V(D)J recombination: mechanisms of initiation. Annu Rev Genet. 2011;45:167-202.
149. Villa A, Santagata S, Bozzi F, Giliani S, Frattini A, Imberti L, et al. Partial V(D)J recombination activity leads to Omenn syndrome. Cell. 1998;93(5):885-96.
150. Santagata S, Besmer E, Villa A, Bozzi F, Allingham JS, Sobacchi C, et al. The RAG1/RAG2 complex constitutes a 3' flap endonuclease: implications for junctional diversity in V(D)J and transpositional recombination. Mol Cell. 1999;4(6):935-47.
151. Sobacchi C, Marrella V, Rucci F, Vezzoni P, Villa A. RAG-dependent primary immunodeficiencies. Hum Mutat. 2006;27(12):1174-84.
152. Omenn GS. FAMILIAL RETICULOENDOTHELIOSIS WITH EOSINOPHILIA. N Engl J Med. 1965;273:427-32.
153. Mombaerts P, Iacomini J, Johnson RS, Herrup K, Tonegawa S, Papaioannou VE. RAG-1-deficient mice have no mature B and T lymphocytes. Cell. 1992;68(5):869-77.

154. Shinkai Y, Rathbun G, Lam KP, Oltz EM, Stewart V, Mendelsohn M, et al. RAG-2-deficient mice lack mature lymphocytes owing to inability to initiate V(D)J rearrangement. Cell. 1992;68(5):855-67.
155. Schwarz K, Gauss GH, Ludwig L, Pannicke U, Li Z, Lindner D, et al. RAG mutations in human B cell-negative SCID. Science. 1996;274(5284):97-9.
156. Giblin W, Chatterji M, Westfield G, Masud T, Theisen B, Cheng HL, et al. Leaky severe combined immunodeficiency and aberrant DNA rearrangements due to a hypomorphic RAG1 mutation. Blood. 2009;113(13):2965-75. PMCID: 2662642.
157. Marrella V, Poliani PL, Casati A, Rucci F, Frascoli L, Gougeon ML, et al. A hypomorphic R229Q Rag2 mouse mutant recapitulates human Omenn syndrome. J Clin Invest. 2007;117(5):1260-9. PMCID: 1857243.
158. Walter JE, Rucci F, Patrizi L, Recher M, Regenass S, Paganini T, et al. Expansion of immunoglobulin-secreting cells and defects in B cell tolerance in Rag-dependent immunodeficiency. J Exp Med. 2010;207(7):1541-54. PMCID: 2901061.
159. Villa A, Notarangelo LD, Roifman CM. Omenn syndrome: inflammation in leaky severe combined immunodeficiency. J Allergy Clin Immunol. 2008;122(6):1082-6.
160. Roberts SA, Strande N, Burkhalter MD, Strom C, Havener JM, Hasty P, et al. Ku is a 5'-dRP/AP lyase that excises nucleotide damage near broken ends. Nature. 2010;464(7292):1214-7. PMCID: 2859099.
161. Blunt T, Gell D, Fox M, Taccioli GE, Lehmann AR, Jackson SP, et al. Identification of a nonsense mutation in the carboxyl-terminal region of DNA-dependent protein kinase catalytic subunit in the scid mouse. Proc Natl Acad Sci U S A. 1996;93(19):10285-90. PMCID: 38376.
162. Spagnolo L, Rivera-Calzada A, Pearl LH, Llorca O. Three-dimensional structure of the human DNA-PKcs/Ku70/Ku80 complex assembled on DNA and its implications for DNA DSB repair. Mol Cell. 2006;22(4):511-9.
163. Carroll AM, Hardy RR, Bosma MJ. Occurrence of mature B (IgM+, B220+) and T (CD3+) lymphocytes in scid mice. J Immunol. 1989;143(4):1087-93.
164. Nussenzweig A, Chen C, da Costa Soares V, Sanchez M, Sokol K, Nussenzweig MC, et al. Requirement for Ku80 in growth and immunoglobulin V(D)J recombination. Nature. 1996;382(6591):551-5.
165. Zhu C, Bogue MA, Lim DS, Hasty P, Roth DB. Ku86-deficient mice exhibit severe combined immunodeficiency and defective processing of V(D)J recombination intermediates. Cell. 1996;86(3):379-89.
166. Danska JS, Holland DP, Mariathasan S, Williams KM, Guidos CJ. Biochemical and genetic defects in the DNA-dependent protein kinase in murine scid lymphocytes. Mol Cell Biol. 1996;16(10):5507-17. PMCID: 231550.
167. Jhappan C, Morse HC, 3rd, Fleischmann RD, Gottesman MM, Merlino G. DNA-PKcs: a T-cell tumour suppressor encoded at the mouse scid locus. Nat Genet. 1997;17(4):483-6.
168. Kurimasa A, Ouyang H, Dong LJ, Wang S, Li X, Cordon-Cardo C, et al. Catalytic subunit of DNA-dependent protein kinase: impact on lymphocyte

development and tumorigenesis. Proc Natl Acad Sci U S A. 1999;96(4):1403-8. PMCID: 15475.
169. Taccioli GE, Amatucci AG, Beamish HJ, Gell D, Xiang XH, Torres Arzayus MI, et al. Targeted disruption of the catalytic subunit of the DNA-PK gene in mice confers severe combined immunodeficiency and radiosensitivity. Immunity. 1998;9(3):355-66.
170. Gu Y, Seidl KJ, Rathbun GA, Zhu C, Manis JP, van der Stoep N, et al. Growth retardation and leaky SCID phenotype of Ku70-deficient mice. Immunity. 1997;7(5):653-65.
171. van der Burg M, van Dongen JJ, van Gent DC. DNA-PKcs deficiency in human: long predicted, finally found. Curr Opin Allergy Clin Immunol. 2009;9(6):503-9.
172. Woodbine L, Neal JA, Sasi NK, Shimada M, Deem K, Coleman H, et al. PRKDC mutations in a SCID patient with profound neurological abnormalities. J Clin Invest. 2013;123(7):2969-80.
173. Meek K, Kienker L, Dallas C, Wang W, Dark MJ, Venta PJ, et al. SCID in Jack Russell terriers: a new animal model of DNA-PKcs deficiency. J Immunol. 2001;167(4):2142-50.
174. Ding Q, Bramble L, Yuzbasiyan-Gurkan V, Bell T, Meek K. DNA-PKcs mutations in dogs and horses: allele frequency and association with neoplasia. Gene. 2002;283(1-2):263-9.
175. Gu Y, Sekiguchi J, Gao Y, Dikkes P, Frank K, Ferguson D, et al. Defective embryonic neurogenesis in Ku-deficient but not DNA-dependent protein kinase catalytic subunit-deficient mice. Proc Natl Acad Sci U S A. 2000;97(6):2668-73. PMCID: 15987.
176. Gao Y, Sun Y, Frank KM, Dikkes P, Fujiwara Y, Seidl KJ, et al. A critical role for DNA end-joining proteins in both lymphogenesis and neurogenesis. Cell. 1998;95(7):891-902.
177. de Villartay JP. V(D)J recombination deficiencies. Adv Exp Med Biol. 2009;650:46-58.
178. Moshous D, Pannetier C, Chasseval Rd R, Deist Fl F, Cavazzana-Calvo M, Romana S, et al. Partial T and B lymphocyte immunodeficiency and predisposition to lymphoma in patients with hypomorphic mutations in Artemis. J Clin Invest. 2003;111(3):381-7. PMCID: 151863.
179. van der Burg M, Verkaik NS, den Dekker AT, Barendregt BH, Pico-Knijnenburg I, Tezcan I, et al. Defective Artemis nuclease is characterized by coding joints with microhomology in long palindromic-nucleotide stretches. Eur J Immunol. 2007;37(12):3522-8.
180. Bosma GC, Fried M, Custer RP, Carroll A, Gibson DM, Bosma MJ. Evidence of functional lymphocytes in some (leaky) scid mice. J Exp Med. 1988;167(3):1016-33. PMCID: 2188881.
181. Ferguson DO, Sekiguchi JM, Chang S, Frank KM, Gao Y, DePinho RA, et al. The nonhomologous end-joining pathway of DNA repair is required for genomic stability and the suppression of translocations. Proc Natl Acad Sci U S A. 2000;97(12):6630-3. PMCID: 18682.

182. Frank KM, Sekiguchi JM, Seidl KJ, Swat W, Rathbun GA, Cheng HL, et al. Late embryonic lethality and impaired V(D)J recombination in mice lacking DNA ligase IV. Nature. 1998;396(6707):173-7.
183. O'Driscoll M, Gennery AR, Seidel J, Concannon P, Jeggo PA. An overview of three new disorders associated with genetic instability: LIG4 syndrome, RS-SCID and ATR-Seckel syndrome. DNA Repair (Amst). 2004;3(8-9):1227-35.
184. Murray JE, Bicknell LS, Yigit G, Duker AL, van Kogelenberg M, Haghayegh S, et al. Extreme Growth Failure is a Common Presentation of Ligase IV Deficiency. Hum Mutat. 2013.
185. Li G, Alt FW, Cheng HL, Brush JW, Goff PH, Murphy MM, et al. Lymphocyte-specific compensation for XLF/cernunnos end-joining functions in V(D)J recombination. Mol Cell. 2008;31(5):631-40. PMCID: 2630261.
186. Costantini S, Woodbine L, Andreoli L, Jeggo PA, Vindigni A. Interaction of the Ku heterodimer with the DNA ligase IV/Xrcc4 complex and its regulation by DNA-PK. DNA Repair (Amst). 2007;6(6):712-22.
187. Enders A, Fisch P, Schwarz K, Duffner U, Pannicke U, Nikolopoulos E, et al. A severe form of human combined immunodeficiency due to mutations in DNA ligase IV. J Immunol. 2006;176(8):5060-8.
188. Buck D, Moshous D, de Chasseval R, Ma Y, le Deist F, Cavazzana-Calvo M, et al. Severe combined immunodeficiency and microcephaly in siblings with hypomorphic mutations in DNA ligase IV. Eur J Immunol. 2006;36(1):224-35.
189. Valencia M, Bentele M, Vaze MB, Herrmann G, Kraus E, Lee SE, et al. NEJ1 controls non-homologous end joining in Saccharomyces cerevisiae. Nature. 2001;414(6864):666-9.
190. Frank-Vaillant M, Marcand S. NHEJ regulation by mating type is exercised through a novel protein, Lif2p, essential to the ligase IV pathway. Genes Dev. 2001;15(22):3005-12. PMCID: 312823.
191. Kegel A, Sjostrand JO, Astrom SU. Nej1p, a cell type-specific regulator of nonhomologous end joining in yeast. Curr Biol. 2001;11(20):1611-7.
192. Ooi SL, Shoemaker DD, Boeke JD. A DNA microarray-based genetic screen for nonhomologous end-joining mutants in Saccharomyces cerevisiae. Science. 2001;294(5551):2552-6.
193. Wilson TE. A genomics-based screen for yeast mutants with an altered recombination/end-joining repair ratio. Genetics. 2002;162(2):677-88. PMCID: 1462309.
194. Shiloh Y. Ataxia-telangiectasia and the Nijmegen breakage syndrome: related disorders but genes apart. Annu Rev Genet. 1997;31:635-62.
195. Callebaut I, Malivert L, Fischer A, Mornon JP, Revy P, de Villartay JP. Cernunnos interacts with the XRCC4 x DNA-ligase IV complex and is homologous to the yeast nonhomologous end-joining factor Nej1. J Biol Chem. 2006;281(20):13857-60.
196. Hentges P, Ahnesorg P, Pitcher RS, Bruce CK, Kysela B, Green AJ, et al. Evolutionary and functional conservation of the DNA non-homologous end-joining protein, XLF/Cernunnos. J Biol Chem. 2006;281(49):37517-26.

197. Pavlicek A, Jurka J. Positive selection on the nonhomologous end-joining factor Cernunnos-XLF in the human lineage. Biol Direct. 2006;1:15. PMCID: 1552050.
198. Deshpande RA, Wilson TE. Modes of interaction among yeast Nej1, Lif1 and Dnl4 proteins and comparison to human XLF, XRCC4 and Lig4. DNA Repair (Amst). 2007;6(10):1507-16. PMCID: 2064958.
199. Barlow C, Hirotsune S, Paylor R, Liyanage M, Eckhaus M, Collins F, et al. Atm-deficient mice: a paradigm of ataxia telangiectasia. Cell. 1996;86(1):159-71.
200. Weemaes CM, Hustinx TW, Scheres JM, van Munster PJ, Bakkeren JA, Taalman RD. A new chromosomal instability disorder: the Nijmegen breakage syndrome. Acta Paediatr Scand. 1981;70(4):557-64.
201. de Miranda NF, Bjorkman A, Pan-Hammarstrom Q. DNA repair: the link between primary immunodeficiency and cancer. Ann N Y Acad Sci. 2011;1246:50-63.
202. Waltes R, Kalb R, Gatei M, Kijas AW, Stumm M, Sobeck A, et al. Human RAD50 deficiency in a Nijmegen breakage syndrome-like disorder. Am J Hum Genet. 2009;84(5):605-16. PMCID: 2681000.
203. Hernandez D, McConville CM, Stacey M, Woods CG, Brown MM, Shutt P, et al. A family showing no evidence of linkage between the ataxia telangiectasia gene and chromosome 11q22-23. J Med Genet. 1993;30(2):135-40. PMCID: 1016271.
204. Klein C, Wenning GK, Quinn NP, Marsden CD. Ataxia without telangiectasia masquerading as benign hereditary chorea. Mov Disord. 1996;11(2):217-20.
205. Taylor AM, Groom A, Byrd PJ. Ataxia-telangiectasia-like disorder (ATLD)-its clinical presentation and molecular basis. DNA Repair (Amst). 2004;3(8-9):1219-25.
206. Maser RS, Monsen KJ, Nelms BE, Petrini JH. hMre11 and hRad50 nuclear foci are induced during the normal cellular response to DNA double-strand breaks. Mol Cell Biol. 1997;17(10):6087-96. PMCID: 232458.
207. Stracker TH, Theunissen JW, Morales M, Petrini JH. The Mre11 complex and the metabolism of chromosome breaks: the importance of communicating and holding things together. DNA Repair (Amst). 2004;3(8-9):845-54.
208. Paull TT, Gellert M. The 3' to 5' exonuclease activity of Mre 11 facilitates repair of DNA double-strand breaks. Mol Cell. 1998;1(7):969-79.
209. Moreau S, Ferguson JR, Symington LS. The nuclease activity of Mre11 is required for meiosis but not for mating type switching, end joining, or telomere maintenance. Mol Cell Biol. 1999;19(1):556-66. PMCID: 83913.
210. Reina-San-Martin B, Nussenzweig MC, Nussenzweig A, Difilippantonio S. Genomic instability, endoreduplication, and diminished Ig class-switch recombination in B cells lacking Nbs1. Proc Natl Acad Sci U S A. 2005;102(5):1590-5. PMCID: 547831.
211. Helmink BA, Bredemeyer AL, Lee BS, Huang CY, Sharma GG, Walker LM, et al. MRN complex function in the repair of chromosomal Rag-mediated DNA double-strand breaks. J Exp Med. 2009;206(3):669-79. PMCID: 2699138.

212. Mason JM. The SNM1B nuclease plays important roles in maintaining genome stability. Ann Arbor: University of Michigan; 2010.
213. Pannicke U, Honig M, Schulze I, Rohr J, Heinz GA, Braun S, et al. The most frequent DCLRE1C (ARTEMIS) mutations are based on homologous recombination events. Hum Mutat. 2010;31(2):197-207.

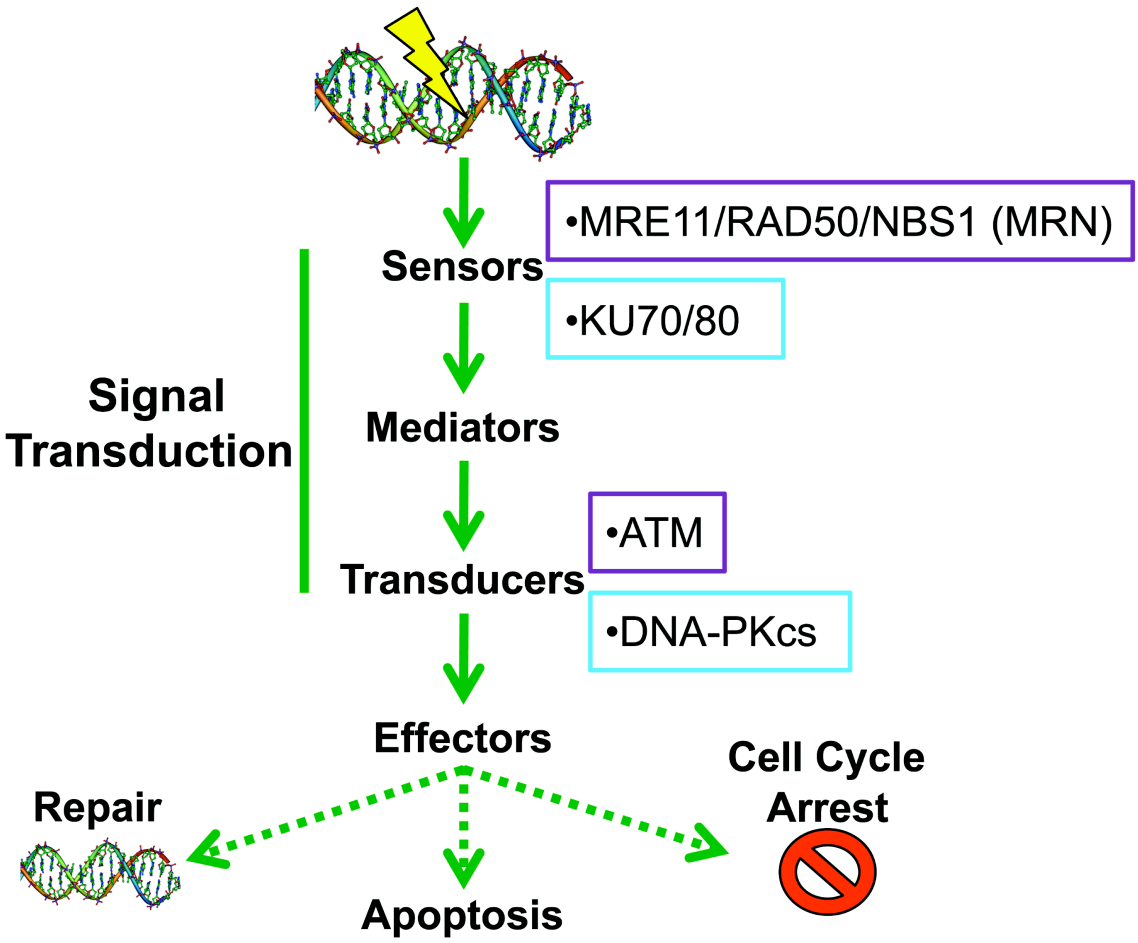

Figure 1.1 DNA damage occurs via exogenous or endogenous insults. DNA damage can occur as a result of exogenous insults such as radiation or as a result of endogenous insults such as due to cellular metabolism or replication errors. After initial damage, the resulting lesion is sensed and bound by particular DNA end-binding factors (KU70/80 or MRN) which help to mediate the DNA damage response and activate kinases (KU70/80 activate DNA-PKcs and MRN activates ATM) that are capable of transducing the DNA damage signal to effector proteins that mediate a response such as cell cycle check point activation, transcriptional program activation, DNA repair, and cellular apoptosis (1).

DNA repair mechanism	Lesions	Protein components	Human disease
Mismatch repair	DNA mismatches insertion/deletion loops	MSH2-MSH6, MSH2-MSH3, MLH1-PMS2, MLH1-PMS1	HNPCC
Nucleotide excision repair	Abnormal DNA bases, single strand breaks	XP family of proteins CSA, CSB	Xeroderma pigmentosum Cockayne syndrome, RTS
Base excision repair	Lesions distorting helix, bulky base adducts, UV photo-products	DNA glycosylases, APEI endonucleases, FEN1	Adenomatous colorectal polyposis
Nonhomologous end joining	double strand breaks	KU70/80, DNA-PKcs, ARTEMIS, LIG4, XLF XRCC4	Lig4 syndrome RS-SCID, Omenn syndrome
Homologous recombination	double strand breaks	BRCA1, BRCA2, RAD51, RPA, WRN,	Werners syndrome Bloom syndrome
Interstrand crosslinks	interstrand crosslinks	FA proteins TLS polymerases	Fanconi Anemia

Figure 1.2 DNA repair mechanisms.
The cellular response to various DNA damage is complex and includes multiple pathways that repair certain types of lesions. Summarized above are the multiple DNA repair pathways that repair specific types of lesions and the factors involved. Summarized from (20, 21, 212).

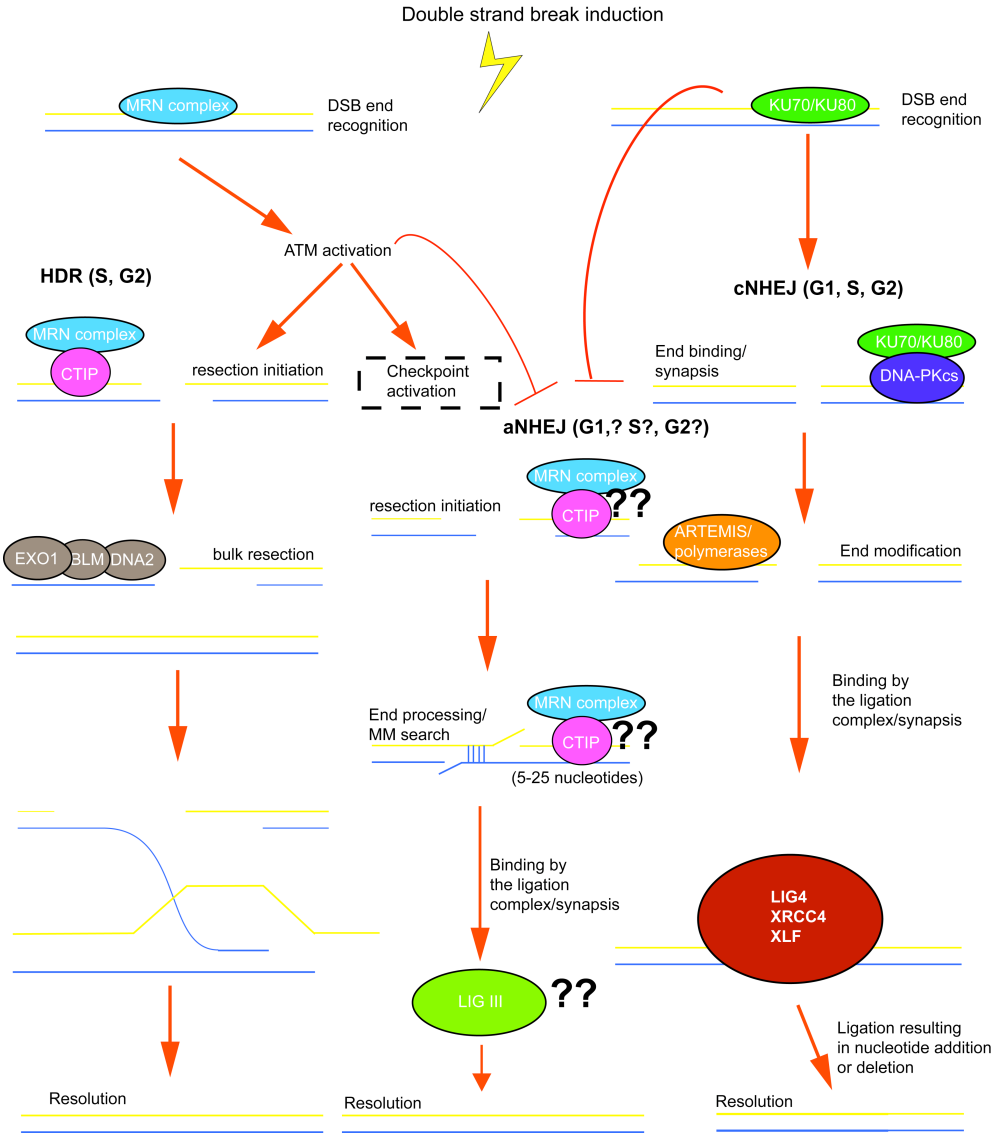

Figure 1.3 The bulk of DSB repair utilizes homologous recombination and nonhomologous end joining. Diagrammed above is a simple schematic of the homology directed repair (HDR) or homologous recombination pathway which utilizes a homologous template (sister chromatid) to direct repair of DSBs. Also illustrated are the classical nonhomologous end joining (cNHEJ) and alternative nonhomologous end joining (aNHEJ) pathways that direct repair via direct end-to-end binding and/or using regions of short homology, respectively. In this figure, MRN denotes the MRE11 complex.

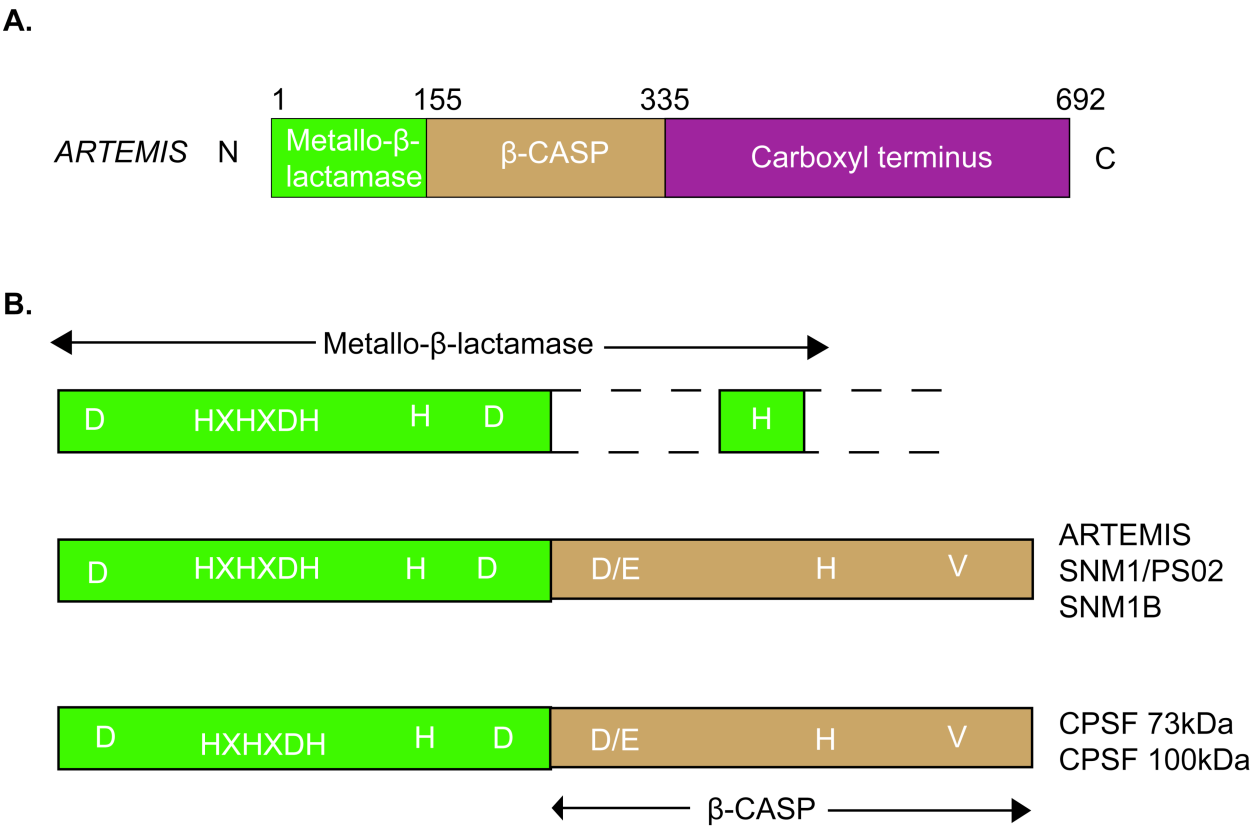

Figure 1.4 ARTEMIS is a part of the Metallo-β-lactamase/β-CASP family of enzymes. (A) ARTEMIS has three recognizable motifs: 1) the β-Lact homology domain 2) the β-CASP region and 3) the COOH-terminal domain. The β-CASP region is specific to members of the β-Lact superfamily of enzymes that acts on nucleic acids while metallo-β-lactamases are enzymes that were first described in bacteria due to their cleavage of the β-lactam ring of certain antibiotics. These domains of ARTEMIS comprise its catalytic core where ARTEMIS is responsible for 'nicking' open hairpin DNA ends and endonucleolytic cleavage of overhangs. **(B)** The metallo-β-lactamase/β-CASP domain is present in ARTEMIS and other DNA repair factors such as SNM1 and SNM1B, both critical in DNA repair mechanisms. This suggests a common role of these nucleases in processing DNA ends during DNA repair. (96).

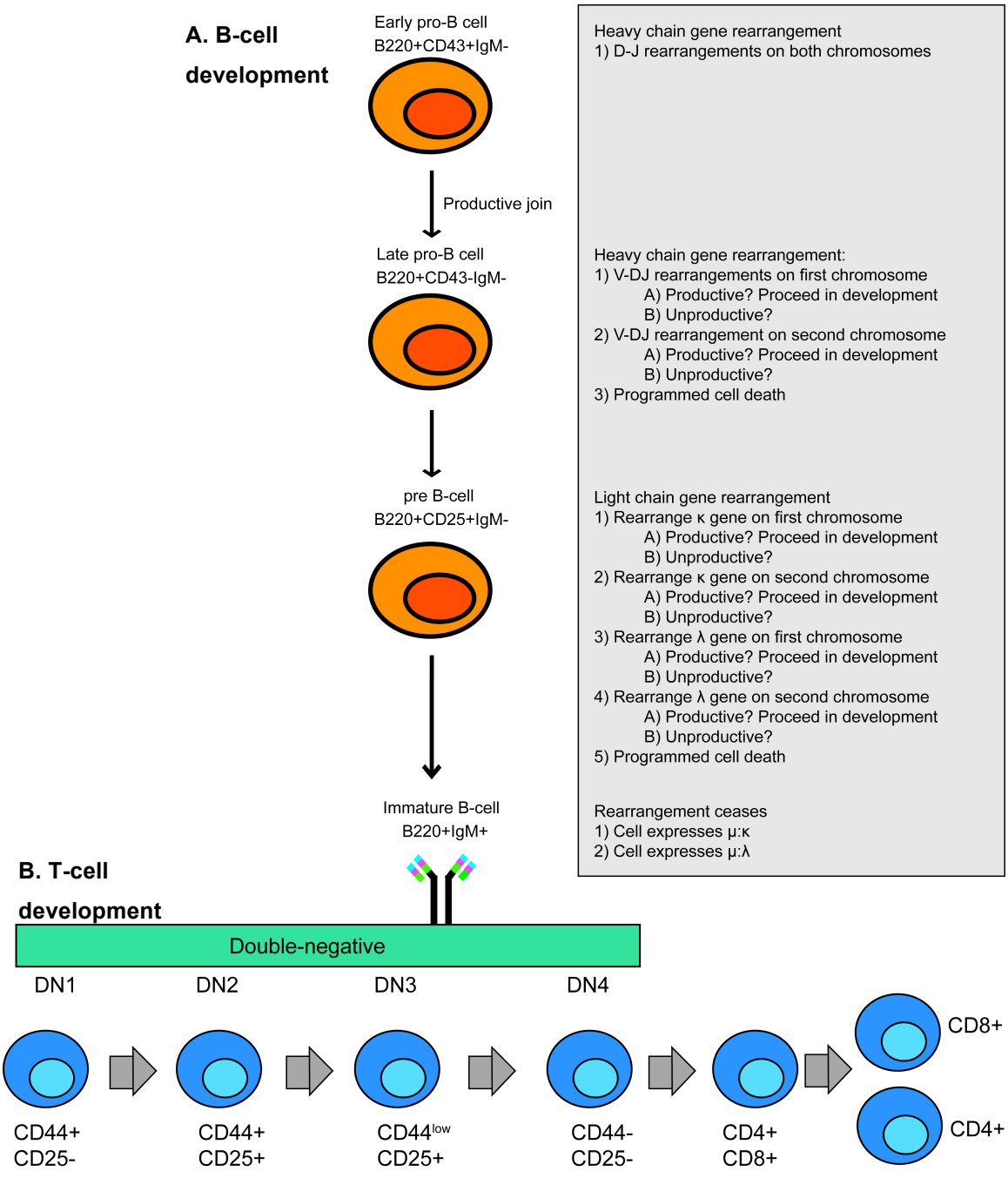
A. B-cell development
Early pro-B cell
B220+CD43+IgM-
Productive join
Late pro-B cell
B220+CD43-IgM-
pre B-cell
B220+CD25+IgM-
Immature B-cell
B220+IgM+
Heavy chain gene rearrangement
1) D-J rearrangements on both chromosomes
Heavy chain gene rearrangement:
1) V-DJ rearrangements on first chromosome
A) Productive? Proceed in development
B) Unproductive?
2) V-DJ rearrangement on second chromosome
A) Productive? Proceed in development
B) Unproductive?
3) Programmed cell death
Light chain gene rearrangement
1) Rearrange κ gene on first chromosome
A) Productive? Proceed in development
B) Unproductive?
2) Rearrange κ gene on second chromosome
A) Productive? Proceed in development
B) Unproductive?
3) Rearrange λ gene on first chromosome
A) Productive? Proceed in development
B) Unproductive?
4) Rearrange λ gene on second chromosome
A) Productive? Proceed in development
B) Unproductive?
5) Programmed cell death
Rearrangement ceases
1) Cell expresses μ:κ
2) Cell expresses μ:λ
B. T-cell development
Double-negative
DN1
DN2
DN3
DN4
CD44+
CD25-
CD44+
CD25+
CD44low
CD25+
CD44-
CD25-
CD4+
CD8+
CD8+
CD4+

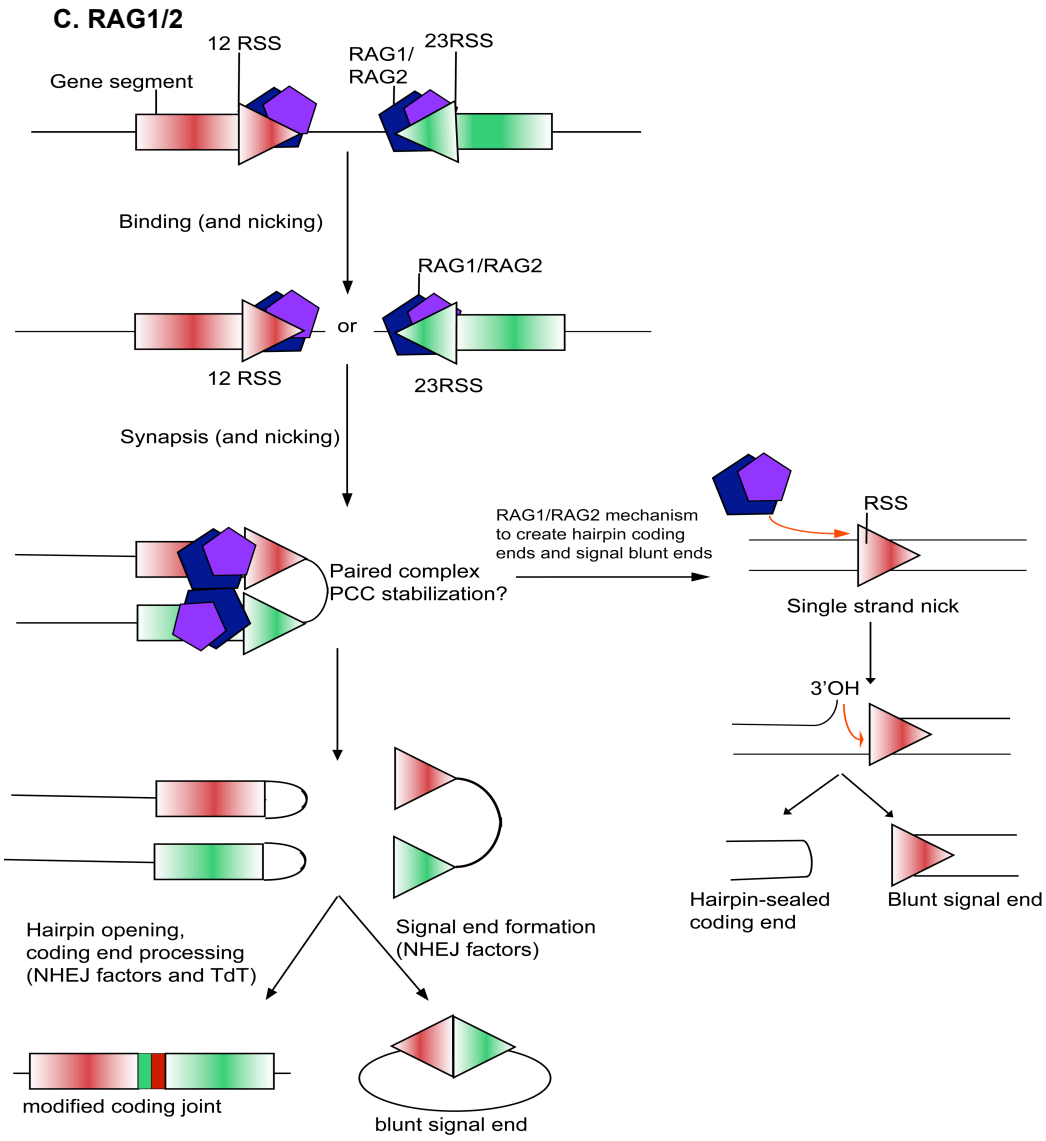

Figure 1.5 V(D)J recombination is initiated by the RAG1/2 complex. **(A)** B-cell development occurs early in development and is a highly regulated process that begins with rearrangement of V, D, or J gene segments, mediated by RAG1/2. Productive rearrangement of both the heavy and light chain results in expression of the variable region of the antigen receptor on the cell surface. **(B)** T-cell development relies upon productive rearrangements to progress to various developmental stages, initiated by the RAG1/2 complex. Productive rearrangements result in expression of an antigen receptor on the cell surface. **(C)** V, D, or J gene segments are flanked by a 12 recombination signal sequence (12RSS) or by a 23RSS. RAG proteins bind to the 12RSS/23RSS, forming the 12/23 signal complex, respectively. Capture of the second RSS (a process termed synapsis) results in the formation of the paired complex, within which the RAG proteins introduce DSBs between the gene segments and the RSSs resulting in two different DNA end structures that are repaired by cNHEJ (102) (109).

A.

cNHEJ genes	Patient phenotype	Murine phenotype; p53+		Murine phenotype; p53 null
Ku70$^{-/-}$ *Ku80*$^{-/-}$	Not reported	Growth retardation; Immunocomp		Immunocomp; cancer predisposition, **proB**
PRKDC-truncation mutants *Prkdc1*$^{-/-}$ *(DNA-Pkcs)*	Immunocomp	Immunocomp		Immunocomp; cancer predisposition, **proB**
DCLRE1C-C terminal truncation mutants *Dclre1c*$^{-/-}$ (Artemis)	Immunocomp; cancer predisposition (C-terminal truncation mutants)	Immunocomp; cancer predisposition (C-terminal truncation mutants)		Immunocomp; cancer predisposition, **proB**
LIG4-truncation mutants *Lig4*$^{-/-}$	Immunocomp; cancer predisposition	Embryonic lethal; Immunocomp		Immunocomp; cancer predisposition, **proB**
Xrcc4$^{-/-}$	Not reported	Embryonic lethal; Immunocomp		Immunocomp; cancer predisposition, **proB**
XLF-truncation mutants *Xlf*$^{-/-}$	Microcephaly; growth retardation; Immunocomp	Immunocomp		Immunocomp; cancer predisposition

B.

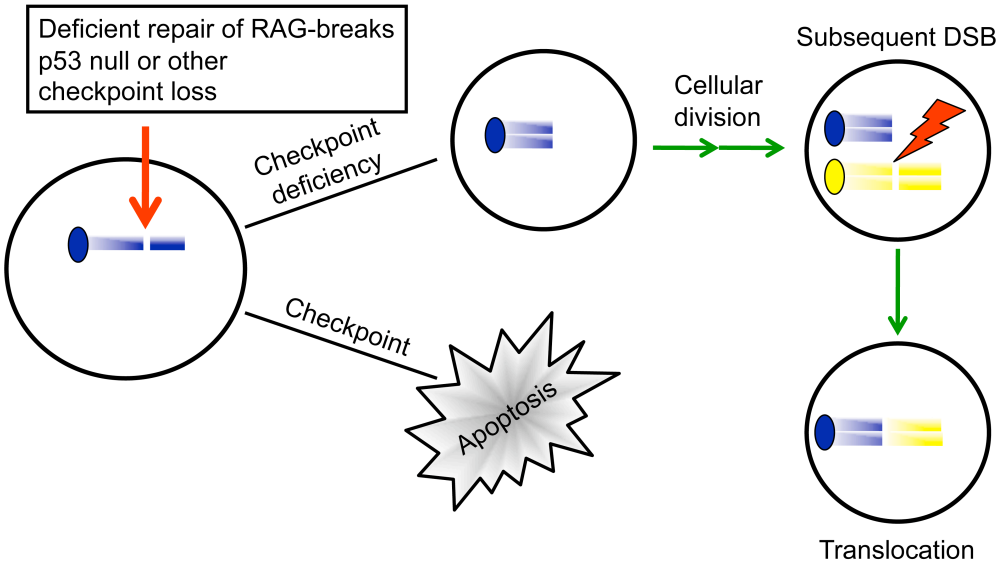

Figure 1.6 cNHEJ gene mutations result in immunodeficiency syndromes and cancer predisposition. (A) NHEJ factors are critical in the repair of RAG1/2-generated DSBs during V(D)J recombination as deficiency of any factor results in a developmental block in antigen receptor gene assembly and thus, antigen receptor expression. Murine mouse models of NHEJ patient mutations recapitulate the patient phenotype of immunodeficiency. **(B)** Combined cNHEJ/p53 mouse models are hypothesized to be predisposed to pro-B lymphoma due to defective checkpoints and misrepair of unrepaired RAG1/2-generated DSBs. In this figure, immunocomp is short for immunocompromised.

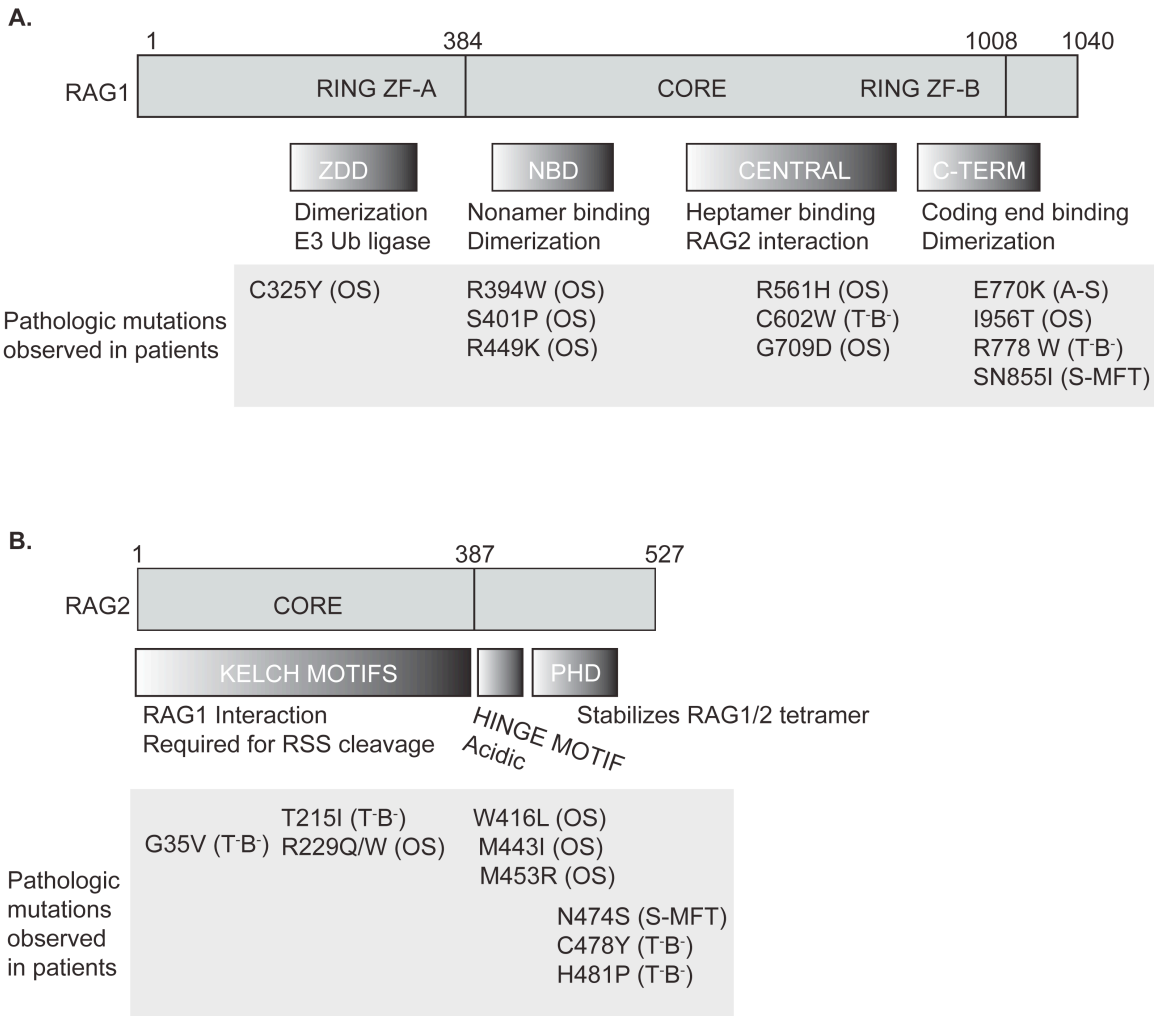

Figure 1.7 Diagram of RAG1 and RAG2 proteins with annotated patient mutations. (A) and **(B)** RAG1/2 mutations have been identified that cause a complete or partial loss of physiological V(D)J recombination activity and are associated with a spectrum of severe immune deficiency disorders ranging from classical T^-B^-SCID (T-B-) to slightly milder variants, such as complete or incomplete Omenn syndrome (OS), and RAG deficiency with γδ T cell expansion (A-S), granuloma formation, or maternofetal engraftment (S-MFT) (148).

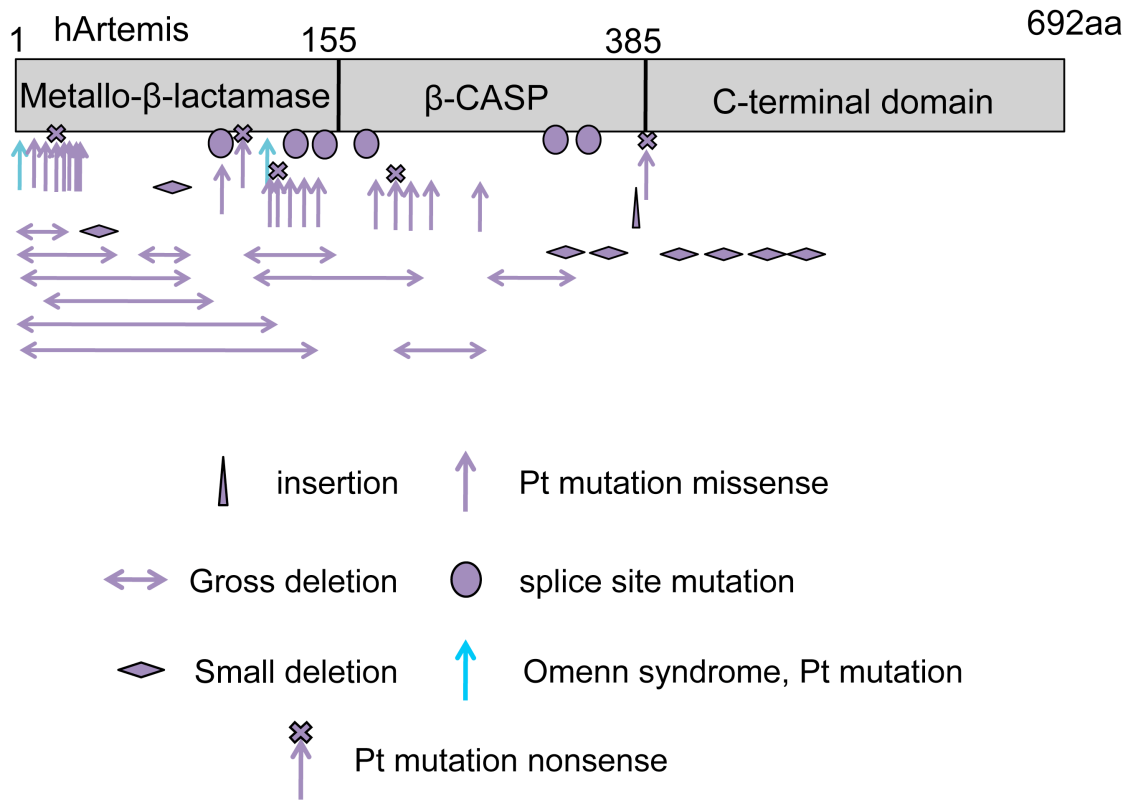

Figure 1.8 Schematic representation of the ARTEMIS protein with mutations annotated. Mutations cluster within the metallo-β-lactamase/β-CASP domain (aa 1-385) that comprises the nucleolytic core of ARTEMIS. A subset of mutations within this region result in inactivating, null ARTEMIS mutations. Some mutations outside of this region cluster within the non-conserved ARTEMIS C-terminus. These mutations result in partial immunodeficiency and predisposition to lymphoma (93, 152, 178, 213). Pt, point mutation. Mutations in violet result in immunodeficiency syndromes of varying severity. Mutations in bright turquoise result in Omenn syndrome, an autoimmunity disorder.

Disease	Gene	Cancer susceptibility	Immuno-deficiency	Other phenotypes
Ataxia Telangiecatasia-Like Disorder (ATLD)	*MRE11*	+/−	+/−?	Neuronal degeneration
Nijmegen Breakage Syndrome (NBS)	*NBS1*	+	+	Mental impairment Microcephaly
NBS-Like Disorder (NBSLD)	*RAD50*	?	−	Mental impairment Microcephaly
Ataxia Telangeictasia (AT)	*ATM*	+	+	Neuronal degeneration Ataxia
T^-B^- SCID	*PRKDC (DNA-PKcs)*	?	+	Immuno-deficiency
T^-B^- RS-SCID Omenn syndrome	*DCLRE1C (ARTEMIS)*	+/−	+	Radiosensitive Immuno-deficient Auto-immunitiy
Lig4 Syndrome	*LIG4*	+/−	+	Radiosensitive Growth defects Microcephaly
RS-SCID	*XLF*	−	+	Immuno-deficiency Radiosensitive Microcephaly

Figure 1.9 Deficiencies in DNA repair factors important for lymphocyte development can predispose to primary immunodeficiencies and lymphomas/leukemias. Summarized above is a list of DNA repair genes important for V(D)J recombination and CSR. The primary immunodeficiency phenotype largely affects both T- and B-cell development. Most deficiencies lead to cancer associated with translocations to the immunoglobulin (Ig) or T-cell receptor (TCR) loci (130, 134, 178, 201).

Allele	Allele type	Phenotypes
NBN$^{657\Delta5}$	Transgene, N-terminal trunction	S/G2 checkpoints, damage sensitivity, chromsomal instability, reduced ATM activity, impaired T-cell development, subfertility
NBN^{H45A}	Transgene, point mutation	S/G2 checkpoint defects, reduced ATM activity
NBN$^{S278/343A}$	Transgene, point mutation	None described
NBN^{tr735}	Transgene, C-terminal truncation	Apoptosis defect, reduced ATM activity
Mre11$^{\Delta}$	Conditional deletion	Embryonic lethality, reduced class swith recombination and DSB repair in B-cells (Cd19-Cre driven Cre), damage sensitivity
Mre11^{ATLD1}	C-terminal truncation	S/G2 checkpoint defects, damage sensitivity, chromosomal instability, reduced ATM activation and activity, defective apoptosis, reduced fertility
Mre11^{H129N}	Conditional allele with point mutation	Embryonic lethality, reduced class switch recombination in B-cells (Cd19-Cre), DNA repair defects and damage sensitivity, ATM activation independent of nuclease activities
Nbs1$^{\Delta6}$	Targeted deletion	Early embryoinic lethality
Nbs1$^{\Delta B}$	N-terminal truncation	S/G2 checkpoint defects, damage sensitivity, chromosomal instability, reduced ATM activity, subfertility
Nbs1$^{\Delta BC}$	N- and C-terminal truncations	S/G2 checkpoint defects, damage sensitivity, chromosomal instability, reduced ATM activity, subfertility, apoptosis defect
Nbs1$^{\Delta C}$	C-terminal truncation	Apoptosis defect, S phase checkpoint defect, reduced ATM activity
Nbs1^{F6}	Conditional deletions	Reduced class switch recombination in B-cells (Cd19-Cre), microcephaly, neuronal apoptossi, cerebellar defects and ataxia (nestin-Cre), lymphopenia, T-cell development defects (Lck-Cre)
Nbs1^{m}	N-terminal truncation	S/G2 checkpoint defects, damage sensitivity, chromosomal instability, reduced ATM activity, subfertility, cancer
Rad50$^{\Delta}$	Targeted deletion	Early embryonic lethality
Rad50^{ind} *Rad50*$^{-}$	Conditional deletion	Chromosomal instability and death in dividing cells(MX1-Cre, PCP2-Cre)
Rad50^{S}	Knock-in point mutation	Embryonic lethality, bone marrow failure, cancer predisposition sensitivity to topoisomerases

Figure 1.10 *Mre11* complex alleles and their associated phenotypes. Above is a summary explaining the various *Mre11* complex alleles and their associated phenotypes. Null alleles of the *Mre11* complex result in embryonic lethality. Conditional or hypomorphic *Mre11* complex alleles have enabled further characterization highlighting the importance of the complex in checkpoint activation, chromosomal stability, and lymphocyte development (42).

II. CHAPTER 2

A hypomorphic Artemis human disease allele causes aberrant chromosomal rearrangements and tumorigenesis

Cheryl Jacobs[1]*,Ying Huang[2]*, Tehmina Masud[1]*, William Lu[3], Gerwin Westfield[2], William Giblin[1] and JoAnn M. Sekiguchi[1,2,3]

[1]Department of Human Genetics, [2]Internal Medicine and [3]Cellular and Molecular Biology Program, University of Michigan Medical School, Ann Arbor, MI 48109, USA

Jacobs contribution: Western blot (Figure 3A), immunofluorescence (Figure 3C), Southern blot (Figure 5A, 5B), fluorescence in situ hybridization (Figure 6C)

This study resulted in a co-first author publication sited below:

Hum Mol Genet. 2011 Feb 15;20(4):806-19. doi: 10.1093/hmg/ddq524. Epub 2010 Dec 8.

Abstract

The *ARTEMIS* gene encodes a DNA nuclease that plays important roles in classical nonhomologous end joining (cNHEJ), a major double strand break (DSB) repair pathway in mammalian cells. cNHEJ factors repair general DSBs as well as programmed breaks generated during the lymphoid-specific DNA rearrangement, V(D)J recombination, which is required for lymphocyte development. Mutations that inactivate *ARTEMIS* cause a human severe combined immunodeficiency syndrome associated with cellular radiosensitivity. In contrast, hypomorphic *ARTEMIS* mutations result in combined immunodeficiency syndromes of varying severity, but, in addition, are hypothesized to predispose to lymphoid malignancy. To elucidate the distinct molecular defects caused by hypomorphic compared with inactivating *ARTEMIS* mutations, we examined tumor predisposition in a mouse model harboring a targeted partial loss-of-function disease allele. We find that, in contrast to *Artemis* nullizygosity, the hypomorphic mutation leads to increased aberrant intra- and interchromosomal V(D)J joining events. We also observe that dysfunctional ARTEMIS activity combined with p53 inactivation predominantly predisposes to thymic lymphomas harboring clonal translocations distinct from those observed in *Artemis* nullizygosity. Thus, the *Artemis* hypomorphic allele results in unique molecular defects, tumor spectrum and oncogenic chromosomal rearrangements. Our findings have significant implications for disease outcomes and treatment of patients with different *ARTEMIS* mutations.

Introduction

ARTEMIS (*DCLRE1C*, DNA crosslink repair 1C, OMIM#605988, but by convention it is annotated as *ARTEMIS*) was initially identified as the gene mutated in a human T^-B^- severe combined immunodeficiency associated with cellular radiosensitivity (RS-SCID) (1-3). ARTEMIS is a DNA nuclease that plays critical roles in the context of the classical nonhomologous end joining (cNHEJ) pathway of DNA double strand break repair (DSB) (4). The cNHEJ factors are required for processing and joining chromosomal ends during general DSB repair as well as V(D)J recombination, a lymphoid-specific DNA rearrangement (5, 6). V(D)J recombination is the process by which the vast array of antigen receptor genes are assembled from component V, D and J coding exons. During early lymphocyte development, the RAG1/2 endonuclease generates DSBs at specific recombination signal sequences (RSSs) that flank the numerous rearranging segments (6-8). Cleavage by RAG1/2 produces two end structures: covalently closed hairpin coding ends and 5′ phosphorylated, blunt RS ends. Prior to ligation, the hairpin coding ends are nicked open by the ARTEMIS endonuclease, which is activated upon interaction with the DNA-dependent protein kinase catalytic subunit (DNA-PKcs), a central cNHEJ factor (9). In the absence of ARTEMIS function, unopened hairpin coding ends accumulate in developing lymphocytes and remain unjoined (10). Thus, mutations that abrogate or reduce ARTEMIS activity result in defective V(D)J recombination and impaired B and T lymphocyte development.

Various mutant *ARTEMIS* alleles have been identified in association with inherited combined immunodeficiency syndromes, including missense, splice-site and nonsense mutations, gross exonic and smaller deletions and a small insertion (2, 11). The majority of mutations are located within a region encoding a highly conserved metallo-β-lactamase/βCASP N-terminal domain (aa 1–385) (12). A smaller subset of *ARTEMIS* alleles resides within a nonconserved C-

terminus (aa 386–692), and these mutations are small nucleotide deletions or insertions resulting in frameshifts followed by premature translation termination (12). Patients harboring null mutations suffer from an absence of B and T lymphocytes, whereas partial loss-of-function *ARTEMIS* alleles are associated with immunodeficiency syndromes of varying severity, including $B^{-/low}T^{-/low}$ SCID, $B^{-/low}$ SCID, chronic inflammatory bowel disease and Omenn syndrome (1, 11-24).

The unjoined DNA ends that accumulate in lymphocytes due to defects in the cNHEJ pathway can be misrepaired via alternative repair pathways, thereby leading to genome instability and potentially detrimental chromosomal aberrations, including oncogenic translocations (25). In this regard, partial B and T immunodeficiency and aggressive B cell lymphoma was observed in patients harboring a premature translation termination ARTEMIS mutation within exon 14, which encodes the non-conserved C-terminal domain (D451fsX10, referred to as P70, herein) (12). These lymphoid tumors were associated with Epstein-Barr virus. However, molecular analyses revealed that the lymphomas were of clonal origin, as evidenced by the rearrangement status of the immunoglobulin heavy chain locus, and also harbored chromosomal anomalies and increased genome instability (12). These features suggest that aberrant ARTEMIS activity contributes to oncogenesis; however, it has not yet been established whether hypomorphic ARTEMIS mutations can predispose to tumorigenesis. To date, patients harboring null *ARTEMIS* alleles have not been reported to exhibit lymphoid malignancies. These findings raise the possibility that partial loss of *ARTEMIS* alleles that lead to truncation of the nonconserved C-terminus may have greater oncogenic potential compared with complete null alleles.

ARTEMIS forms a complex with DNA-PKcs, a serine–threonine protein kinase, via interactions within the C-terminal domain (9). The ARTEMIS:DNA-PKcs complex possesses intrinsic endonucleolytic activities that can cleave DNA at single-to-double-strand transitions, including hairpins and 5′ or 3′ overhangs, as well as single strands (4, 9, 26-28). The ARTEMIS C-terminus undergoes extensive phosphorylation by DNA-PKcs (29-31). In vitro biochemical studies

with mutant forms of ARTEMIS harboring site-specific mutations revealed that DNA-PKcs-dependent phosphorylation is not required for activation of endonucleolytic activity (29). However, C-terminally truncated forms of ARTEMIS that retain stable interaction with DNA-PKcs but that lack the majority of phosphorylation sites, including the lymphoma-associated ART-P70 protein, exhibit reduced DNA-PKcs-dependent endonucleolytic activity (26, 32). In previous studies, we demonstrated that a mouse model harboring the ART-P70 mutation recapitulated the partial B and T immunodeficiency phenotypes observed in patients (32). We determined that lymphocyte development was impaired due to substantially reduced, but not abrogated, hairpin opening activity catalyzed by the ART-P70 mutant protein. Together, these results indicate that the ARTEMIS C-terminal domain plays important roles in modulating biochemical and in vivo ARTEMIS activities, in addition to facilitating DNA-PKcs interaction.

In this study, we examine the impact of the *Art-P70* hypomorphic allele on predisposition to tumorigenesis. We observe that loss of a functional region within the nonconserved ARTEMIS C-terminus leads to aberrant intra- and interchromosomal rearrangements within the antigen receptor loci. In addition, we find that the *Art-P70* allele in the context of p53 inactivation predisposes to a spectrum of B and T lymphoid malignancies that is distinct from that observed in Artemis nullizygosity. The tumors arising in an *Art-P70/p53* background are associated with clonal chromosomal translocations involving the rearranging loci due to misrepair of RAG1/2-generated DNA breaks. Together, these findings provide insights into the molecular basis of tumorigenesis associated with defective, but not abrogated, V(D)J recombination activity. In addition, the results uncover potential roles for ARTEMIS function in contributing to DNA end complex stability of RAG1/2-generated chromosomal breaks

Results

The *Artemis-P70* mutation results in elevated interchromosomal V(D)J rearrangements

We previously observed that the *Art-P70* homozygous mutation led to an accumulation of hairpin coding ends in developing lymphocytes; however, the levels were notably lower compared with *Artemis* nullizygosity (32). The presence of coding ends led us to determine whether the unjoined DSB intermediates engage in aberrant chromosomal rearrangements. To this end, we employed a nested polymerase chain reaction (PCR) approach to examine the levels of interchromosomal V(D)J rearrangements between the TCRβ (chr. 6) and TCRγ (chr. 13) loci in *Artemis*$^{P70/P70}$ and *Artemis*$^{-/-}$ thymocytes, followed by Southern blot analysis. Interchromosomal trans-rearrangement is a global predictor of chromosomal translocation (33, 34) and occurs at elevated frequencies in lymphocytes harboring mutations in genes that predispose to lymphoid neoplasia, including *Atm* (35-39), *Prkdcs (DNA-Pkcs)* (34), *Nbs1* (33, 38), and *53bp1* (40).

Initially, we examined levels of normal TCRγ V-to-J and TCRβ D-to-J rearrangements by PCR amplification. As previously reported, we observed that TCRβ D-to-J rearrangements in *Artemis*$^{P70/P70}$ thymocytes were reduced and were not readily detected in *Artemis*$^{-/-}$ thymocytes (Figure 1A) (10, 32). In comparison, products corresponding to TCRγ intrachromosomal V-to-J rearrangements were not significantly decreased in *Artemis*$^{P70/P70}$ and *Artemis*$^{-/-}$ thymocytes compared with controls. These findings indicate that the *Artemis*$^{P70/P70}$ and *Artemis*$^{-/-}$ mutations impair rearrangement at the TCRγ locus to a lesser extent compared with TCRβ rearrangements, as has been observed at the TCRδ locus in cNHEJ-deficient backgrounds, including *Artemis* nullizygosity (41-44).

Next, we determined whether trans-rearrangement occurs between loci on different chromosomes using PCR primers located upstream of TCRγV3S1 and downstream of TCRβJ2. As anticipated, we detected robust levels of trans-rearrangement between TCRγ and TCRβ in *Atm* null thymocytes (35-39). PCR products corresponding to interchromosomal V(D)J rearrangements in wild type or $p53^{-/-}$ thymocytes were not readily observed, as previously reported (Figure 2.1A) (33, 38, 45). Similar to $Atm^{-/-}$ lymphocytes, we detected substantially increased levels of interchromosomal events involving TCRγV3S1 and TCRβJ2 in $Artemis^{P70/P70}$ thymocytes (n=5) compared with controls, despite harboring lower levels of Dβ2-to-Jβ2 intrachromosomal rearrangements (Figure 2.1A, data not shown). On the contrary, we observed a lower frequency of trans-rearrangement in $Artemis^{-/-}$ thymocytes. In this regard, two of seven *Artemis* null mice harbored PCR products corresponding to TCRγ-to-TCRβ interchromosomal rearrangements (Figure 2.1A, data not shown), and the events appeared to be clonal as only a single band was observed, compared with multiple bands observed in $Artemis^{P70/P70}$ and $Atm^{-/-}$ thymocytes. Thus, the ART-P70 mutation increases the propensity of unrepaired coding ends to engage in aberrant interchromosomal translocations involving rearranging V(D)J loci. Moreover, this phenotype is distinct from that observed in *Artemis* null thymocytes which exhibit infrequent trans-rearrangements despite harboring a higher level of unjoined hairpin coding ends.

We next examined the frequency of interchromosomal rearrangements in *Art-P70* heterozygous thymocytes to determine whether the hypomorphic mutation results in a dominant phenotype. TCRγV3S1 to TCRβJ2 trans-rearrangements were readily detected in $Artemis^{+/P70}$ thymocytes in more than half (six of ten) of the mice examined (Figure 2.1B). However, fewer PCR products corresponding to distinct rearrangements and lower levels of interchromosomal events were observed in $Artemis^{+/P70}$ compared with $Artemis^{P70/P70}$ and $Atm^{-/-}$ thymocytes. The levels of TCRβ D-to-J rearrangements in $Artemis^{+/P70}$ thymocytes were similar to those observed in wild-type controls (Figure 2.1B). These findings indicate that the C-terminally truncated ART-P70

protein does not substantially disrupt proper coding end processing and joining, yet increases chromosomal anomalies, even when the wild-type enzyme is present.

The nested PCR products from ART-P70 mutant thymocytes were cloned and sequenced in order to verify that they represent the predicted interchromosomal events. We obtained several unique clones from four *Artemis*$^{P70/P70}$ mice containing flanking sequence from TCRγV3S1 and TCRβJ2, thereby indicating that the PCR primers indeed amplified V(D)J trans-rearrangements (Figure 2.1C). The junctions contained non-templated (N) and palindromic (P) nucleotides and small deletions, similar to the coding joints analyzed from intrachromosomal V(D)J recombination events in the *Artemis*$^{P70/P70}$ mice (32). We also cloned and sequenced the PCR products corresponding to the interchromosomal rearrangements obtained from *Artemis*$^{-/-}$ thymocytes. Sequencing of multiple clones yielded one unique sequence, thereby indicating that the single PCR product likely represents a clonal event (Figure 2.1C). These results support the notion that aberrant end processing due to the hypomorphic *Artemis*$^{P70/P70}$ mutation generates V(D)J ends that engage in chromosomal translocations at an elevated frequency compared with a complete absence of ARTEMIS.

The *Artemis-P70* mutation results in increased deletional chromosomal hybrid joining

Hybrid joint formation occurs between a coding and an RSS end and represents an unproductive V(D)J rearrangement. Inversional chromosomal rearrangements require that the two coding and two RSS ends generated by the RAG1/2 endonuclease are maintained in proximity in order to facilitate coordinated processing and ligation. Increased levels of deletional chromosomal hybrid joining during inversional V(D)J rearrangement are hypothesized to result from inappropriate release of RAG1/2-generated ends from DNA end complexes, thereby leading to the loss of the intervening genomic fragment (41, 46, 47). Our observations of increased interchromosomal rearrangements in *Artemis*$^{P70/P70}$, but not *Artemis*$^{-/-}$ lymphocytes, led us to examine the frequency of deletional

hybrid joining in these mutant backgrounds. To this end, we examined hybrid joint formation during IgL-k locus rearrangements in splenocytes. Productive rearrangement between Vk and Jk segments occurs via inversion; thus, hybrid joining results in deletion of the intervening DNA segment (Figure 2.2A). Using a nested PCR approach, we readily detected Vk to Jk hybrid joints in *Artemis*$^{P70/P70}$ splenocytes in the majority (three of four) of mutant mice analyzed (Figure 2.2A). The levels were lower than those observed in ATM deficiency, but markedly higher compared with wild type and *Artemis*$^{-/-}$ splenocytes. We also observed decreased levels of Vk to Jk coding joining in ART-P70 mutant splenocytes compared with controls; therefore, the relative frequency of deletional hybrid joining compared with inversional coding joining within the IgLk locus is substantially increased by the ART-P70 mutation. Within the TCRβ locus, Vβ14-to-DJβ2 rearrangements also occur via inversion; thus, we examined deletional hybrid joining between Vβ14 and Dβ2 via nested PCR. We detected increased levels of Vβ14–Dβ2 hybrid joints in Artemis$^{P70/P70}$ thymocytes (two of four), albeit at lower levels compared with ATM deficiency (Figure 2.2B). Hybrid joints were not detected in *Artemis*$^{-/-}$ thymocytes, as previously reported (Figure 2.2B) (48). Given our findings that interchromosomal rearrangements were detected in *Artemis*$^{+/P70}$ thymocytes, we assessed the impact of *Artemis-P70* heterozygosity on Vβ14–Dβ2 hybrid joining (Figure 2.2B). We also detected hybrid joints in a subset of *Artemis*$^{+/P70}$ mice examined (two of five), thereby providing additional evidence that the *Artemis-P70* allele may have a dominant effect in promoting aberrant rearrangements.

Examination of ATM- and MRN-dependent DNA damage responses in ARTEMIS-P70 cells

The increased levels of interchromosomal rearrangements and deletional hybrid joining observed in *Artemis*$^{P70/P70}$ lymphocytes parallel the phenotypes observed in *Atm*, *Mre11* and *Nbs1* mutant lymphocytes (41, 46, 47). These findings raise the possibility that the *Artemis-P70* allele impairs ATM-dependent responses to DNA DSBs and/or disrupts the functional MRE11/RAD50/NBS1 (MRN) complex. To address these questions, I examined key ATM-dependent

cellular responses to ionizing radiation (IR)-induced DSBs in *Artemis*$^{P70/P70}$ murine embryonic fibroblasts (MEFs). Upon exposure to IR, the ATM protein kinase undergoes autophosphorylation in an MRN-dependent manner (49, 50) and subsequently phosphorylates downstream targets, including the histone variant, H2AX (38, 51) and the transcriptional co-repressor, KAP1 (52). I examined the levels of phospho-ATM (p-ATM), phospho-H2AX (γH2AX) and phospho-KAP-1 (p-KAP1) in *Artemis*$^{P70/P70}$, *Artemis*$^{-/-}$ and wild type MEFs at 1 h post-irradiation by western blotting. I observed similar levels of IR-induced phosphorylation of ATM, H2AX and KAP1 in wild type, *Artemis*$^{P70/P70}$ and *Artemis*$^{-/-}$ cells (Figure 2.3A). These findings indicate that the *Artemis-P70* and null alleles do not significantly impair ATM-dependent responses to DSBs. We next assessed the impact of the *Artemis-P70* allele on the stability and localization of the MRN complex. We examined the levels of MRE11, RAD50 and NBS1 in whole-cell lysates and upon immunoprecipitation of the complex using anti-MRE11 antibodies in *Artemis*$^{P70/P70}$ MEFs and wild type controls by western blotting. We observed that the overall levels of MRE11, RAD50 and NBS1 in *Artemis*$^{P70/P70}$ MEFs were not different from those observed in control cells (Figure 2.3B). Furthermore, we observe similar levels of MRE11, RAD50 and NBS1 upon co-immunoprecipitation of MRE11 from *Artemis*$^{P70/P70}$ and wild type cells, thereby indicating that the MRN complex was not disrupted by the *Artemis-P70* allele (Figure 2.3B).

During repair of IR-induced DSBs, MRE11 localizes to sites of damage and forms repair foci that can be visualized as punctate staining by immunofluorescence (49, 53). It is thought that these foci gather at damaged DNA and represent large macromolecular complexes comprised of DNA repair factors in the DNA damage response. MRE11 foci formation requires the presence of an intact and functional MRN complex (49). I exposed *Artemis*$^{P70/P70}$, *Artemis*$^{-/-}$ and wild type MEFs to IR and quantitated the number of untreated and irradiated cells containing MRE11 foci. I observed that the *Artemis*$^{P70/P70}$ and *Artemis* null alleles did not reduce IR-induced MRE11 foci formation (Figure 2.3C). These results indicate that the ART-P70 mutation does not impair ATM-

and MRN-dependent DNA damage responses. Thus, these findings are consistent with the notion that the aberrant rearrangements observed in *Artemis*$^{P70/P70}$ lymphocytes are due to defects in ARTEMIS function at RAG1/2-generated DSBs.

Artemis-P70 predisposes to lymphoma in a p53 mutant background

The increased levels of aberrant rearrangements in *Artemis*$^{P70/P70}$ lymphocytes suggested that the ART-P70 mutation may increase the frequency of RAG1/2-generated DNA ends that engage in oncogenic translocations. To address this question, we examined cohorts of *Artemis*$^{P70/P70}$, *Artemis*$^{-/-}$ and wild type mice over a period of 12 months to determine whether the ART-P70 mutation predisposes to lymphoid or other tumors. We observed that two of fourteen *Artemis*$^{P70/P70}$ mice became moribund at 7 and 9 months of age as a result of large thymic masses (Figure 2.4A). Flow cytometric analyses revealed that the thymic lymphomas were primarily of a $CD4^+CD8^+TCR\beta^-$ origin (Figure 2.4B). In comparison, the wild type and *Artemis*$^{-/-}$ control cohorts survived tumor-free within the 12-month period, which is consistent with previous reports (54, 55). To further assess the oncogenic potential of the *Artemis-P70* hypomorphic allele, we examined the impact of p53 mutation on tumor predisposition through mouse breeding. The experimental cohorts were on a closely matched 129Sv/C57BL6 background, thereby minimizing potential strain background effects. However, a subtle impact of genetic background cannot be entirely ruled out. Inactivation of the p53-dependent cell-cycle checkpoint in ARTEMIS mutant lymphocytes allows cells harboring unrepaired DSBs or activated oncogenes to survive (56-60). We observed that *Artemis-P70/p53* double mutant mice exhibit significantly decreased survival compared with *p53*$^{-/-}$ controls (median survival of 11 and 18 weeks, respectively; p=0.001; Figure 2.4A). As previously reported, we found that *Artemis*$^{-/-}$*p53*$^{-/-}$ mice also exhibited decreased survival compared with *p53* null controls, and the median survival (13 weeks) was similar to that observed for *Art-P70/p53* double-deficient cohort (Figure 2.4A). We found that the *Artemis*$^{-/-}$*p53*$^{-/-}$ and *Artemis*$^{P70/P70}$*p53*$^{-/-}$ mice succumbed to lymphoid tumors. Flow cytometric analysis of the tumors revealed that *Artemis*$^{-/-}$*p53*$^{-/-}$ mice were

predominantly predisposed to disseminated $B220^+CD43^+IgM^-$ pro-B lymphomas, as has been previously reported (Figure 2.4B) (55). In contrast, the majority of tumors that arose in the *Art-P70/p53* double mutant background were $CD4^+CD8^+$ $TCR\beta^-$ thymic lymphomas (Figure 2.4B). $B220^+CD43^+IgM^-$ pro-B lymphomas were also observed in *Artemis*$^{P70/P70}$*p53*$^{-/-}$ mice, similar to *Artemis/p53* double null mice (Figure 2.4B) (55) albeit at a significantly lower frequency (p=0.014; two-tailed Fisher's exact test). These findings indicate that the *Artemis-P70* allele predisposes to lymphoid malignancies in a p53-deficient background, and the lymphoma spectrum observed in *Artemis*$^{P70/P70}$*p53*$^{-/-}$ mice is distinct from that observed in most cNHEJ/p53 double null backgrounds, including *Artemis*$^{-/-}$*p53*$^{-/-}$ mice (55, 60).

Distinct chromosomal anomalies associated with Art-P70/p53 lymphoid tumors

I next examined the status of the rearranging TCRβ and IgH loci in the lymphomas that arose in the *Artemis*$^{P70/P70}$*p53*$^{-/-}$ and *Artemis*$^{P70/P70}$ mice. Genomic DNA isolated from the primary tumors was digested with EcoRI and analyzed by Southern blotting. I used a probe located within the TCR Dβ1 to Jβ1 region to examine rearrangement status of the TCRβ locus. I observed that the *Artemis*$^{P70/P70}$*p53*$^{-/-}$ thymic tumors exhibited clonal rearrangements on one or both alleles, as evidenced by hybridization of specific bands that are distinct from the germline, unrearranged band or deletion of the hybridizing region (Figure 2.5A). Similarly, the two *Artemis*$^{P70/P70}$ tumors exhibited clonal D to Jβ rearrangements (data not shown). These results indicate that the thymic lymphomas emanated from a clonal event within the population of developing ART-P70 mutant thymocytes.

I also analyzed the rearrangement status of the IgH locus in *Art-P70/p53* pro-B lymphomas by Southern blotting EcoRI digested genomic DNA from primary tumors (Figure 2.5B). Previous analyses of *Artemis*$^{-/-}$*p53*$^{-/-}$ pro-B lymphomas by Southern blotting revealed clonal rearrangements and amplification of the J_H locus. I observed these similar events in one *Artemis*$^{P70/P70}$*p53*$^{-/-}$ pro-B lymphoma (C263). However, pro-B tumors, C219 and

C318, did not exhibit clonal IgH rearrangement or amplification, as only the germline band was present. It is possible that the region encompassing the probe was deleted from one of the two rearranging IgH alleles. Thus, I further analyzed the molecular events occurring in the *Art-P70/p53* double mutant tumors. One recurrent event within the IgH locus observed in *Artemis*$^{-/-}$*p53*$^{-/-}$ pro-B lymphomas is amplification of regions downstream of the J_H region. I used probes comprised the Cμ constant region and 3′ enhancer regulatory region located approximately 5 and 170 kb, respectively, from the rearranging J_H segments. I observed amplification with the more distal probes in tumor C263, but not in the other *Artemis*$^{P70/P70}$*p53*$^{-/-}$ pro-B lymphomas analyzed (Figure 2.5B). I next examined the status of the *c-myc* and *n-myc* loci, as amplification of either genomic region is associated with *Artemis*$^{-/-}$*p53*$^{-/-}$ pro-B tumors. Southern blotting revealed genomic amplification of the *n-myc* locus in tumor C263 (Figure 2.5B), and I determined that N-MYC expression was elevated by northern blot and semi-quantitative RT-PCR analyses (Figure 2.5C, data not shown). Thus, this Artemis$^{P70/P70}$p53$^{-/-}$ pro-B lymphoma harbors the established hallmark events observed in *Art/p53* double-mutant tumors, i.e. increased copy number of the IgH and *n-myc* genomic loci. However, I did not observe genomic amplification of either *c-myc* or *n-myc* in the C219 and C318 *Artemis*$^{P70/P70}$*p53*$^{-/-}$ pro-B tumors, providing further distinction between lymphomas arising in the *Artemis-P70* versus *Artemis* null backgrounds.

Spectral karyotyping and fluorescence in situ hybridization analyses of *Art-P70/p53* double-mutant lymphomas

I next examined the cytogenetic events occurring in *Art-P70/p53* double-mutant lymphomas using spectral karyotyping (SKY) and fluorescence in situ hybridization (FISH) analyses. I performed SKY on metaphase spreads from seven *Artemis*$^{P70/P70}$*p53*$^{-/-}$ thymic lymphomas. I observed that all of the *Art-P70/p53* tumors analyzed contained non-reciprocal clonal translocations involving chromosomes harboring rearranging loci (Figure 2.6A and 2.6B). In this regard, five tumors harbored clonal events involving chr. 14, the location of the TCRαδ locus, translocated to chr. 1, 2, 4 or 12 (Figure 2.6A). It is of interest to note that the IgH locus is located on chr. 12, and in addition to the t(12;14)

translocation in tumor C306, I also observed t(12;11) and t(12;1) clonal events in tumors C262 and C268, respectively. One tumor, C227, also harbored clonal events involving chr. 13 (TCRγ) translocated to chr. 6 (TCRβ) (Figure 2.6A and 2.6B). I analyzed one *Artemis*$^{P70/P70}$*p53*$^{-/-}$ pro-B lymphoma, C219, by SKY and observed that, similar to other reported *cNHEJ/p53* double null tumors, it harbored a t(12;15) non-reciprocal translocation (Figure 2.6A).

SKY analyses can effectively identify gross chromosomal anomalies; however, genomic loci that may be amplified or co-localized cannot be accurately detected using this technique. Thus, I further analyzed the metaphases from *Art-P70/p53* lymphomas using a two-color FISH approach. I established that thymic lymphomas, C325 and C306, harbored clonal chr. 14 anomalies using bacterial artificial chromosome (BAC) probes comprised of genomic sequences located upstream and downstream of the rearranging TCRαδ locus. In this regard, I observed co-localization of the probes in control metaphases, whereas the two probes were clearly located on different chromosomes in metaphases from the *Artemis*$^{P70/P70}$*p53*$^{-/-}$ thymic tumors (Supplementary Material, Figure 2S7). In tumor C306, we also observed co-localization of the IgH and TCRαδ BAC probes, as anticipated based on the t(12;14) identified by SKY (Figure 2.6C). Likewise, I found co-localization of BAC probes containing TCRβ and TCRγ genomic sequences in tumor C227. Tumor C262 harbored separated single-copy FISH signals using BACs located upstream and downstream of the IgH locus on chr. 12 (Supplementary Material, Figure 2S7). Thus, the *Artemis*$^{P70/P70}$*p53*$^{-/-}$ thymic lymphomas harbored chromosomal aberrations and translocation events that involved the loci undergoing V(D)J recombination. However, I did not observe amplification of the rearranging loci examined in the thymic lymphomas (Figure 2.6C and Supplementary Material, Figure 2S7). FISH analyses of metaphases from *Art-P70/p53* pro-B lymphoma, C219, revealed separation of single-copy signals using the upstream and downstream IgH probes, thereby suggesting that RAG1/2-generated DSBs within the rearranging locus initiated the aberrant events (Supplementary Material, Figure 2S7). I also observed co-localization of the FISH signals corresponding to c-myc (chr. 15) and IgH loci, as predicted

based on the SKY results. However, distinct from the hallmark co-amplification observed in other *cNHEJ/p53* double null pro-B tumors, no amplification of either signal was found (Figure 2.6C). These findings are consistent with the Southern blot analyses that did not detect amplification using probes within the c-myc, JH, Cμ or HS3A loci.

Previous studies of other *cNHEJ/p53* double null pro-B lymphomas, including *Artemis*$^{-/-}$*p53*$^{-/-}$ tumors, established that genomic amplification of the *c-myc* locus was associated with elevated C-MYC expression levels in the tumor cells (55, 60). As I did not observe amplification of *c-myc* by Southern or FISH analyses, we sought to determine whether the oncogene may be dysregulated by a distinct mechanism in the *Artemis*$^{P70/P70}$*p53*$^{-/-}$ tumor, C219, which harbored the t(12;15) translocation and co-localization of *c-myc* and IgH FISH probes. Thus, we examined expression levels of C-MYC in primary tumor cells compared with control cells by semiquantitative RT-PCR (Figure 2.5C). We observed a substantial increase in C-MYC expression in the C219 *Art-P70/p53* pro-B lymphoma, comparable to that observed in a control *Artemis*$^{-/-}$*p53*$^{-/-}$ tumor (C405) which harbored the hallmark *c-myc* and IgH amplicon (Figure 2.5C and Supplementary Material, Figure 2S7). These results suggest that elevated C-MYC expression observed in the *Art-P70/p53* mutant background results from a mechanism independent of genomic amplification and thus distinct from that observed in *Artemis*$^{-/-}$*p53*$^{-/-}$ tumors.

Discussion

In this study, we demonstrate that a hypomorphic *Artemis* mutation that results in partial B and T immunodeficiency and EBV-associated lymphoma in patients increases the frequency of aberrant chromosomal rearrangements in primary lymphocytes and predisposes to lymphoid malignancy in a mouse model harboring the human disease allele. The ART-P70 mutation, which truncates the non-conserved C-terminus, results in elevated levels of V(D)J trans-rearrangements between loci located on different chromosomes and deletional hybrid joining in homozygous and heterozygous mutant lymphocytes. In comparison, undetectable or substantially lower levels of these chromosomal anomalies are present in *Artemis* null lymphocytes, thereby indicating that loss of functional regions within the C-terminal domain increases the potential for the DSB intermediates to engage in aberrant repair events.

Previously, we demonstrated that a mutant ARTEMIS protein modeled after the *Artemis-P70* allele, ART-D451X, interacted stably with DNA-PKcs and exhibited reduced DNA-PKcs-dependent endonucleolytic activity (32). In addition, we found that loss of the C-terminal 241 amino acids markedly reduced DNA-PKcs-dependent phosphorylation due to deletion of the majority of phosphorylation sites. We hypothesized that these defects may impair the ability of ARTEMIS to associate with and properly act upon DNA ends. Consistent with this notion, hairpin coding ends accumulate in *Artemis*$^{P70/P70}$ developing lymphocytes, whereas nicked hairpins with blunt or 5′ or 3′ overhanging ends are not detected (32). In the current study, we observed increased levels of interchromosomal V(D)J rearrangements and deletional hybrid joints within the IgLk and TCRβ loci in *Artemis*$^{P70/P70}$ primary lymphocytes. The mechanism underlying these events presumably involves inappropriate release of RAG-generated DNA ends from post-cleavage complexes prior to joining (41, 46, 47). In contrast, these aberrant rearrangements occur infrequently in *Artemis* null

lymphocytes (Figure 2.1 and Figure 2.2) (48), despite harboring significantly higher levels of hairpin coding ends compared with ART-P70 mutant lymphocytes (32). Although open hairpins are not detected in *Artemis*$^{P70/P70}$ lymphocytes, it is possible that a low level of nicked coding ends is present, and these end structures may be more likely to engage in aberrant events. However, interchromosomal rearrangements and deletional hybrid joining occur infrequently in wild type lymphocytes in which hairpins are efficiently cleaved by ARTEMIS. Likewise, coding ends in normal lymphocytes rarely serve as substrates for oncogenic translocations, even in a p53-deficient background which permits RAG1/2-generated ends to persist throughout the cell cycle (40, 41, 55, 56, 61-66). Thus, the *Artemis-P70* allele likely causes molecular defects in coding end processing and joining beyond impaired hairpin nicking.

Mutations in *Atm*, *Mre11* or *Nbs1* significantly increase the frequency of aberrant chromosomal rearrangements in mutant lymphocytes, including interchromosomal trans-rearrangements and deletional hybrid joint formation (33, 35-37, 39, 41, 42, 46, 47). These observations led to the hypothesis that the ATM kinase and MRN complex function during V(D)J recombination to enhance DNA end complex stability and promote proper joining of RAG1/2-generated breaks (41, 46, 47). Our findings suggest that truncation of the C-terminus impairs functions of ARTEMIS within post-cleavage DNA end complexes, thereby leading to inappropriate release and altered handling of V(D)J recombination intermediates. It is of interest to note that ATM phosphorylates ARTEMIS at residues S503, S516 and S645, which are located within the C-terminal region that is deleted in the ART-P70 mutant protein (29). ATM does not play a direct role in V(D)J recombination per se as ATM-deficient cells exhibit wild-type levels of V(D)J recombination on extra-chromosomal plasmid substrates (67). However, ATM deficiency in mice leads to accumulation of V(D)J coding end intermediates, impaired lymphocyte development and aberrant, potentially oncogenic, chromosomal rearrangements (39, 68-72). Although ATM-dependent phosphorylation of ARTEMIS is not required to activate intrinsic endonucleolytic activity in vitro nor is it required for V(D)J recombination on model plasmid

substrates in cells (29), our findings raise the possibility that ATM phosphorylation may modulate ARTEMIS functions during chromosomal V(D)J rearrangements to facilitate the stabilization of DNA end complexes in vivo.

We propose that the ART-P70 mutant protein is recruited to DNA ends via interaction with DNA-PKcs (32), and activation of DNA-PKcs upon autophosphorylation induces large conformational changes to allow the nuclease access to the hairpins (29, 73, 74). Truncation of the ARTEMIS C-terminal region that contains ATM and DNA-PKcs phosphorylation sites may prevent stable association within conformationally altered DNA end complexes that are poised for further end processing events. Inappropriate release of the RAG1/2-generated ends from aborted post-cleavage complexes would render the ends more susceptible to misrepair, thereby increasing their potential to generate chromosomal aberrations, including oncogenic translocations (41).

We demonstrate that the ART-P70 mutation in a p53 null background accelerates the timing of tumor onset compared with p53 mutation alone. *Art-P70/p53* double mutant mice predominantly succumb to $CD4^+CD8^+TCR\beta^-$ thymic lymphomas that are associated with clonal chromosomal translocations involving the TCR or IgH loci; however, the majority of tumors do not harbor the hallmark gene amplification events observed in *cNHEJ/p53* double null lymphomas, including those arising in *Artemis*$^{-/-}$*p53*$^{-/-}$ mice (55). We found that the *Artemis*$^{P70/P70}$*p53*$^{-/-}$ and *Artemis*$^{-/-}$*p53*$^{-/-}$ lymphomas arise with a similar latency, despite our observation of substantially higher levels of aberrant interchromosomal rearrangements in ART-P70 mutant lymphocytes. One potential explanation for these observations is that the timing of lymphoma incidence is influenced by the particular oncogenic events associated with tumorigenesis. In this regard, genomic amplification leading to elevated expression of *c-myc* or *n-myc* in Artemis$^{-/-}$p53$^{-/-}$ lymphomas may lead to a higher proliferative potential compared with oncogenic events in the Artemis$^{P70/P70}$p53$^{-/-}$ background, thereby accelerating tumorigenesis in *Artemis/p53* double null mice.

The frequently arising *Artemis*$^{P70/P70}$*p53*$^{-/-}$ thymic lymphomas are associated with clonal translocations involving chr. 6, 12, 13 and 14 which harbor

the murine TCRβ, IgH, TCRγ and TCRαδ loci, respectively, with chr. 14 translocations observed in the majority of the tumors analyzed. Cytogenetic analyses of activated T-cells isolated from human lymphoma patients harboring the hypomorphic allele modeled in the ART-P70 mouse and a similar C-terminal truncating mutation (T432SfsX16) revealed a translocation of chr. 7 and 14 and inversion of chr. 7, respectively (75). In humans, the rearranging IgH and TCRαδ loci reside on chr. 14, whereas TCRγ and TCRβ reside on chr. 7. Thus, the *Artemis-P70* hypomorphic allele results in translocations involving chromosomes that undergo V(D)J recombination in both human and murine lymphocytes.

The precise mechanisms underlying the distinct molecular events observed in *Art-P70/p53* lymphomas have not yet been elucidated. Inactivation of the p53-dependent cell-cycle checkpoint has been hypothesized to allow unrepaired RAG-induced DNA ends generated during G1 to persist throughout the cell cycle and undergo mis-repair by alternative DSB repair pathways (56, 60, 76). We speculate that unjoined coding ends in *Artemis*$^{P70/P70}$ versus *Artemis* null lymphocytes may be repaired by distinct pathways that function during different cell-cycle phases. Consistent with this notion, the junctional sequences of both intra- and interchromosomal V(D)J rearrangements in Artemis$^{P70/P70}$ lymphocytes are characteristic of joining mediated by the cNHEJ pathway (Figure 1) (32). In comparison, an alternative pathway generates aberrant V(D)J junctions containing large deletions and long P-nucleotide additions in *Artemis*$^{-/-}$ lymphocytes (10) and microhomology mediated translocations in *Artemis*$^{-/-}$*p53*$^{-/-}$ lymphomas (55). An alternative, though not mutually exclusive, hypothesis is that defects in DNA end complex stability in ART-P70 mutant lymphocytes allow unrepaired breaks to be aberrantly localized in three-dimensional space and engage in translocations that do not require the chromosomal partner to be located in proximity. In this regard, recent studies have provided evidence that loci involved in recurrent oncogenic translocations are located in proximity in lymphocytes (77-79). This hypothesis does not preclude amplification from occurring in the ART-P70 background, and indeed we did observe *n-myc* amplification in one *Artemis*$^{P70/P70}$*p53*$^{-/-}$ pro-B lymphoma (C263). It will be of

significant interest to further define the molecular mechanisms underlying the oncogenic translocations in *Art-P70/p53* tumors.

Together, these studies provide insight into the consequence of truncation of the ARTEMIS C-terminal domain on the fate of chromosomal DNA ends during endogenous V(D)J rearrangements. Our findings support the notion that loss of the ARTEMIS C-terminus impacts the proper processing and joining of DNA ends via destabilization of end bound complexes that coordinate recombination events. These findings have important clinical implications in the identification and treatment of human immunodeficiency patients harboring similar *ARTEMIS* mutations that may predispose to aberrant rearrangements and lymphoid malignancy.

Materials and Methods

Mice

Gene-targeted *Atm* null, *Artemis* null and *Artemis-P70* mice (mixed 129Svev/C57BL6 genetic background) were previously generated (10, 32, 80, 81). p53 mutant mice (Trp53tm1Tyj) in a 129S2/Sv background were obtained from Jackson Laboratory and bred with *Artemis*$^{-/-}$ and *Artemis*$^{P70/P70}$ animals. Double heterozygous *Artemis*$^{+/-}$*p53*$^{+/-}$ and *Artemis*$^{+/P70}$*p53*$^{+/-}$ mice were subsequently interbred to generate progeny of the desired genotypes for the tumorigenesis studies (i.e. *Artemis*$^{+/+}$*p53*$^{+/+}$, *Artemis*$^{-/-}$*p53*$^{+/+}$, *Artemis*$^{-/-}$*p53*$^{-/-}$, *Artemis*$^{P70/P70}$*p53*$^{+/+}$, *Artemis*$^{P70/P70}$*p53*$^{-/-}$ and *Artemis*$^{+/+}$*p53*$^{-/-}$). The single- and double-mutant mice as well as wild type controls used in this study were approximately 75% 129Sv and 25% C57Bl6; thus, the experimental cohorts are closely strain matched. Mice were housed in a specific pathogen-free facility in a room dedicated to immunocompromised animals.

Interchromosomal V(D)J rearrangements

Nested PCR amplification reactions used to detect TCRγ intrachromosomal and TCRγ-to-TCRβ interchromosomal trans-rearrangements were modified from methods as described previously (34). Genomic DNA (100 ng) obtained from thymocytes isolated from 4- to 5-week-old mice [*Artemis*$^{+/+}$ (n=3), *Artemis*$^{-/-}$ (n=7), *Artemis*$^{P70/P70}$ (n=5), *Artemis*$^{+/P70}$ (n=10)] was amplified in 50 µl of reaction mixture containing set ‘a’primers (10 pmol). The cycling conditions were: denaturation at 95°C, 30 cycles of amplification at 95°C for 15 s, 55°C for 15 s, 72°C for 30 s with a 6-s increment per cycle followed by 10 min elongation at 72°C. The products from the first reaction (5 µl) were used in a nested PCR reaction with the same conditions using primers set ‘b’. The final PCR products (25 µl) were run on a 1.5% agarose gel followed by Southern blotting using probes (primers set ‘c’) internal to the primers used for PCR

amplification (see Supplementary Material). The second-round PCR products were subcloned into pCR 2.1-TOPO (Invitrogen; Carlsbad, CA, USA) and individual clones were sequenced. TCRβ Dβ2-to-Jβ2 intrachromosomal rearrangements were PCR amplified from thymic genomic DNA (100 ng) at an annealing temperature of 62°C (35 cycles). Each experiment was repeated at least thrice independently.

Hybrid join analysis

To analyze the levels of coding and hybrid joints between Vκ6–23 and Jκ1, PCR assays were used as described previously (47). Genomic DNA (0.5 μg) isolated from mouse splenocytes for each genotype (*Artemis*$^{P70/P70}$; n=4) was PCR amplified in 50 μl with 15 pmol of each primer. PCR conditions were as follows: 95°C for 5 min followed by 17 cycles of 94°C (30 s), 64°C (30 s), 72°C (30 s). A second PCR reaction was carried out under the same conditions for 25 amplification cycles using 4-fold dilutions of the first PCR reaction and nested primer pairs. The HJ and CJ PCR products were transferred to Zetaprobe membrane and hybridized with pβg oligonucleotide. For normalization, 4-fold dilutions starting with 0.5 μg of genomic DNA were PCR amplified. For Vβ14 coding and hybrid joint analysis, genomic DNA (0.5 μg) was isolated from mouse thymocytes for each genotype [*Artemis*$^{P70/P70}$ (n=2), *Artemis*$^{+/P70}$ (n=5)], and PCR analysis was performed as described (47). The PCR products were analyzed by Southern blotting using the pβg oligonucleotide as a probe.

Western blot analysis of ATM-dependent responses to IR

Artemis$^{+/+}$, *Artemis*$^{-/-}$, *Artemis*$^{P70/P70}$ and *Atm*$^{-/-}$ mouse embryonic fibroblasts (SV40 large T-antigen immortalized) were plated at a density of 3.5×10^6 cells per 10-cm dish then exposed to 10 Gy of γ-rays from a 137Cs source. The cells were allowed to recover for 1 hour and then harvested in Laemmli buffer (4% sodium dodecyl sulfate, 20% glycerol, 120 mM Tris–HCl, pH 6.8). Equivalent amounts of whole-cell lysates were resolved on either a 12 or 6% sodium dodecyl sulfate–polyacrylamide gel electrophoresis (SDS–PAGE) gel and transferred to polyvinylidene fluoride membrane. Primary antibodies used were: γH2AX S139

(1:1000, Millipore; Billerica, MA, USA); pKAP1 S824 (1:500, Bethyl Laboratories; Montgomery, TX, USA); pATM S1981 (1:500, Rockland; Gilbertsville, PA, USA). This experiment was repeated thrice independently.

Co-immunoprecipitation of the MRN complex

Artemis$^{+/+}$ and *Artemis*$^{P70/P70}$ mouse embryonic fibroblasts were grown to confluency, harvested and then lysed in a buffer containing 25 mM HEPES, pH 7.4, 150 mM KCl, 10 mM $MgCl_2$, 10% glycerol, 2 mM DTT and protease inhibitors (Roche; Basel, Switzerland). Protein concentrations were determined using the Bradford assay. Lysates (6 mg) were pre-cleared for 1 hour with protein G beads (GE Healthcare) at 4°C, then incubated with α-MRE11 antibody (4.5 µg; Cell Signaling) and protein G beads overnight at 4°C with constant rotation. The beads were washed twice with lysis buffer followed by two washes in lysis buffer containing 300 mM KCl. The immunoprecipitates were analyzed by 8% SDS–PAGE followed by western blotting with α-MRE11 (Cell Signaling; Danvers, MA, USA), α-Nbs1 (Novus Biologicals; Littleton, CO, USA) and α-Rad50 (Bethyl Laboratories; Montgomery, TX, USA) antibodies. The protein bands were visualized using IRDye800CW-conjugated goat anti-rabbit secondary antibody (LiCor Biosciences; Lincoln, NE, USA). The co-IPs were repeated thrice independently.

Immunofluorescence analysis of MRE11 foci

Artemis$^{+/+}$, *Artemis*$^{-/-}$ and *Artemis*$^{P70/P70}$ mouse embryonic fibroblasts (SV40 large T-antigen immortalized) were plated at a density of $2x10^5$ cells per well of a 12-well dish and then exposed to 10 Gy of γ-rays from a 137Cs source. Cells were allowed to recover for 8 hours and then fixed in 4% paraformaldehyde solution (4% paraformaldehyde, 2% sucrose, pH 7.5) followed by treatment with a permeabilization solution (50 mM NaCl, 3 mM $MgCl_2$, 200 mM sucrose, 10 mM HEPES, pH 7.9, 0.5% Triton X-100), as previously described (82). Fixed cells were incubated for 1 hour in phosphate buffered saline (PBST), 0.1% Tween-20 incubated with primary antibody MRE11 (1:500, Cell Signaling; Danvers, MA, USA) for 1 hour and then incubated with secondary antibody for 1 hour

(AlexaFlour 488, donkey anti-rabbit IgG; Invitrogen). Images were visualized using an Olympus BX-61 microscope. Cells containing greater than 20 Mre11 foci were considered foci-positive, and approximately 40–50 cells were scored for each genotype. The slides were scored blinded, and the experiment was repeated twice independently.

Characterization of tumors

All mice were regularly monitored for tumors and analyzed when moribund. Lymphoid tumors were analyzed by flow cytometry with antibodies against surface B-cell (CD43, B220, IgM) and T-cell (CD4, CD8, CD3, TCRβ, CD44, CD25) markers. Thymic and pro-B lymphomas were cultured in RPMI medium 1640 supplemented with 15% fetal calf serum, 25 U/ml IL-2 (BD Biosciences) and 25 ng/ml of IL-7 (PeproTech, Rocky Hill, NJ, USA). The proportion of pro-B and thymic lymphomas in the *Artemis*$^{P70/P70}$*p53*$^{-/-}$ cohort was calculated to be statistically significantly different from that observed for *Artemis*$^{-/-}$ *p53*$^{-/-}$ lymphomas (P=0.014, two-tailed Fisher's exact test). Data for *Artemis*$^{-/-}$ *p53*$^{-/-}$ tumors also in a mixed 129Sv/C57BL6 genetic background from a previous publication (55) were included in the calculation (total of 13 lymphomas: 10 pro-B and 3 thymic).

Chromosomal analyses of tumor metaphases

Spectral karyotyping was performed on metaphases from cells derived from the primary tumor or early passage cultured tumor cells using an interferometer (Applied Spectral Imaging; Vista, CA, USA) and SkyView software. For fluorescent in situ hybridization analyses, early passage tumor cultures were exposed to 100 ng/ml Colcemid for 5.5 hour BAC probes for fluorescent in situ hybridization analysis were obtained from the RPCI-23 library (Children's Hospital Oakland Research Institute; Oakland, CA, USA) and nick-translated using biotin-11-dUTP or digoxigenin-16-dUTP by standard procedures (Roche; Basel, Switzerland). BAC probes hybridizing to TCRα/δ are as follows: RPCI-23 204N18 (centromeric to TCRα/δ region) and RPCI-23 269E2 (telomeric to TCRα/δ region). BAC probe hybridizing to TCRβ are as follows:

RPCI-23 216J19 (spans TRBD1–TRBV31). BAC probe hybridizing to TCRγ are as follows: RPCI-23 212N5 (within TCRγ). BAC probes hybridizing to IgH are as follows: N-myc BAC A-10-1[54], Bac199 (hybridizes to Cα), Bac 207 (hybridizes to V region). c-myc BAC probe was previously described[83]. At least 10 metaphases for each tumor were analyzed by spectral karyotyping and at least 20 metaphases by fluorescent in situ hybridization.

Southern blot and RT-PCR analyses

Genomic DNA (20 μg) isolated from control tissues (tail or kidney) or *Artemis*$^{P70/P70}$ *p53*$^{-/-}$ tumor masses was digested with EcoRI. Southern blotting was performed with previously characterized probes hybridizing within the TCRβ locus (Drd1), J_H region, HS3a, Cμ, N-myc and c-myc loci. Southern blots were visualized using a Phosphorimager. Band intensities were quantitated using Image Quant TL v2005 software, and relative levels were normalized to a non-lymphoid locus (LR8). Fold amplification was calculated compared with the intensities of bands in the kidney controls on the same membrane. Reverse transcription of total RNA (1 μg) isolated from primary *Artemis*$^{P70/P70}$*p53*$^{-/-}$ (C219, C263) and *Artemis*$^{-/-}$*p53*$^{-/-}$ (C405) pro-B lymphomas and wild type lymphnode was performed using a poly-dT (20) primer and MLV-reverse transcriptase (Invitrogen). PCR amplification of cDNAs was performed using gene-specific primers to *c-myc* (exons 1 and 3) and (exons 2 and 3). cDNA levels were normalized to tubulin. Bands were quantitated using AlphaImager 2200 (Alpha Innotech; Santa Clara, CA, USA). RT-PCR reactions were repeated at least four times

References

1. Moshous D, Callebaut I, de Chasseval R, Corneo B, Cavazzana-Calvo M, Le Deist F, et al. Artemis, a novel DNA double-strand break repair/V(D)J recombination protein, is mutated in human severe combined immune deficiency. Cell. 2001;105(2):177-86.
2. Le Deist F, Poinsignon C, Moshous D, Fischer A, de Villartay JP. Artemis sheds new light on V(D)J recombination. Immunol Rev. 2004;200:142-55.
3. de Villartay JP. V(D)J recombination deficiencies. Adv Exp Med Biol. 2009;650:46-58.
4. Ma Y, Schwarz K, Lieber MR. The Artemis:DNA-PKcs endonuclease cleaves DNA loops, flaps, and gaps. DNA Repair (Amst). 2005;4(7):845-51.
5. Lieber MR. The mechanism of double-strand DNA break repair by the nonhomologous DNA end-joining pathway. Annu Rev Biochem. 2010;79:181-211. PMCID: 3079308.
6. Fugmann SD. RAG1 and RAG2 in V(D)J recombination and transposition. Immunol Res. 2001;23(1):23-39.
7. Gellert M. V(D)J recombination: RAG proteins, repair factors, and regulation. Annu Rev Biochem. 2002;71:101-32.
8. Sekiguchi J, Alt F.W., Oettinger M., Honjo T. Molecular Biology of B Cells. In: W. AF, editor. Elsevier Science2004. p. 57-78.
9. Ma Y, Pannicke U, Schwarz K, Lieber MR. Hairpin opening and overhang processing by an Artemis/DNA-dependent protein kinase complex in nonhomologous end joining and V(D)J recombination. Cell. 2002;108(6):781-94.
10. Rooney S, Sekiguchi J, Zhu C, Cheng HL, Manis J, Whitlow S, et al. Leaky Scid phenotype associated with defective V(D)J coding end processing in Artemis-deficient mice. Mol Cell. 2002;10(6):1379-90.
11. Pannicke U, Honig M, Schulze I, Rohr J, Heinz GA, Braun S, et al. The most frequent DCLRE1C (ARTEMIS) mutations are based on homologous recombination events. Hum Mutat. 2010;31(2):197-207.
12. Moshous D, Pannetier C, Chasseval Rd R, Deist Fl F, Cavazzana-Calvo M, Romana S, et al. Partial T and B lymphocyte immunodeficiency and predisposition to lymphoma in patients with hypomorphic mutations in Artemis. J Clin Invest. 2003;111(3):381-7. PMCID: 151863.
13. Ege M, Ma Y, Manfras B, Kalwak K, Lu H, Lieber MR, et al. Omenn syndrome due to ARTEMIS mutations. Blood. 2005;105(11):4179-86.
14. van der Burg M, Verkaik NS, den Dekker AT, Barendregt BH, Pico-Knijnenburg I, Tezcan I, et al. Defective Artemis nuclease is characterized by coding joints with microhomology in long palindromic-nucleotide stretches. Eur J Immunol. 2007;37(12):3522-8.

15. Musio A, Marrella V, Sobacchi C, Rucci F, Fariselli L, Giliani S, et al. Damaging-agent sensitivity of Artemis-deficient cell lines. Eur J Immunol. 2005;35(4):1250-6.
16. de Villartay JP, Shimazaki N, Charbonnier JB, Fischer A, Mornon JP, Lieber MR, et al. A histidine in the beta-CASP domain of Artemis is critical for its full in vitro and in vivo functions. DNA Repair (Amst). 2009;8(2):202-8.
17. Darroudi F, Wiegant W, Meijers M, Friedl AA, van der Burg M, Fomina J, et al. Role of Artemis in DSB repair and guarding chromosomal stability following exposure to ionizing radiation at different stages of cell cycle. Mutat Res. 2007;615(1-2):111-24.
18. Lagresle-Peyrou C, Benjelloun F, Hue C, Andre-Schmutz I, Bonhomme D, Forveille M, et al. Restoration of human B-cell differentiation into NOD-SCID mice engrafted with gene-corrected CD34+ cells isolated from Artemis or RAG1-deficient patients. Mol Ther. 2008;16(2):396-403.
19. Evans PM, Woodbine L, Riballo E, Gennery AR, Hubank M, Jeggo PA. Radiation-induced delayed cell death in a hypomorphic Artemis cell line. Hum Mol Genet. 2006;15(8):1303-11.
20. Kobayashi N, Agematsu K, Sugita K, Sako M, Nonoyama S, Yachie A, et al. Novel Artemis gene mutations of radiosensitive severe combined immunodeficiency in Japanese families. Hum Genet. 2003;112(4):348-52.
21. Li L, Moshous D, Zhou Y, Wang J, Xie G, Salido E, et al. A founder mutation in Artemis, an SNM1-like protein, causes SCID in Athabascan-speaking Native Americans. J Immunol. 2002;168(12):6323-9.
22. Noordzij JG, Verkaik NS, van der Burg M, van Veelen LR, de Bruin-Versteeg S, Wiegant W, et al. Radiosensitive SCID patients with Artemis gene mutations show a complete B-cell differentiation arrest at the pre-B-cell receptor checkpoint in bone marrow. Blood. 2003;101(4):1446-52.
23. van Zelm MC, Geertsema C, Nieuwenhuis N, de Ridder D, Conley ME, Schiff C, et al. Gross deletions involving IGHM, BTK, or Artemis: a model for genomic lesions mediated by transposable elements. Am J Hum Genet. 2008;82(2):320-32. PMCID: 2427306.
24. Rohr J, Pannicke U, Doring M, Schmitt-Graeff A, Wiech E, Busch A, et al. Chronic inflammatory bowel disease as key manifestation of atypical ARTEMIS deficiency. J Clin Immunol. 2010;30(2):314-20.
25. Brandt VL, Roth DB. Recent insights into the formation of RAG-induced chromosomal translocations. Adv Exp Med Biol. 2009;650:32-45.
26. Niewolik D, Pannicke U, Lu H, Ma Y, Wang LC, Kulesza P, et al. DNA-PKcs dependence of Artemis endonucleolytic activity, differences between hairpins and 5' or 3' overhangs. J Biol Chem. 2006;281(45):33900-9.
27. Yannone SM, Khan IS, Zhou RZ, Zhou T, Valerie K, Povirk LF. Coordinate 5' and 3' endonucleolytic trimming of terminally blocked blunt DNA double-strand break ends by Artemis nuclease and DNA-dependent protein kinase. Nucleic Acids Res. 2008;36(10):3354-65. PMCID: 2425473.
28. Gu J, Li S, Zhang X, Wang LC, Niewolik D, Schwarz K, et al. DNA-PKcs regulates a single-stranded DNA endonuclease activity of Artemis. DNA Repair (Amst). 2010;9(4):429-37. PMCID: 2847011.

29. Goodarzi AA, Yu Y, Riballo E, Douglas P, Walker SA, Ye R, et al. DNA-PK autophosphorylation facilitates Artemis endonuclease activity. EMBO J. 2006;25(16):3880-9. PMCID: 1553186.
30. Soubeyrand S, Pope L, De Chasseval R, Gosselin D, Dong F, de Villartay JP, et al. Artemis phosphorylated by DNA-dependent protein kinase associates preferentially with discrete regions of chromatin. J Mol Biol. 2006;358(5):1200-11.
31. Ma Y, Pannicke U, Lu H, Niewolik D, Schwarz K, Lieber MR. The DNA-dependent protein kinase catalytic subunit phosphorylation sites in human Artemis. J Biol Chem. 2005;280(40):33839-46.
32. Huang Y, Giblin W, Kubec M, Westfield G, St Charles J, Chadde L, et al. Impact of a hypomorphic Artemis disease allele on lymphocyte development, DNA end processing, and genome stability. J Exp Med. 2009;206(4):893-908. PMCID: 2715118.
33. Kang J, Bronson RT, Xu Y. Targeted disruption of NBS1 reveals its roles in mouse development and DNA repair. EMBO J. 2002;21(6):1447-55. PMCID: 125926.
34. Lista F, Bertness V, Guidos CJ, Danska JS, Kirsch IR. The absolute number of trans-rearrangements between the TCRG and TCRB loci is predictive of lymphoma risk: a severe combined immune deficiency (SCID) murine model. Cancer Res. 1997;57(19):4408-13.
35. Lipkowitz S, Stern MH, Kirsch IR. Hybrid T cell receptor genes formed by interlocus recombination in normal and ataxia-telangiectasis lymphocytes. J Exp Med. 1990;172(2):409-18. PMCID: 2188320.
36. Stern MH, Lipkowitz S, Aurias A, Griscelli C, Thomas G, Kirsch IR. Inversion of chromosome 7 in ataxia telangiectasia is generated by a rearrangement between T-cell receptor beta and T-cell receptor gamma genes. Blood. 1989;74(6):2076-80.
37. Kobayashi Y, Tycko B, Soreng AL, Sklar J. Transrearrangements between antigen receptor genes in normal human lymphoid tissues and in ataxia telangiectasia. J Immunol. 1991;147(9):3201-9.
38. Kang J, Ferguson D, Song H, Bassing C, Eckersdorff M, Alt FW, et al. Functional interaction of H2AX, NBS1, and p53 in ATM-dependent DNA damage responses and tumor suppression. Mol Cell Biol. 2005;25(2):661-70. PMCID: 543410.
39. Liyanage M, Weaver Z, Barlow C, Coleman A, Pankratz DG, Anderson S, et al. Abnormal rearrangement within the alpha/delta T-cell receptor locus in lymphomas from Atm-deficient mice. Blood. 2000;96(5):1940-6.
40. Ward IM, Difilippantonio S, Minn K, Mueller MD, Molina JR, Yu X, et al. 53BP1 cooperates with p53 and functions as a haploinsufficient tumor suppressor in mice. Mol Cell Biol. 2005;25(22):10079-86. PMCID: 1280262.
41. Deriano L, Stracker TH, Baker A, Petrini JH, Roth DB. Roles for NBS1 in alternative nonhomologous end-joining of V(D)J recombination intermediates. Mol Cell. 2009;34(1):13-25. PMCID: 2704125.
42. Bogue MA, Jhappan C, Roth DB. Analysis of variable (diversity) joining recombination in DNAdependent protein kinase (DNA-PK)-deficient mice reveals

DNA-PK-independent pathways for both signal and coding joint formation. Proc Natl Acad Sci U S A. 1998;95(26):15559-64. PMCID: 28082.
43. Bogue MA, Wang C, Zhu C, Roth DB. V(D)J recombination in Ku86-deficient mice: distinct effects on coding, signal, and hybrid joint formation. Immunity. 1997;7(1):37-47.
44. Carroll AM, Bosma MJ. T-lymphocyte development in scid mice is arrested shortly after the initiation of T-cell receptor delta gene recombination. Genes Dev. 1991;5(8):1357-66.
45. Giblin W, Chatterji M, Westfield G, Masud T, Theisen B, Cheng HL, et al. Leaky severe combined immunodeficiency and aberrant DNA rearrangements due to a hypomorphic RAG1 mutation. Blood. 2009;113(13):2965-75. PMCID: 2662642.
46. Helmink BA, Bredemeyer AL, Lee BS, Huang CY, Sharma GG, Walker LM, et al. MRN complex function in the repair of chromosomal Rag-mediated DNA double-strand breaks. J Exp Med. 2009;206(3):669-79. PMCID: 2699138.
47. Bredemeyer AL, Sharma GG, Huang CY, Helmink BA, Walker LM, Khor KC, et al. ATM stabilizes DNA double-strand-break complexes during V(D)J recombination. Nature. 2006;442(7101):466-70.
48. Bredemeyer AL, Huang CY, Walker LM, Bassing CH, Sleckman BP. Aberrant V(D)J recombination in ataxia telangiectasia mutated-deficient lymphocytes is dependent on nonhomologous DNA end joining. J Immunol. 2008;181(4):2620-5. PMCID: 3598579.
49. Buis J, Wu Y, Deng Y, Leddon J, Westfield G, Eckersdorff M, et al. Mre11 nuclease activity has essential roles in DNA repair and genomic stability distinct from ATM activation. Cell. 2008;135(1):85-96. PMCID: 2645868.
50. Lee JH, Paull TT. Activation and regulation of ATM kinase activity in response to DNA double-strand breaks. Oncogene. 2007;26(56):7741-8.
51. Burma S, Chen BP, Murphy M, Kurimasa A, Chen DJ. ATM phosphorylates histone H2AX in response to DNA double-strand breaks. J Biol Chem. 2001;276(45):42462-7.
52. Ziv Y, Bielopolski D, Galanty Y, Lukas C, Taya Y, Schultz DC, et al. Chromatin relaxation in response to DNA double-strand breaks is modulated by a novel ATM- and KAP-1 dependent pathway. Nat Cell Biol. 2006;8(8):870-6.
53. Maser RS, Monsen KJ, Nelms BE, Petrini JH. hMre11 and hRad50 nuclear foci are induced during the normal cellular response to DNA double-strand breaks. Mol Cell Biol. 1997;17(10):6087-96. PMCID: 232458.
54. Woo Y, Wright SM, Maas SA, Alley TL, Caddle LB, Kamdar S, et al. The nonhomologous end joining factor Artemis suppresses multi-tissue tumor formation and prevents loss of heterozygosity. Oncogene. 2007;26(41):6010-20.
55. Rooney S, Sekiguchi J, Whitlow S, Eckersdorff M, Manis JP, Lee C, et al. Artemis and p53 cooperate to suppress oncogenic N-myc amplification in progenitor B cells. Proc Natl Acad Sci U S A. 2004;101(8):2410-5. PMCID: 356964.
56. Dujka ME, Puebla-Osorio N, Tavana O, Sang M, Zhu C. ATM and p53 are essential in the cell-cycle containment of DNA breaks during V(D)J recombination in vivo. Oncogene. 2010;29(7):957-65.

57. Guidos CJ, Williams CJ, Grandal I, Knowles G, Huang MT, Danska JS. V(D)J recombination activates a p53-dependent DNA damage checkpoint in scid lymphocyte precursors. Genes Dev. 1996;10(16):2038-54.
58. Zhu C, Mills KD, Ferguson DO, Lee C, Manis J, Fleming J, et al. Unrepaired DNA breaks in p53-deficient cells lead to oncogenic gene amplification subsequent to translocations. Cell. 2002;109(7):811-21.
59. Negrini S, Gorgoulis VG, Halazonetis TD. Genomic instability--an evolving hallmark of cancer. Nat Rev Mol Cell Biol. 2010;11(3):220-8.
60. Mills KD, Ferguson DO, Alt FW. The role of DNA breaks in genomic instability and tumorigenesis. Immunol Rev. 2003;194:77-95.
61. Difilippantonio MJ, Petersen S, Chen HT, Johnson R, Jasin M, Kanaar R, et al. Evidence for replicative repair of DNA double-strand breaks leading to oncogenic translocation and gene amplification. J Exp Med. 2002;196(4):469-80. PMCID: 2196056.
62. Liao MJ, Zhang XX, Hill R, Gao J, Qumsiyeh MB, Nichols W, et al. No requirement for V(D)J recombination in p53-deficient thymic lymphoma. Mol Cell Biol. 1998;18(6):3495-501. PMCID: 108930.
63. Haines BB, Ryu CJ, Chang S, Protopopov A, Luch A, Kang YH, et al. Block of T cell development in P53-deficient mice accelerates development of lymphomas with characteristic RAG-dependent cytogenetic alterations. Cancer Cell. 2006;9(2):109-20.
64. Bassing CH, Suh H, Ferguson DO, Chua KF, Manis J, Eckersdorff M, et al. Histone H2AX: a dosage-dependent suppressor of oncogenic translocations and tumors. Cell. 2003;114(3):359-70.
65. Celeste A, Difilippantonio S, Difilippantonio MJ, Fernandez-Capetillo O, Pilch DR, Sedelnikova OA, et al. H2AX haploinsufficiency modifies genomic stability and tumor susceptibility. Cell. 2003;114(3):371-83.
66. Vanasse GJ, Halbrook J, Thomas S, Burgess A, Hoekstra MF, Disteche CM, et al. Genetic pathway to recurrent chromosome translocations in murine lymphoma involves V(D)J recombinase. J Clin Invest. 1999;103(12):1669-75. PMCID: 408389.
67. Hsieh CL, Arlett CF, Lieber MR. V(D)J recombination in ataxia telangiectasia, Bloom's syndrome, and a DNA ligase I-associated immunodeficiency disorder. J Biol Chem. 1993;268(27):20105-9.
68. Barlow C, Hirotsune S, Paylor R, Liyanage M, Eckhaus M, Collins F, et al. Atm-deficient mice: a paradigm of ataxia telangiectasia. Cell. 1996;86(1):159-71.
69. Elson A, Wang Y, Daugherty CJ, Morton CC, Zhou F, Campos-Torres J, et al. Pleiotropic defects in ataxia-telangiectasia protein-deficient mice. Proc Natl Acad Sci U S A. 1996;93(23):13084-9. PMCID: 24050.
70. Xu Y, Baltimore D. Dual roles of ATM in the cellular response to radiation and in cell growth control. Genes Dev. 1996;10(19):2401-10.
71. Borghesani PR, Alt FW, Bottaro A, Davidson L, Aksoy S, Rathbun GA, et al. Abnormal development of Purkinje cells and lymphocytes in Atm mutant mice. Proc Natl Acad Sci U S A. 2000;97(7):3336-41. PMCID: 16240.

72. Callen E, Jankovic M, Difilippantonio S, Daniel JA, Chen HT, Celeste A, et al. ATM prevents the persistence and propagation of chromosome breaks in lymphocytes. Cell. 2007;130(1):63-75.
73. Mahaney BL, Meek K, Lees-Miller SP. Repair of ionizing radiation-induced DNA double-strand breaks by non-homologous end-joining. Biochem J. 2009;417(3):639-50. PMCID: 2975036.
74. Hammel M, Yu Y, Mahaney BL, Cai B, Ye R, Phipps BM, et al. Ku and DNA-dependent protein kinase dynamic conformations and assembly regulate DNA binding and the initial non-homologous end joining complex. J Biol Chem. 2010;285(2):1414-23. PMCID: 2801267.
75. Moshous D, Callebaut I, de Chasseval R, Poinsignon C, Villey I, Fischer A, et al. The V(D)J recombination/DNA repair factor artemis belongs to the metallo-beta-lactamase family and constitutes a critical developmental checkpoint of the lymphoid system. Ann N Y Acad Sci. 2003;987:150-7.
76. Rooney S, Chaudhuri J, Alt FW. The role of the non-homologous end-joining pathway in lymphocyte development. Immunol Rev. 2004;200:115-31.
77. Zha S, Bassing CH, Sanda T, Brush JW, Patel H, Goff PH, et al. ATM-deficient thymic lymphoma is associated with aberrant tcrd rearrangement and gene amplification. J Exp Med. 2010;207(7):1369-80. PMCID: 2901073.
78. Osborne CS, Chakalova L, Mitchell JA, Horton A, Wood AL, Bolland DJ, et al. Myc dynamically and preferentially relocates to a transcription factory occupied by Igh. PLoS Biol. 2007;5(8):e192. PMCID: 1945077.
79. Wang JH, Gostissa M, Yan CT, Goff P, Hickernell T, Hansen E, et al. Mechanisms promoting translocations in editing and switching peripheral B cells. Nature. 2009;460(7252):231-6. PMCID: 2907259.
80. Zha S, Sekiguchi J, Brush JW, Bassing CH, Alt FW. Complementary functions of ATM and H2AX in development and suppression of genomic instability. Proc Natl Acad Sci U S A. 2008;105(27):9302-6. PMCID: 2453730.
81. Rooney S, Alt FW, Sekiguchi J, Manis JP. Artemis-independent functions of DNA-dependent protein kinase in Ig heavy chain class switch recombination and development. Proc Natl Acad Sci U S A. 2005;102(7):2471-5. PMCID: 548986.
82. Theunissen JW, Petrini JH. Methods for studying the cellular response to DNA damage: influence of the Mre11 complex on chromosome metabolism. Methods Enzymol. 2006;409:251-84.

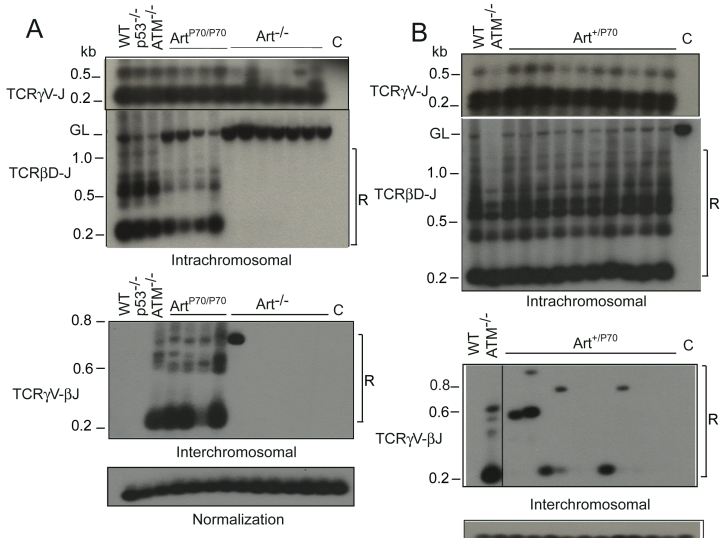

C

TCRγV3	NT Added	TCRβJ2	# Clones
ArtP70/P70			
GCTAAAG		CTCCTATGAAC	Jβ2S7
GC	CTC	TATGAAC	1
GC	AG	TGAAC	1
GCTAA	GGGGAGGC	CCTATGAAC	1
GC	GA	CTCCTATGAAC	2
GCTAAAG	CTAAGG	CTATGAAC	1
GC	AA	CTCCTATGAAC	1
		AGTCAAAACAC	Jβ2S4
GCT	CATCT	AGTCAAAACAC	1
GCT	CT	AGTCAAAACAC	1
		AACCAAGACACCCA	Jβ2S5
G	-	AGACACCCA	1
GCTAA	CGTCCCT	A	1
GCTAAA	TC	CCAAGACACCCA	1
G	ATG	AAGACACCCA	1
G	GAAGG	AAGACACCCA	1
Art-/-			
GCTAAAG		AGTGCAGAAA	Jβ2S3
GCTAA	CTCACT	AGTGCAGAAA	15

Figure 2.1 Aberrant rearrangements in Artemis-P70 lymphocytes. (A) Examination of V(D)J trans-rearrangements. Intrachromosomal TCRγ V-to-J (chr. 13) and TCRβ Dβ2-to-Jβ2 (chr 6) rearrangements (top) and interchromosomal TCRγV–TCRβJ transrearrangements (bottom) were PCR amplified from genomic thymocyte DNA isolated from wild type, *Artemis*$^{P70/P70}$, *Artemis*$^{-/-}$, *Atm*$^{-/-}$ and *p53*$^{-/-}$ mice, as indicated. Nested PCR products were detected by Southern blot analysis. Levels of rearrangements were normalized to PCR-amplified non-rearranging locus. GL, germline, unrearranged band; R, bands corresponding to rearrangements; C, PCR amplification of kidney genomic DNA. Representative results are shown. **(B)** Examination of V(D)J trans-rearrangements in *Artemis-P70* heterozygous mice. Nested PCR analyses of intrachromosomal TCRγ V-to-J, TCRβ Dβ2-to-Jβ2 (top) and interchromosomal TCRγV–TCRβJ trans-rearrangements (bottom) were performed with genomic DNA isolated from *Artemis*$^{+/P70}$ thymocytes, as described above. Representative results are shown. **(C)** Sequence analysis of trans-rearrangement PCR products. Trans-rearrangement PCR products detected from Southern blot analysis were subcloned and sequenced. Coding sequences are shown in boxes. Nucleotides added include P-nucleotides (underlined) as well as N nucleotides.

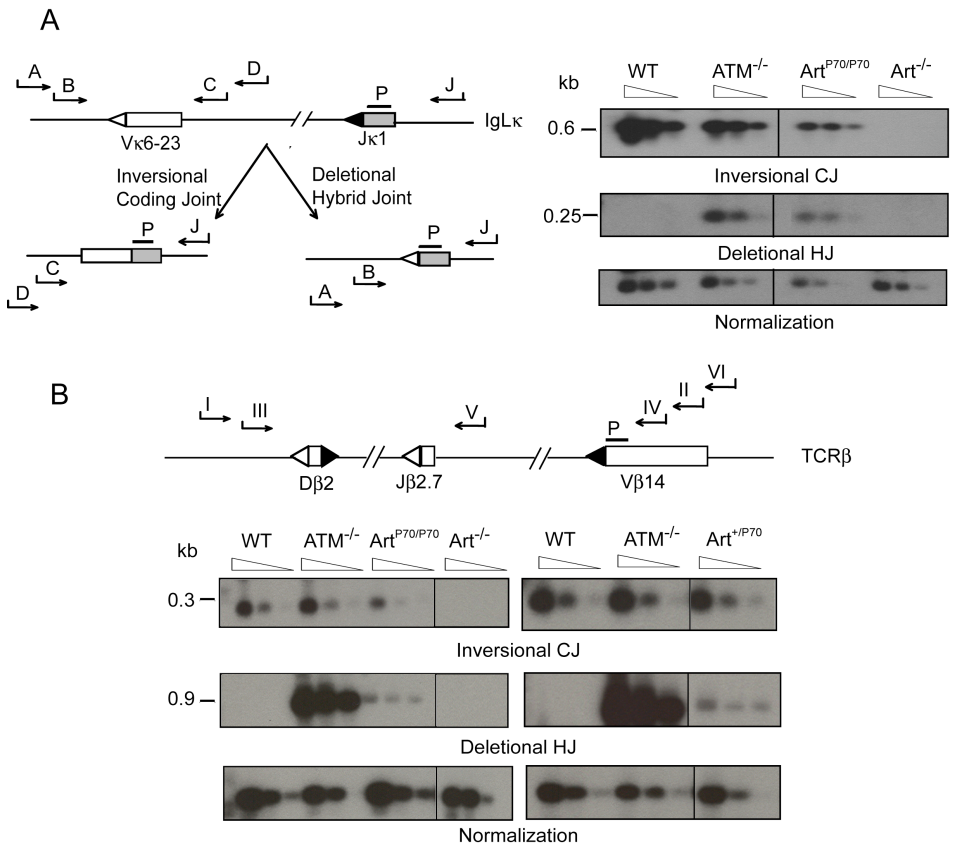

Figure 2.2 Deletional hybrid joint formation in Art-P70 mutant lymphocytes. **(A)** Left panel: Schematic representation of nested PCR strategy for detecting coding and hybrid joints within the IgLκ locus. Relative orientation of Vκ6-23 and Jκ1 coding (rectangles) and RSSs (triangles) within the IgLk locus. Inversional (CJ) and deletional (HJ) products are depicted. Positions of primers (J = pκJa, A = pκ6a, B = pκ6b, C = pκ6c, D = pκ6d) and probe (P) are shown. Right panel: PCR analysis of Vκ6-23 to Jκ1 coding joins (CJs) and hybrid joins (HJs). Genomic splenocyte DNA was isolated from WT, *Atm*$^{-/-}$, *Artemis*$^{-/-}$ and *Artemis*$^{P70/P70}$ mice and amplified using primers (pκJa and pκ6d for CJ and pκJa and pκ6a for HJ). Serial 4-fold dilutions of the PCR reaction were amplified using nested primer pairs (pκJa and pκ6c for CJ, and pκJa and pκ6b for HJ). CJ and HJ bands are 0.6 and 0.25 kb, respectively. **(B)** Deletional hybrid joining and coding joining within the TCRβ locus. Upper panel: Schematic of nested PCR strategy. Relative orientation of Vβ14, Dβ2 and Jβ2.3 coding (rectangles) and RSSs (triangles) within the TCRβ locus. Positions of primers (I = pβa, II = pβb, III = pβc, IV = pβd, V = pβe, VI = pβf) and probe (P = pβg) are shown. Lower panel: PCR analysis of Vβ14 to Jβ2 coding and hybrid joints. Left panel shows CJ and HJ PCR analyses of genomic thymocyte DNA isolated from WT, *Atm*$^{-/-}$, *Artemis*$^{-/-}$ and *Artemis*$^{P70/P70}$ mice. Right panel shows CJ and HJ PCR analyses of Art$^{+/P70}$ and control thymocyte genomic DNA, as indicated. Primers for CJ were pβe and pβf. Primary primers for HJ were pβa and pβb. Serial 4-fold dilutions of this primary HJ reaction were amplified using primers pβc and pβd. CJ and HJ bands are 0.3 and 0.9 kb, respectively.

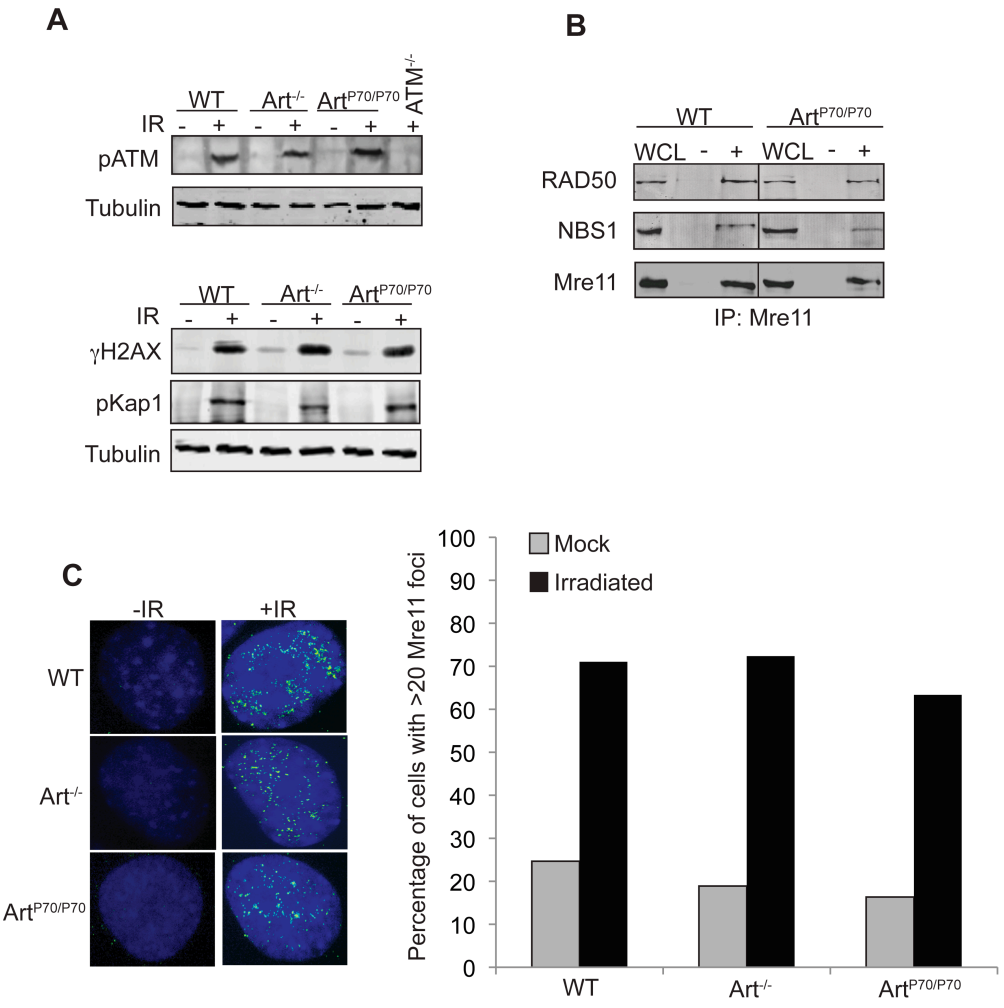

Figure 2.3 ATM- and MRN-dependent responses to IR-induced breaks in ART-P70 mutant cells. (A) ART-P70 mutation does not impair ATM-dependent DNA damage responses to IR. *Artemis*$^{+/+}$, *Artemis*$^{-/-}$, *Artemis*$^{P70/P70}$ and *Atm*$^{-/-}$ MEFs, as indicated, were unirradiated (−) or exposed to IR (10 Gy, +) and then harvested at 1 h post-irradiation. Whole-cell lysates were analyzed by western blotting using the indicated antibodies. Tubulin was used as a loading control. **(B)** The MRN complex is intact in ART-P70 mutant cells. The MRN complex was co-immunoprecipitated from whole-cell lysates generated from wild type or *Artemis*$^{P70/P70}$ MEFs using α-MRE11 antibodies. The immunoprecipitates were washed with 300 mM KCl, and the proteins were analyzed on an 8% SDS–PAGE followed by western blotting with the indicated antibodies. WCL, whole-cell lysate; −, no antibody; +, α-MRE11 antibody. **(C)** MRE11 foci formation is not impaired in ART-P70 mutant cells. *Artemis*$^{+/+}$, *Artemis*$^{-/-}$ and *Artemis*$^{P70/P70}$ MEFs were grown on coverslips then irradiated (10 Gy). The irradiated cells and unirradiated controls were fixed in paraformaldehyde and then stained with α-MRE11 antibodies. The number of cells containing >20 Mre11 foci were scored. Left panels, representative images of nuclei. Right panels, quantitative results of MRE11 foci-positive cells. Average of two independent experiments is shown.

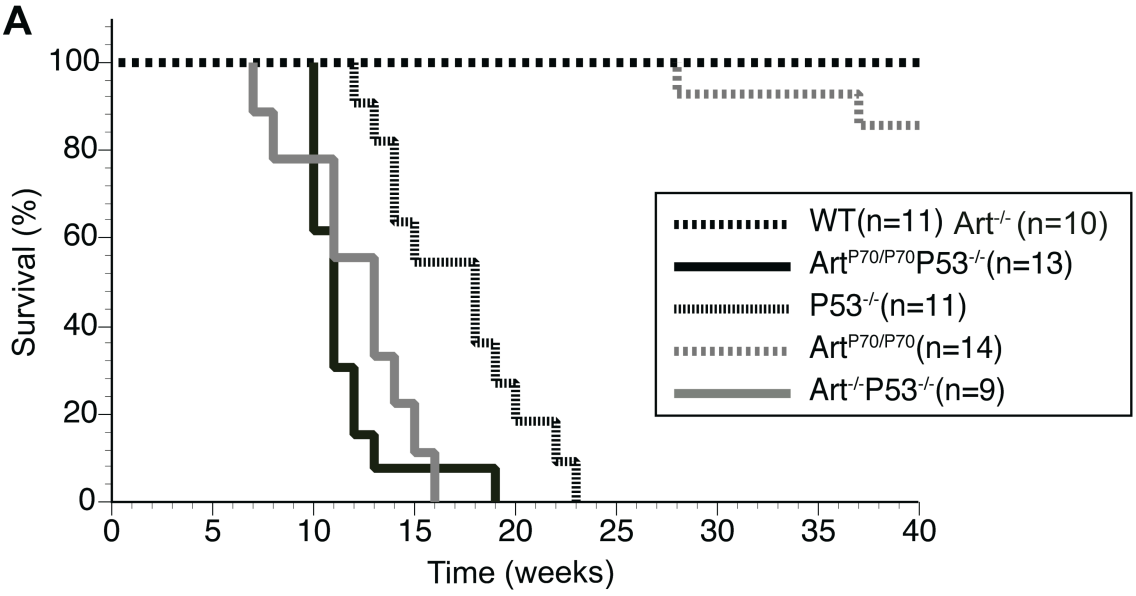

B

Tumor spectrum in Art-P70/p53 mice

Tumor type	$Art^{P70/P70}$	$Art^{-/-}$	$Art^{P70/P70}$ $p53^{-/-}$	$Art^{-/-}$ $p53^{-/-}$	$p53^{-/-}$
Total number	2	0	13	8	11
ProB lymphoma	0	0	4	6	0
Mature B lymphoma	0	0	0	0	1
TCRβ⁻ T-cell lymphoma	2	0	9	2	0
TCRβ+ T-cell lymphoma	0	0	0	0	10
Sarcoma	0	0	0	0	0

Figure 2.4 Art-P70/p53 double-mutant mice are predisposed to thymic lymphomas with chromosomal translocations. (A) Decreased survival of *Art-P70/p53 mice*. Survival of a cohort of wild type (n= 11), *Artemis*$^{-/-}$ (n= 10), *p53*$^{-/-}$ (n= 11), *Artemis*$^{P70/P70}$ (n= 14), *Artemis*$^{P70/P70}$*p53*$^{-/-}$ (n= 13) and *Artemis*$^{-/-}$*p53*$^{-/-}$ (n= 9) mice was observed for a period of 40 weeks. Shown are Kaplan–Meier survival curves representing the percentage of survival of cohort mice versus age in weeks. **(B)** Distinct tumor spectrum exhibited by *Art-P70/p53* mice. Table summarizing the number of the different tumor types observed in mice of the indicated genotypes.

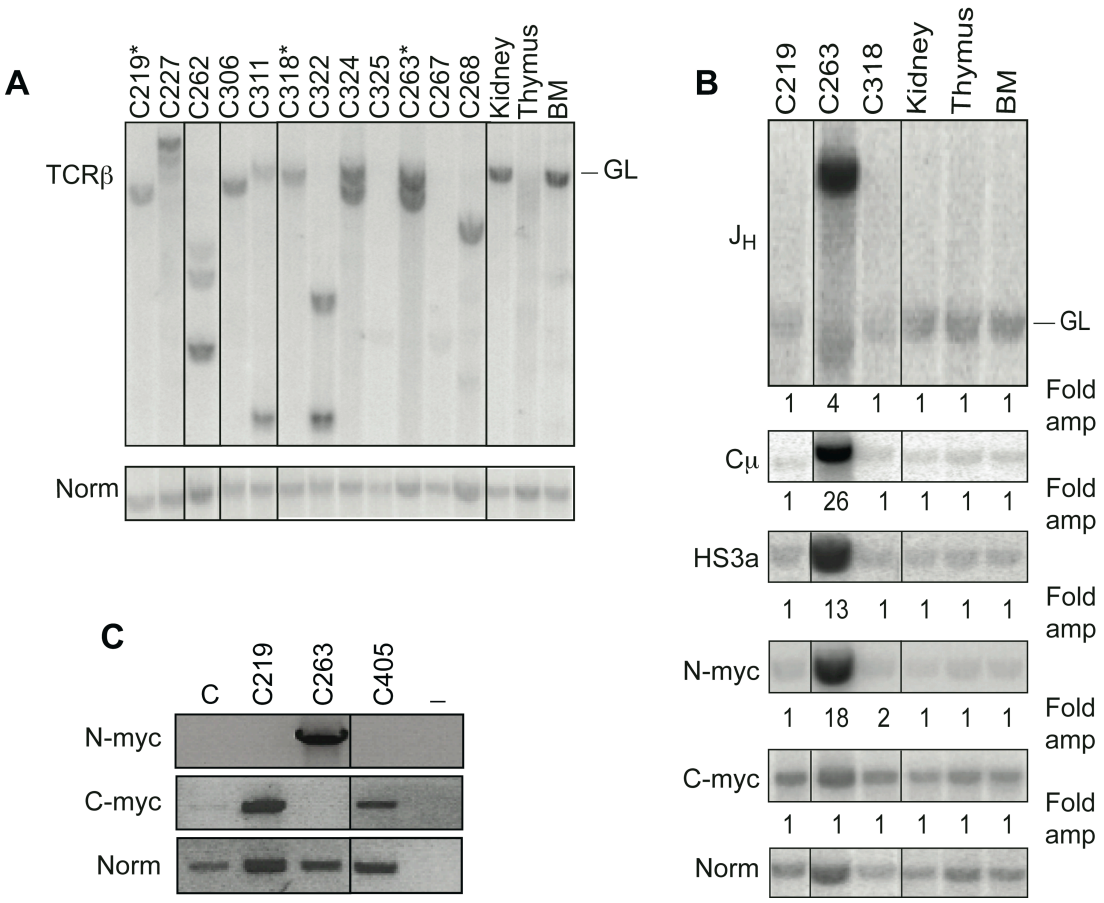

Figure 2.5 Clonal rearrangements involving recombining loci in Art-P70/p53 tumors. (A) Analysis of TCR rearrangement status in *Art-P70/p53* thymic lymphomas. Genomic DNA isolated from *Artemis*$^{P70/P70}$*p53*$^{-/-}$ tumors was digested with EcoRI and then analyzed by Southern blotting. Individual tumors are indicated (top). Thymus, kidney and bone marrow (BM), control tissues; GL, unrearranged, germline band. Amounts of input DNA were normalized to a non-rearranging locus (LR8). *, pro-B lymphomas (C219, C263, C318). **(B)** Analysis of *Art-P70/p53* pro-B lymphomas by Southern blotting. Genomic DNA isolated from *Art-P70/p53* double-mutant lymphomas was digested with EcoRI and then analyzed by Southern blotting. Previously characterized probes that hybridized to the J_H, Cμ and HS3A regions of the IgH locus, N-myc on chr. 12 and c-myc on chr. 15 were used, as indicated. Individual tumors are indicated, top; Thymus, kidney, and bone marrow (BM), control tissues; GL, unrearranged, germline band. Amounts of input DNA were normalized to a non-rearranging locus (LR8). Fold amplification compared with the non-rearranging locus was calculated as described in Materials and methods. **(C)** Semi-quantitative RT-PCR of N-MYC and C-MYC transcript levels. Total RNA was isolated from primary tumor cells, and RT-PCR was performed. cDNAs were PCR amplified using *n-myc* (exons 2 and 3), *c-myc* (exons 1–3) and tubulin-specific primers. Tumor numbers, as indicated; C, total RNA from normal, wild type LN; −, no-RT control.

A **Spectral karyotyping of Art-P70/p53 tumor metaphases**

Tumor	Translocations	Flow cytometry
C227	t(13;6) t(14;1)	$CD4^+$ $CD8^+$ $TCR\beta^-$
C267	t(14;4)	$CD4^+$ $CD8^+$ $TCR\beta^-$
C268	t(12;1)	$CD4^+$ $CD8^+$ $TCR\beta^-$
C325	t(4;14)	$CD4^+$ $CD8^+$ $TCR\beta^-$
C306	t(12;14) t(1;14)	$CD4^+$ $CD8^+$ $TCR\beta^-$
C262	t(12;11) t(19;2)	$CD4^+$ $CD8^+$ $TCR\beta^-$
C324	t(14;2)	$CD4^+$ $CD8^+$ $TCR\beta^-$
C219	t(12;15)	IgM^-, $B220^+$, $CD43^+$

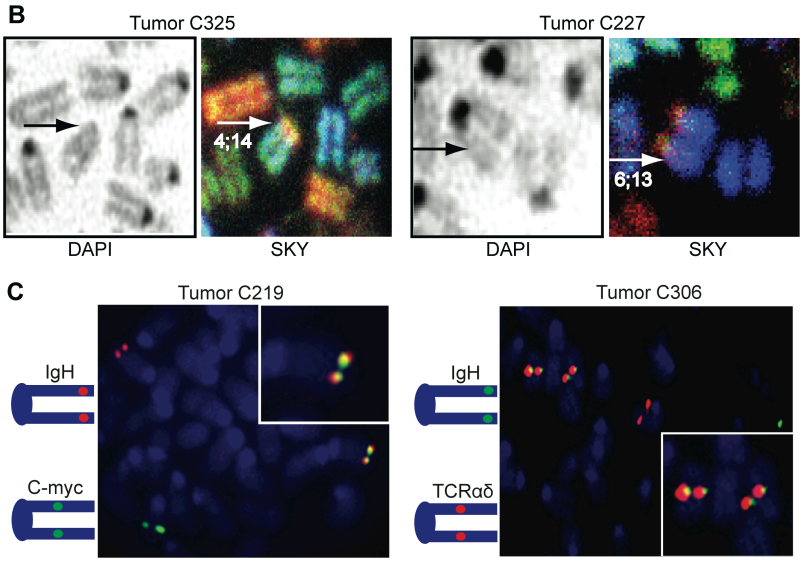

Figure 2.6 Art-P70/p53 tumors harbor clonal chromosomal translocations. **(A)** Table summarizing clonal translocations observed in *Art-P70/p53* tumors. Metaphases from primary tumor cells or early passage tumor cell cultures were analyzed by SKY. At least 10 metaphases from each tumor were scored. **(B)** SKY images of metaphase chromosomes from *Art-P70/p53* tumors. DAPI staining (left panels) and SKY analysis (right panels) of tumor C325 and C227 containing clonal t(4;14) and t(6;13) translocations, respectively. Arrows indicate translocated chromosomes. **(C)** FISH analyses of metaphases from *Art-P70/p53* tumors. Representative FISH analyses of metaphases from *Art-P70/p53* tumors. Left panel, pro-B lymphoma, C219. Left panel, thymic tumor C306. At least 20 metaphases were scored for each tumor. Diagrams indicate the relative chromosomal positions and fluorescent colors of BAC probes. Inset, enlarged images of co-localized probes.

Supplementary Figure 2S7

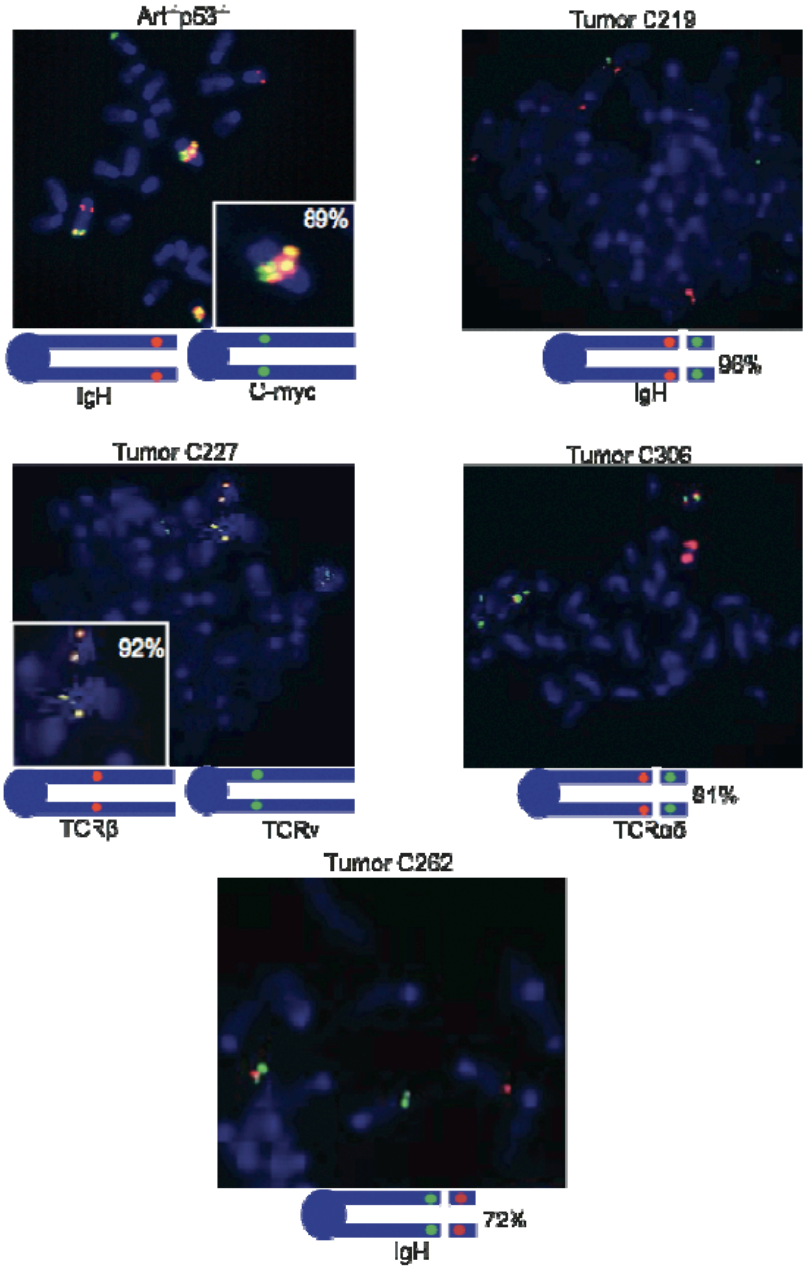

Supplementary Figure 2S7. FISH analyses of Art-P70/p53 tumor metaphases. Chromosomal anomalies in metaphases from primary tumors or early passage cultured tumor cells were analyzed by FISH using the indicated BAC probes. Red and green fluorescent signals, as diagramed. *Artemis*$^{-/-}$*p53*$^{-/-}$ (C405), C219, pro-B lymphomas; C227, C306, C262, thymic lymphomas. Representative metaphase images are shown. Percentage of metaphases with the indicated anomalies is indicated. At least 20 metaphases from each tumor were analyzed.